

**An-Najah National University**  
**Faculty of Graduate Studies**

**TiO<sub>2</sub> and ZnO photocatalysts for degradation of widespread pharmaceutical wastes: Effect of particle size and support**

**By**  
**Shadya Ahmed Hussni Hejjawi**

**Supervisors**  
**Prof. Hikmat Hilal**  
**Dr. Ahed Zyoud**

**This Thesis is Submitted in Partial Fulfillment of the Requirements for the Degree of Master of Science in Chemistry, Faculty of Graduate Studies, An-Najah National University, Nablus, Palestine.**

**2013**

**TiO<sub>2</sub> and ZnO photocatalysts for degradation of widespread pharmaceutical wastes: Effect of particle size and support**

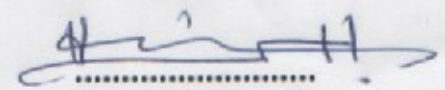
By  
**Shadya Ahmed Hussni Hejjawi**

This Thesis was defended successfully on 30/5/2013 and approved by:

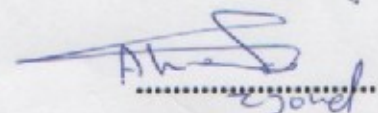
**Defense Committee Members**

**Signature**

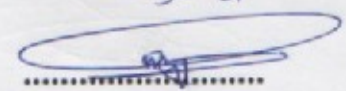
1. Prof. Hikmat Hilal / Supervisor



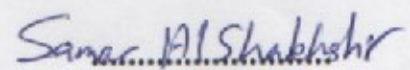
2. Dr. Ahed Zyoud/ Co-Supervisor



3. Dr. Wadie Sultan / External Examiner



4. Dr. Samar Al-Shakhshir / Internal Examiner



## **Dedication**

*To my Mother, Father, Sister, Brothers and, last but in no way least, to my Husband, for their continuous support with my appreciation.*

## **Acknowledgment**

Praise be to Allah who enable me to complete this work.

Thanks and deepest appreciation to my supervisors, Prof. Hikmat Hilal for his guidance, support and great help throughout this research. Thanks for Dr. Ahed Zyoud for his encouragement, and continuous theoretical and practical help and for his useful discussions.

I would like to thank the technical staff in Chemistry. Thanks are due to Laboratories of the Department of Chemistry at King Saud University, Riyadh, Saudi Arabia, for measuring XRD, with special thank to Dr. Ismail Warrad and Dr. Bajia.

Thanks are due to Dr. Guy Campet and his research group, ICMCB, University of Bordeaux, France, for SEM measurement. The auther acknowledges support from Al- Maqdisi Project to this work.

My great thanks are due to my father for endless support. I also say my prayers for my mother who passed away while giving me full support and guidance.

I wish to thank all my friends, especially research lab mates.

## الإقرار

أنا الموقعة أدناه مقدمة الرسالة التي تحمل العنوان:

### **TiO<sub>2</sub> and ZnO photocatalysts for degradation of widespread pharmaceutical wastes: Effect of particle size and support**

استخدام TiO<sub>2</sub> و ZnO كحفازات ضوئية في تحطيم المخلفات الصيدلانية المنتشرة:  
تأثير حجم حبيبة الحفاز وتثبيتته على السطوح

أقر بأن ما اشتملت عليه هذه الرسالة هو نتاج جهدي الخاص، باستثناء ما تمت الإشارة إليه  
حيثما ورد، وأن هذ الرسالة ككل أو أي جزء منها لم يقدم من قبل لنيل أي درجة أو لقب علمي  
أو بحثي لدى أي مؤسسة تعليمية أو بحثية أخرى.

### **Declaration**

The work provide in this thesis, unless otherwise referenced, is the  
researcher's own work, and has not been submitted elsewhere for any other  
degrees or qualifications.

**Student's name:**

اسم الطالب:

**Signature:**

التوقيع:

**Date:**

التاريخ:

## List of Contents

No.	Contents	Page
	Dedication	iii
	Acknowledgment	iv
	Declaration	v
	List of abbreviations	xiv
	List of contents	vi
	List of tables	ix
	List of figures	xi
	Abstract	xv
	<b>Chapter 1 Introduction</b>	1
1.1	Ultraviolet purification	2
1.2	Semiconductor photocatalysis	2
1.2.1	Titanium dioxide	5
1.2.2	Zinc oxide	9
1.3	Mechanism of photodegradation	13
1.3.1	TiO <sub>2</sub> photocatalytic reaction mechanism	14
1.3.2	ZnO photocatalytic reaction mechanism	17
1.4	Reaction parameters studied	19
1.5	Examples of contaminant studied	19
1.6	Photodegradation of paracetamol	21
1.7	General objective of this work	23
1.8	Novelty of this work	24
1.9	Hypothesis	24
	<b>Chapter 2 Materials and Methods</b>	26
2.1	Materials	26
2.1.1	Zinc oxide	26
2.1.2	Titanium dioxide	26
2.1.3	Paracetamol	27
2.1.4	Other chemicals	27
2.2	Instrument	27
2.2.1	UV lamp	27
2.2.2	UV-visible spectrophotometry	29
2.2.3	Lux meter	29
2.2.4	pH meter	29
2.2.5	Thermometer	29
2.2.6	Centrifuge	29
2.2.7	XRD	29
2.2.8	SEM	30

2.3	Catalyst preparation	30
2.3.1	Preparation of TiO <sub>2</sub> powder	30
2.3.2	Nanoparticle zinc oxide preparation	30
2.3.3	AC/catalyst (TiO <sub>2</sub> , ZnO) preparation	31
2.3.4	Stock solution preparation	31
2.4	Calibration curve	32
2.5	Photo-catalytic experiments	33
	<b>Chapter 3 Results and Discussion</b>	34
3.1	Introduction	34
3.2	Photocatalyst characterization results	34
3.2.1	TiO <sub>2</sub> system	34
	X-ray diffraction (XRD) of TiO <sub>2</sub>	34
	Scanning electron microscopy (SEM) of TiO <sub>2</sub>	37
	TiO <sub>2</sub> photoluminescence (PL) spectra	38
	UV/visible spectral characterization of TiO <sub>2</sub>	39
3.2.2	ZnO system	40
	UV/visible spectral characterization of ZnO	40
	Photoluminescence (PL) spectra of ZnO	41
	XRD study of ZnO	42
	SEM results of ZnO	44
3.3	Photocatalytic reaction results	45
3.3.1	Commercial catalyst system	45
3.3.1.1	Commercial TiO <sub>2</sub> catalyst system	45
	Effect of contaminant concentration	45
	Effect of catalyst concentration	48
	Effect of pH	51
3.3.1.2	Commercial ZnO catalyst system	53
	Effect of contaminant concentration	53
	Effect of catalyst concentration	54
3.3.2	Nano-catalyst systems	56
3.3.2.1	TiO <sub>2</sub> system	56
3.3.2.2	ZnO system	57
3.3.2.3	TiO <sub>2</sub> and ZnO nano-systems	58
3.3.3	AC-supported catalyst systems	59
	Effect of contaminant concentration	60
	Effect of pH	63
	AC/TiO <sub>2</sub> rutile	63
	AC/TiO <sub>2</sub> anatase	64
	AC/ZnO commercial	60
	AC/TiO <sub>2</sub> nano-particles and AC/ZnO nano-	68

	particles	
	AC/TiO <sub>2</sub> anatase and AC/TiO <sub>2</sub> rutile	68
3.4	General discussion	70
3.4.1	Catalytic reaction results	71
3.4.1.1	Commercial catalyst systems	71
3.4.1.1.1	Commercial TiO <sub>2</sub> systems	71
	Effect of contaminant concentration	71
	Effect of catalyst concentration	71
	Effect of pH	72
3.4.1.1.2	Commercial ZnO system	73
	Effect of contaminant concentration	73
	Effect of catalyst concentration	74
3.4.1.2	Activated carbon-supported commercial catalysts (AC/catalysts)	74
3.4.1.2.1	AC/TiO <sub>2</sub> System	75
3.4.1.2.2	AC/ZnO System	75
	Effect of contaminant concentration	76
	Effect of pH	77
3.4.1.3	Nano-particle catalyst systems	78
3.4.1.3.1	Nano TiO <sub>2</sub> system	78
3.4.1.3.2	Nano ZnO system	79
3.4.1.4	AC/catalyst nano-particle systems	80
	Conclusions	82
	Suggestions for further work	83
	References	84
	الملخص	ب

## List of Tables

No.	Table	Page
(1.1)	A general mechanism of semiconductor photocatalysis at TiO <sub>2</sub> .	15
(2.1)	UV lamp specification.	28
(3.1)	Effect of contaminant concentration on values of turnover number (T.N.), turnover frequency (T.F.) (min <sup>-1</sup> ), quantum yield (Q.Y.) and overall rate for paracetamol degradation after 60 min, using the TiO <sub>2</sub> anatase system under UV light.	47
(3.2)	Effect of catalyst concentration on values of turnover number, turnover frequency (min <sup>-1</sup> ), quantum yield and overall rate for paracetamol degradation after 60 min, using TiO <sub>2</sub> in anatase form under UV light.	49
(3.3)	Effect of catalyst concentration on values of turnover number, turnover frequency (min <sup>-1</sup> ), quantum yield and overall rate for paracetamol degradation after 60 min, using TiO <sub>2</sub> catalyst in the rutile form under UV light.	50
(3.4)	Effect of pH on values of turnover number, turnover frequency (min <sup>-1</sup> ), quantum yield and overall rate for paracetamol degradation after 60 min, using rutile form under UV light.	52
(3.5)	Effect of pH on values of turnover number, turnover frequency (min <sup>-1</sup> ), quantum yield and overall rate for paracetamol degradation after 60 min, using anatase form under UV light.	53
(3.6)	Effect of initial paracetamol concentration on values of turnover number, turnover frequency (min <sup>-1</sup> ), quantum yield and overall rate for paracetamol degradation after 60 min, using ZnO commercial under UV light.	54
(3.7)	Effect of ZnO catalyst concentration on values of turnover number, turnover frequency (min <sup>-1</sup> ), quantum yield and overall rate for paracetamol degradation after 60 min, using ZnO commercial under UV light.	55
(3.8)	Effect of TiO <sub>2</sub> systems on values of turnover number, turnover frequency (min <sup>-1</sup> ), quantum yield and overall rate for paracetamol degradation after 60 min, using TiO <sub>2</sub> nano-particles and TiO <sub>2</sub> commercial under direct	57

	sun light.	
(3.9)	Effect of ZnO nano-particles and commercial on values of turnover number, turnover frequency ( $\text{min}^{-1}$ ), quantum yield and overall rate for paracetamol degradation after 60 min under direct sun light.	58
(3.10)	Effect of $\text{TiO}_2$ and ZnO nano-catalyst on values of turnover number, turnover frequency ( $\text{min}^{-1}$ ), quantum yield and overall rate for paracetamol degradation after 60 min under direct sun light.	59
(3.11)	Effect of paracetamol concentration on values of turnover number, turnover frequency ( $\text{min}^{-1}$ ), quantum yield and overall rate for paracetamol degradation after 60 min, using different commercial catalyst systems under UV light.	63
(3.12)	Effect of pH on values of turnover number, turnover frequency ( $\text{min}^{-1}$ ), quantum yield and overall rate for paracetamol degradation after 60 min, using AC/ $\text{TiO}_2$ rutile system with UV light.	64
(3.13)	Effect of pH on values of turnover number, turnover frequency ( $\text{min}^{-1}$ ), quantum yield and overall rate for paracetamol degradation after 60 min, using AC/ $\text{TiO}_2$ anatase system with UV light.	65
(3.14)	Effect of pH on values of turnover number, turnover frequency ( $\text{min}^{-1}$ ), quantum yield and overall rate for paracetamol degradation after 60 min using AC/ZnO (commercial) catalyst with UV light.	67
(3.15)	Effect of catalyst on values of turnover number, turnover frequency ( $\text{min}^{-1}$ ), quantum yield and overall rate for paracetamol degradation after 60 min, using AC/Catalyst nano. under direct sun light.	68
(3.16)	Effect of AC/ $\text{TiO}_2$ commercial catalysts (anatase and rutile) on values of turnover number, turnover frequency ( $\text{min}^{-1}$ ), quantum yield and overall rate for paracetamol degradation after 60 min under UV light.	69

## List of Figures

No.	Figure	Page
(1.1)	Mechanism of photocatalysis in organic degradation processes.	3
(1.2)	Schematic drawing show different crystal structures for TiO <sub>2</sub> (a) rutile (b) anatase (c) brookite.	6
(1.3)	SEM image of commercial TiO <sub>2</sub> showing particles of about 150 nm.	8
(1.4)	UV/Visible spectrum of TiO <sub>2</sub> sample.	8
(1.5)	Crystal structures for both ZnO types A) wurtzite crystal structure, B) zinblende unit cell.	10
(1.6)	XRD pattern of prepared ZnO nanoparticles.	11
(1.7)	Imagaes for ZnO nanoparticles, (a) SEM images of ZnO nanoparticles at different magnifications, and (b) High-resolution transmission electron microscopic (TEM) pictures of ZnO nanoparticles.	12
(1.8)	UV-vis absorbtion spectrum for ZnO nanoparticles.	12
(1.9)	Photoluminescence spectrum for prepared ZnO nanoparticles (Excitation using $\lambda = 320$ nm).	13
(1.10)	The important features of the major destructive methods to purify water.	14
(1.11)	A schematic showing how ZnO semiconductor photocatalyst functions in degrading organic contaminants in water.	18
(1.12)	The commercial manufacture steps of paracetamol.	22
(2.1)	Spectrograms for the a) sun, b) mercury vapor c) halogen lamps.	28
(2.2)	UV-visible spectrum of paracetamol.	32
(2.3)	A calibration curve showing a plot of absorbance vs. paracetamol concentration (ppm). Measurements were conducted in aqueous media, at room temperature.	32
(3.1)	X-ray diffraction pattern for prepared TiO <sub>2</sub> nano-particles.	35
(3.2)	X-ray diffraction pattern for commercial TiO <sub>2</sub> rutile.	35
(3.3)	X-ray diffraction pattern for commercial TiO <sub>2</sub> anatase.	36
(3.4)	SEM images for prepared nano-particles of TiO <sub>2</sub> .	38
(3.5)	Photoluminescence spectra measured for TiO <sub>2</sub> : a) commercial anatase sample, b) commercial rutile sample, c) prepared nano-size, excitation wavelength was 226 nm.	39

(3.6)	Solid state electronic absorption spectra measured for TiO <sub>2</sub> a) commercial anatase form, b) commercial rutile form, c) nano-particles powder.	40
(3.7)	Electronic absorption spectra for a) commercial ZnO catalyst, b) ZnO nano-particles, suspension inside water.	41
(3.8)	Photoluminescence spectra measured for a) ZnO commercial, b) ZnO nano-particles, excitation wavelength was 325 nm.	42
(3.9)	X-ray diffraction pattern for the prepared ZnO nano-particles.	43
(3.10)	Literature X-ray diffraction pattern of nano zinc oxide (ZnO) particles.	43
(3.11)	X-ray diffraction pattern for commercial ZnO.	44
(3.12)	SEM images for the prepared ZnO nanoparticles.	45
(3.13)	Effect of contaminant concentration on degradation of paracetamol using the TiO <sub>2</sub> anatase system under UV light and neutral conditions: a) 15 ppm, b) 30 ppm, c) 45 ppm.	46
(3.14)	Effect of contaminant concentration on degradation of paracetamol using the TiO <sub>2</sub> rutile system under UV light and neutral conditions: a) 15 ppm, b) 30 ppm, c) 45 ppm.	48
(3.15)	Effect of concentration of TiO <sub>2</sub> in anatase form on photodegradation of paracetamol by varying its amount: a) 0.05g, b) 0.1g, c) 0.2g under UV light and neutral conditions.	49
(3.16)	The photodegradation rate of paracetamol by varying the concentration of TiO <sub>2</sub> catalyst in the rutile form: a) 0.05g, b) 0.1g, c) 0.2g under UV light and neutral conditions.	50
(3.17)	Effect of pH on reaction rates of paracetamol degradation with UV-light lamp using TiO <sub>2</sub> rutile: a) Neutral, b) Acidic, c) Basic.	51
(3.18)	Effect of pH on reaction rates of paracetamol degradation with UV-light lamp using TiO <sub>2</sub> anatase: a) Neutral, b) Acidic, c) Basic.	52
(3.19)	Effect of initial paracetamol concentration on overall rate of degradation under UV light and neutral conditions using ZnO commercial: a) 15 ppm, b) 30 ppm, c) 45 ppm.	53
(3.20)	Effect of ZnO catalyst concentration on degradation of paracetamol under UV light and neutral conditions: a) 0.05 g, b) 0.1 g, c) 0.2 g.	55

(3.21)	Photodegradation of neutral 30 ppm paracetamol solution under direct solar light using TiO <sub>2</sub> nano-particles and TiO <sub>2</sub> commercial: a) TiO <sub>2</sub> nano-particle, b) TiO <sub>2</sub> R, c) TiO <sub>2</sub> A.	56
(3.22)	ZnO nano-particles and commercial in photodegradation of neutral paracetamol solution (30 ppm) under direct sun light: a) ZnO nano-particle, b) ZnO commercial.	57
(3.23)	TiO <sub>2</sub> and ZnO nano-catalysts in photodegradation of neutral 30 ppm paracetamol solution: a) TiO <sub>2</sub> nano-particle, b) ZnO nano-particle.	59
(3.24)	Effect of initial paracetamol concentration on overall reaction rate of degradation for different catalyst systems (a: AC/TiO <sub>2</sub> R, b: AC/TiO <sub>2</sub> A, c: AC/ZnO) under UV light and neutral conditions: i) 60 ppm, ii) 70 ppm, iii) 85 ppm, iv) 100 ppm.	62
(3.25)	Paracetamol degradation reaction using AC/TiO <sub>2</sub> rutile system at different pH values in the range (3.5- 10) under UV light: a) Neutral, b) Acidic, c) Basic.	64
(3.26)	Paracetamol degradation reaction using AC/TiO <sub>2</sub> anatase system using different pH values under UV light: a) Neutral, b) Acidic, c) Basic.	65
(3.27)	Effect of pH on reaction rate of paracetamol degradation with UV light lamp using AC/ZnO (commercial) catalyst: a) Neutral, b) Acidic, c) Basic.	66
(3.28)	AC/TiO <sub>2</sub> and AC/ZnO nano-particles for photodegradation of neutral 60 ppm paracetamol solution (100 mL) under direct sun light: a) AC/ZnO nano-particle, b) AC/TiO <sub>2</sub> nano-particle.	67
(3.29)	AC/TiO <sub>2</sub> forms (anatase and rutile) for photodegradation of acidic 70 ppm paracetamol solution (100 mL) under UV light: a) AC/TiO <sub>2</sub> rutile, b) AC/TiO <sub>2</sub> anatase.	68

## List of Abbreviations

<b>Symbol</b>	<b>Abbreviation</b>
<b>UV</b>	Ultraviolet light
<b>AOP</b>	Advanced oxidation processes
<b>AC</b>	Activated carbon
<b>VB</b>	Valence band
<b>CB</b>	Conduction band
<b>PL</b>	Photoluminescence
<b>SEM</b>	Scanning electron microscopy
<b>XRD</b>	X-Ray diffraction
<b>TEM</b>	Transmission electron microscopy
<b>FWHM</b>	Full width at half maximum
<b>eV</b>	Electron volt
<b>e<sup>-</sup></b>	Electron
<b>h<sup>+</sup></b>	Hole
<b>E<sub>bg</sub></b>	Energy band gap
<b>R</b>	Rutile
<b>A</b>	Anatase
<b>λ</b>	Wavelength
<b>h<sub>vb</sub><sup>+</sup></b>	Photohole
<b>e<sub>cb</sub><sup>-</sup></b>	Photoelectron
<b>&gt;TiOH:TiO<sub>2</sub></b>	Surface group
<b>Red</b>	Reductant
<b>Ox</b>	Oxidant
<b>M</b>	Contaminant molecule
<b>S</b>	Semiconductor surface
<b>M<sub>ads</sub></b>	Adsorbed molecule
<b>ppm</b>	Part per million
<b>T.N.</b>	Turnover number
<b>T.F.</b>	Turnover frequency
<b>Q.Y.</b>	Quantum yield

**TiO<sub>2</sub> and ZnO photocatalysts for degradation of widespread pharmaceutical wastes: Effect of particle size and support****By****Shadya Ahmed Hussni Hejjawi****Supervisors****Prof. Hikmat Hilal****Dr. Ahed Zyoud****Abstract**

In our search for safe and economical techniques to eliminate pharmaceutical wastes, in water, this work has been conducted. Solar energy can be used in degrading these compounds in the presence of suitable photo-catalysts. TiO<sub>2</sub> and ZnO were examined as photo-catalysts in degradation of pharmaceutical waste of a well-known compound, namely paracetamol. Both catalysts were used, each in different phase commercial (micro-sized particles) and synthetic (nano-sized particles). Commercial and prepared catalyst powders, of TiO<sub>2</sub> and ZnO, were characterized by XRD, SEM, photoluminescence and electronic absorption spectra before being used as photocatalysts. The commercial phase catalysts were studied using UV light, while prepared catalyst phases were used under direct solar light. On the other hand, both catalyst systems (commercial and synthetic) were supported on activated carbon surface. The photodegradation reaction of paracetamol was investigated under different reaction conditions, such as contaminant concentration, catalyst concentration and pH. Under neutral conditions, the commercial TiO<sub>2</sub> (both anatase and rutile) slowly catalyzed the photo-degradation of paracetamol under the used UV lamp radiation. Under direct sun light, the commercial anatase TiO<sub>2</sub> showed higher efficiency than the synthetic TiO<sub>2</sub>. Rutile TiO<sub>2</sub>

showed efficiency with UV only under higher pH values. Different kinetic parameters were studied.

The commercial ZnO showed sound efficiency under UV light and direct sun light. Under direct solar light, synthetic ZnO showed lower efficiency than the commercial ZnO system. Effects of different reaction conditions onto commercial ZnO catalyst were studied.

Depending on reaction conditions, the commercial TiO<sub>2</sub> in anatase form was mainly more efficient than the commercial ZnO in paracetamol photodegradation under UV. Under direct solar light, the commercial ZnO was more efficient than commercial TiO<sub>2</sub> in anatase form. Under direct solar light, synthetic ZnO showed more efficiency than synthetic TiO<sub>2</sub>.

Supporting commercial TiO<sub>2</sub> onto activated carbon surfaces enhanced its catalytic activity under UV. The supported anatase phase showed higher efficiency than the rutile counterpart. Supporting synthetic TiO<sub>2</sub> onto activated carbon surfaces also enhanced its catalytic activity under direct solar light. The supported synthetic TiO<sub>2</sub> was more effective than supported commercial TiO<sub>2</sub> under direct solar light. Supporting commercial ZnO increased its efficiency under UV radiation, whereas supporting synthetic ZnO increased the efficiency under direct solar light.

The supported commercial ZnO was more efficient than the supported commercial anatase TiO<sub>2</sub> under UV. The supported commercial anatase TiO<sub>2</sub> and the supported commercial ZnO catalyst systems showed different behaviors when paracetamol concentration and pH were varied. The supported synthetic ZnO was more effective than the supported synthetic TiO<sub>2</sub> under direct sun light. The study shows that supporting TiO<sub>2</sub> and ZnO systems has the advantage of increasing their catalytic efficiencies, and making their separation easier.

# Chapter 1

## Introduction

Many human activities have the potential to cause pollution. With respect to water quality, pollutants may enter surface or groundwater directly, run-off the surrounding catchment, or be deposited from the atmosphere. They may enter a system through a point source discharge (e.g. discharges through pipes), or may be more dispersed and diffused (e.g. agricultural run-off). However, pollution from both point and diffuse sources may be exacerbated by a number of factors such as weather [1].

Water pollution is "*the introduction into fresh or ocean waters of chemical, physical, or biological materials that degrade the quality of the water and affect the organisms living on it. This process ranges from simple addition of dissolved or suspended solids to discharge of the most insidious and persistent toxic pollutants (such as pesticides, heavy metals, and nondegradable, bioaccumulative, chemical compounds)*" [2].

Water purification is necessary to reduce the concentration of contaminants including suspended particles, parasites, bacteria, algae, viruses, fungi, in addition to a range of dissolved and particulate materials. Water quality cannot simply be judged by visual examination. Simple procedures such as boiling or the use of a household activated carbon filters are not sufficient for treating all possible contaminants that may be present in water from an unknown source [3].

Many water purification methods followed in recent years, including physical, biological and chemical processes, are known. Chemical processes have been employed to remove low levels of toxic compounds. They may involve chemicals of powerful oxidizing agents such as ozone or hydrogen peroxide. Such processes involve highly oxidizing hydroxyl radicals, which may degrade contaminants. Some chemical processes involve oxidizing chemicals alone, while others combine such chemicals with UV-visible light irradiation [4].

### **1.1 Ultraviolet purification**

Ultraviolet (UV) light is electromagnetic radiation with a wavelength shorter than that of visible light, but longer than X-rays, in the range 10 nm to 400 nm, and energies from 124 to 3.0 eV. Ultraviolet light (UV) alone may be used to inactivate cysts, in low turbidity water. It can cause chemical reactions, and can cause many substances to glow or fluoresce. Most ultraviolet is classified as non-ionizing radiation. The higher energies of the ultraviolet spectrum from wavelengths about 10 nm to 120 nm ('extreme' ultraviolet) are ionizing, but this type of ultraviolet in sunlight is blocked by normal oxygen in air, and does not reach the ground [5].

### **1.2 Semiconductor photocatalysis**

Another possible strategy to purify water is using semiconducting material photocatalysts. Therefore, it is necessary to give an account on such classes of photocatalyst systems.

A semiconducting material has electrical conductivity intermediate in magnitude between that of a conductor and an insulator. This means conductivity roughly in the range of  $10^{-2}$  to  $10^4$  siemens per centimeter. Semiconductors are the foundation of modern electronics, including radio, computer ....etc. [6].

Many reactions can be promoted by light-activated solids which are not consumed in the over all reaction. Such solids are often referred to as photocatalysis, or photosensitizers, and are invariably semiconductors. Probably the most well-established example of semiconductor photocatalysts is paint chalking, which involves the photodegradation of organic polymer part of the paint sensitized by the semiconductor pigment, usually  $\text{TiO}_2$ . Figure (1.1) explains how semiconducting photocatalysts function in degrading organic contaminants [7, 8].

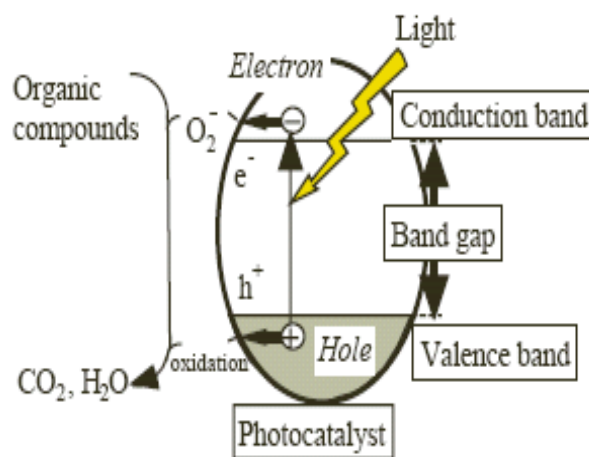
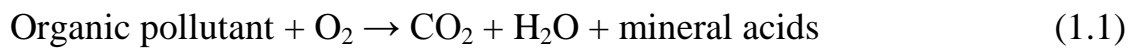


**Figure (1.1):** Mechanism of photocatalysis in organic degradation processes [7].

In recent years, there has been a growing interest in the use of semiconductors as photocatalysts for complete oxidative mineralization of pollutants by oxygen. In water purification by semiconductor photocatalysis, the over all process can be summarized by the following reaction:



In a solid, the electrons occupy energy bands as a consequence of the extended bonding network. In a semiconductor the highest occupied and lowest unoccupied energy bands are separated by a band gap,  $E_{\text{bg}}$ , a region with no energy levels. Activation of a semiconductor photocatalyst is achieved through the absorption of a photon of ultra-band gap energy which results in the promotion of an electron,  $e^-$ , to the conduction band (CB), and a hole,  $h^+$ , remaining in the valance band (VB). For a photocatalyst to be efficient, the different interfacial electron transfer processes, involving  $e^-$  and  $h^+$  reacting with adsorbed species must compete effectively with the major deactivation route of electron-hole recombination [9].

Various metal oxides (i.e.  $\text{TiO}_2$ ,  $\text{ZnO}$ ,  $\text{MoO}_3$ ,  $\text{CeO}_2$ ,  $\text{ZrO}_2$ ,  $\text{WO}_3$ ,  $\text{Fe}_2\text{O}_3$ , and  $\text{SnO}_2$ ) and metal chalcogenides (i.e.  $\text{ZnS}$ ,  $\text{CdS}$ ,  $\text{CdSe}$ ,  $\text{WS}_2$  and  $\text{MoS}_2$ ) are used as semiconductor photocatalysts.  $\text{TiO}_2$  and  $\text{ZnO}$  are most commonly used photocatalysts as they have the advantages of being cheap, efficient, safe, and environmentally friendly [7- 9].

### 1.2.1 Titanium dioxide

Titanium dioxide, also known as titanium (IV) oxide or titania, is the naturally occurring oxide of titanium, with the chemical formula  $\text{TiO}_2$ . When used as a pigment, it is called titanium white, Pigment White 6. Generally it comes in two different forms, rutile (R) and anatase (A). It has a wide range of applications, from paint to sunscreen to food coloring. When used as a food coloring, it has E number E171 [10]. The most common form of  $\text{TiO}_2$  is rutile [11] which is also the equilibrium phase at all temperatures [12]. The metastable anatase and brookite phases both convert to rutile upon heating [13].  $\text{TiO}_2$  is also an effective opacifier in powder form, where it is employed as a pigment to provide whiteness and opacity to products such as paints, coatings, plastics, papers, inks, foods, medicines (i.e. pills and tablets) as well as most toothpastes [10]. Titanium dioxide, particularly in the anatase form, is a photocatalyst under ultraviolet (UV) light. The photocatalytic splitting of water on  $\text{TiO}_2$  electrodes was discovered in 1972 by Fujishima and Honda. The process on the surface of the titanium dioxide was called the **Honda-Fujishima effect** [8, 14]. Thus  $\text{TiO}_2$  exhibits three distinct polymorphs (anatase, rutile and brookite) of which only anatase is functional as a photocatalyst. Anatase is a typical n-type semiconductor and requires about 3.20 eV to be an electrical conductor. Photons with wavelengths shorter than 380 nm are sufficient in energy to excite electrons from the valence band to the conduction band of

this material [15]. Figure (1.2) shows the crystal structures for the three TiO<sub>2</sub> types.

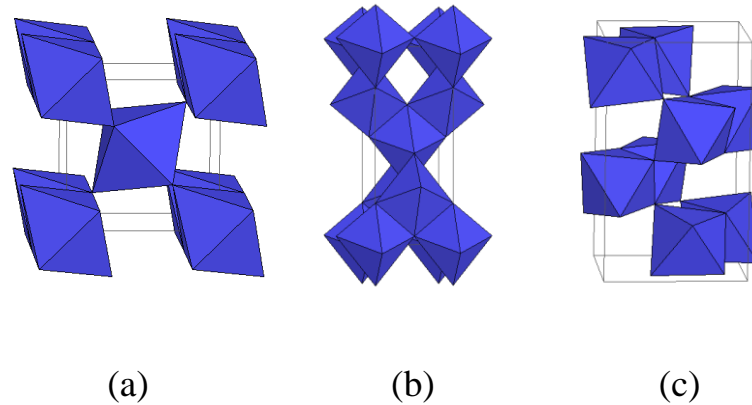


**Figure (1.2):** Schematic drawing show different crystal structures for TiO<sub>2</sub> (a) rutile (b) anatase (c) brookite.

Most TiO<sub>2</sub> photocatalytic studies used pure anatase form, pure rutile form or a mixture of both forms. Brookite is rarely used in photo-catalytic studies, because it is unstable form and is very difficult to prepare [16]. Anatase form of TiO<sub>2</sub> is more widely used than rutile form in photo-catalytic activity. That is because, the excess charge carriers in the rutile tend to have higher recombination rates than in anatase [17]. Anatase has been used as the semiconductor photocatalyst in research. This is due to its non-toxicity, high photo-activity, mechanical stability, low cost and favorable overlap with the ultra-violet portion of the solar spectrum. Although rutile TiO<sub>2</sub> exhibits an energy band gap of 3.02 eV it remains photocatalytically inactive due to intrinsic crystal defects attributed to a quick charge recombination [18]. In 1995 Fujishima and his group discovered the superhydrophilicity phenomenon for titanium dioxide

coated glass exposed to sun light [8]. This resulted in the development of self-cleaning glass and anti-fogging coatings. A photocatalytic cement that uses titanium dioxide as a primary component, produced by Italcementi Group, was included in Time's Top 50 Inventions of 2008 [19].  $\text{TiO}_2$  offers great potential as an industrial technology for detoxification or remediation of wastewater due to several factors [20]:

1. The process occurs under ambient conditions very slowly, direct UV light exposure increases the rate of reaction.
2. The formation of photocyclized intermediate products, unlike direct photolysis techniques, is avoided.
3. Oxidation of the substrates to  $\text{CO}_2$  is complete [21].
4. The photocatalyst is inexpensive and has a high turnover.
5.  $\text{TiO}_2$  can be supported on suitable reactor substrates.

Commercial  $\text{TiO}_2$  powders are commonly purchased as micro-scale particles, as observed in Figure (1.3) [22].

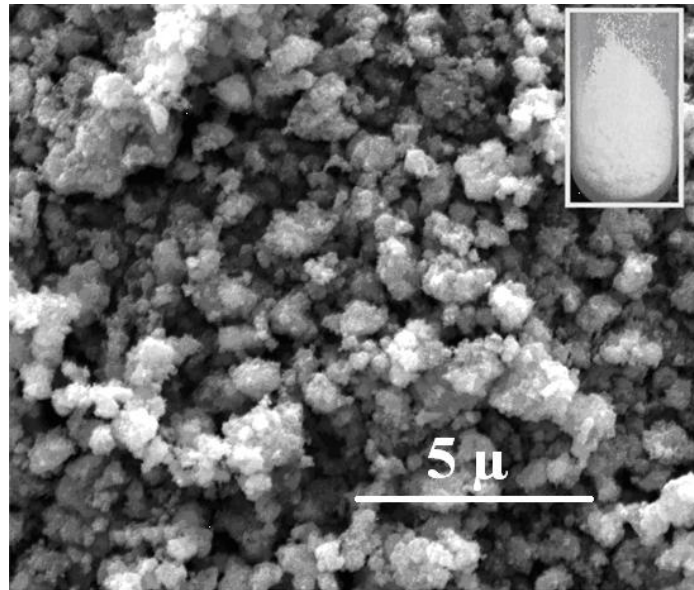


**Figure (1.3):** SEM image of commercial TiO<sub>2</sub> showing particles of about 150 nm [22].

UV/Visible spectra are commonly used to characterize TiO<sub>2</sub> powders.

Figure (1.4) shows that the absorption edge for TiO<sub>2</sub> is 388 nm [23].

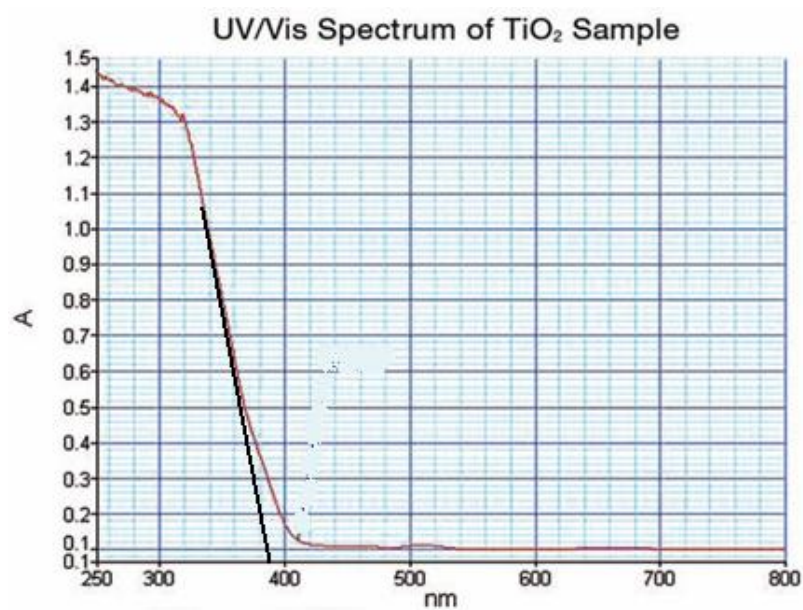


**Figure (1.4):** UV/Visible spectrum of TiO<sub>2</sub> sample [23].

### 1.2.2 Zinc oxide

Zinc oxide is an inorganic compound with the formula ZnO. It is a white powder that is insoluble in water, and widely used as an additive in numerous materials and products including plastics, ceramics, glass, cement, lubricants [24], paints, ointments, adhesives, sealants, pigments, foods (source of Zn nutrient), batteries, ferrites, fire retardants, and first aid tapes. It occurs naturally as the mineral zincite but most zinc oxide is produced synthetically [25]. ZnO is a wide-band gap 3.37 eV (or 375 nm) at room temperature semiconductor. It has several favorable properties, including good transparency, high electron mobility, and strong room-temperature luminescence. Those properties are used in emerging applications for transparent electrodes in liquid crystal displays, in energy-saving or heat-protecting windows and in electronics as thin-film transistors and light-emitting diodes. Zinc oxide is an amphoteric oxide that is soluble in most acids, such as hydrochloric acid [26, 27]:



Bases also degrade the solid to give soluble zincates:



Zinc oxide crystallizes in two main forms, hexagonal wurtzite and cubic zinc blende. The wurtzite structure is most stable at ambient conditions and thus most common. The zinc blende form can be stabilized by growing

ZnO on substrates with cubic lattice structure. In both cases, the zinc and oxide centers are tetrahedral, the most characteristic geometry for Zn(II). In addition to the wurtzite and zinc blende polymorphs, ZnO can be crystallized in the rock-salt motif at relatively high pressures about 10 GPa [28]. Figure (1.5) summarizes crystal structures for both ZnO types.

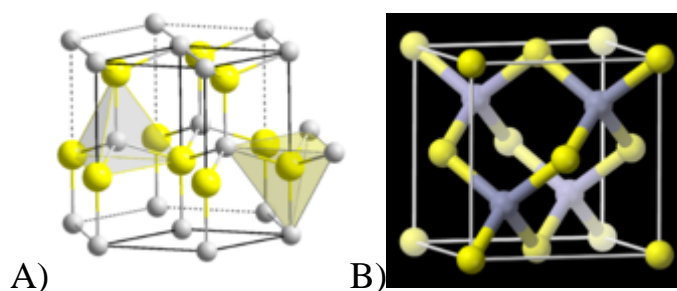


**Figure (1.5):** Crystal structures for both ZnO types. A) wurtzite crystal structure, B) zincblende unit cell [28].

ZnO nanoparticles have been synthesized by precipitation method from zinc nitrate. The powder was characterized by X-ray diffraction (XRD), scanning electron microscopy (SEM), transmission electron microscopy (TEM), selected-area electron diffraction, UV-vis optical absorption and photoluminescence spectroscopy (PL) analyses [29]. XRD patterns showed that ZnO nanoparticles have hexagonal unit cell structure (wurtzite) [30, 31], as shown in Figure (1.6). SEM and TEM pictures reveal the morphology and particle size of prepared ZnO nanoparticles [31, 32], as shown in Figure (1.7a, b). The UV-vis absorption spectrum shows an absorption band at 355 nm due to ZnO nanoparticles [33], as presented in Figure (1.8). The photoluminescence spectrum exhibits two emission peaks, one at 392 nm corresponding to band gap excitonic emission and

another located at 520 nm due to the presence of singly ionized oxygen vacancies [34- 39]. Figure (1.9) summarizes photoluminescence spectra for ZnO nanoparticles. The synthesis method has potential for application in manufacturing units due to easy processing and more economical reagents.

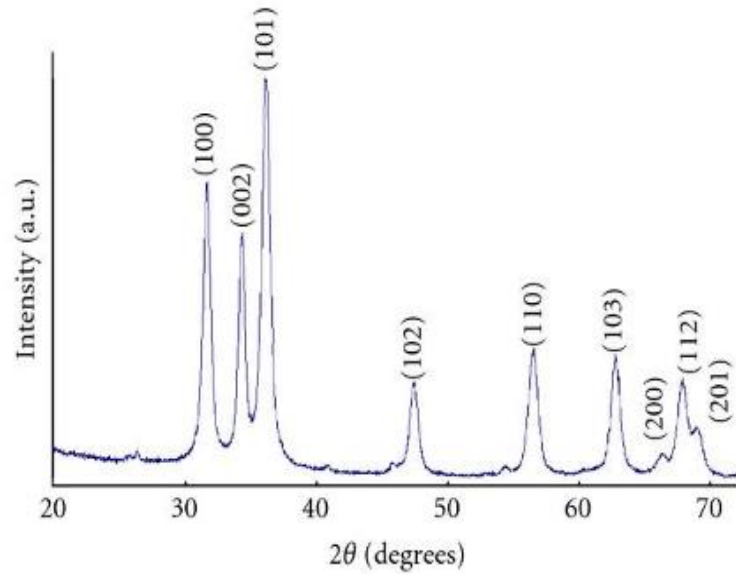
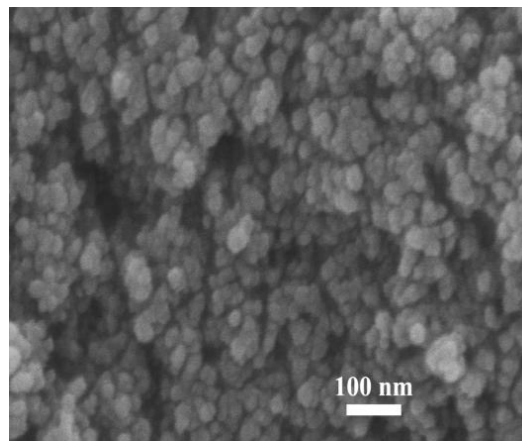
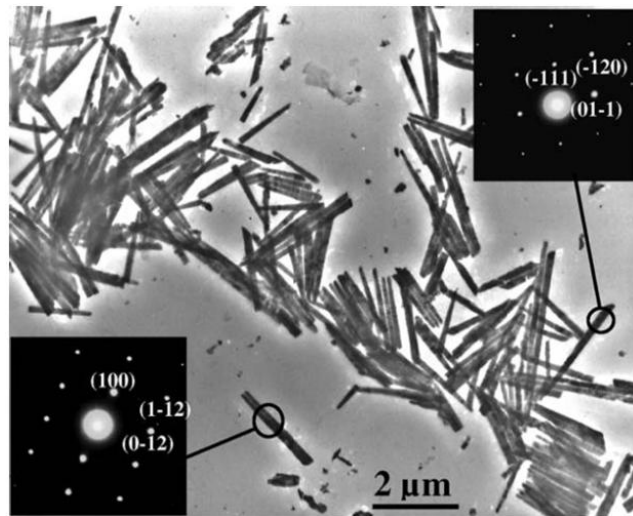


**Figure (1.6):** XRD pattern of prepared ZnO nanoparticles [30, 31].



(a)



(b)

**Figure (1.7):** Images for ZnO nanoparticles, (a) SEM images of ZnO nanoparticles at different magnifications, and (b) High-resolution transmission electron microscopic (TEM) pictures of ZnO nanoparticles [31, 32].

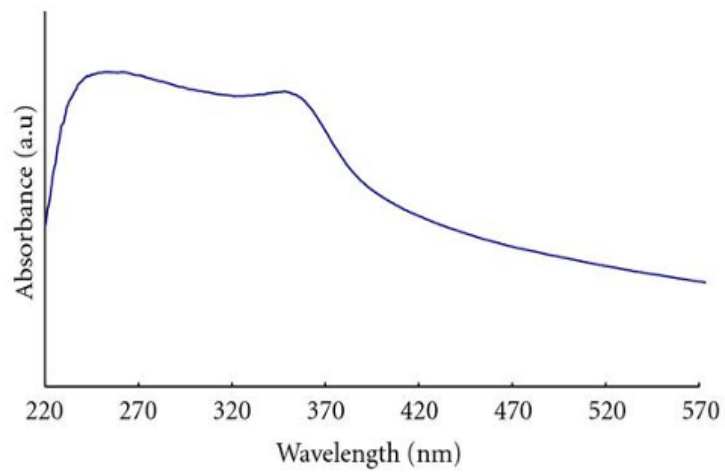


**Figure (1.8):** UV-vis absorption spectrum for ZnO nanoparticles [33].

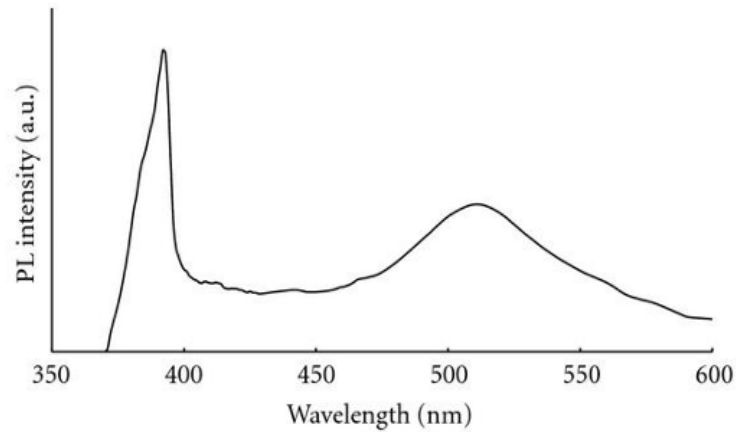


**Figure (1.9):** Photoluminescence spectrum for prepared ZnO nanoparticles (Excitation using  $\lambda = 320$  nm) [34- 39].

### 1.3 Mechanism of photodegradation

Photocatalytic degradation of contaminants is being widely studied. Excitation of electrons from valence band to conduction band is necessary in these processes. Photocatalytic degradation has the advantage of complete oxidation of organic pollutants, as shown in equation (1.1). Figure (1.10) summarizes some destructive methods that are currently used to purify water, and compares them with those of semiconductor photocatalysis. Therefore, research is still needed to improve such technique [40].

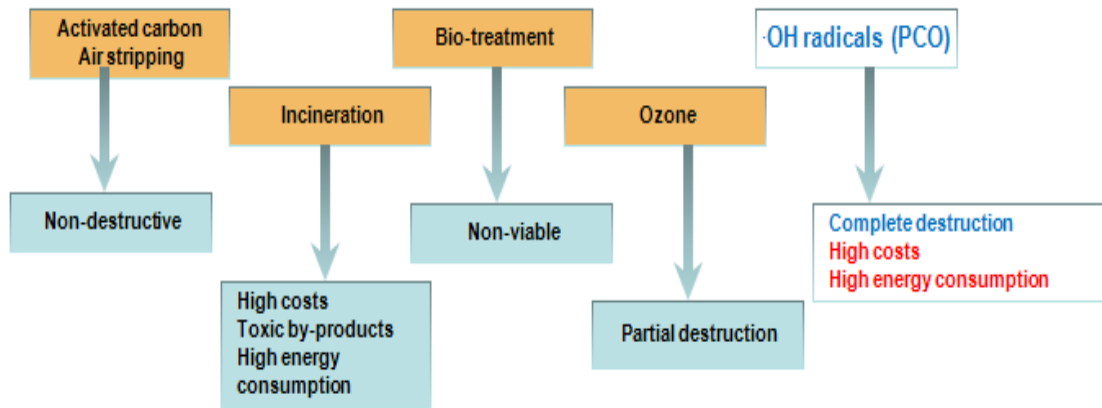


**Figure (1.10):** The important features of the major destructive methods to purify water [40].

### 1.3.1 TiO<sub>2</sub> photocatalytic reaction mechanism

Based on laser flash photolysis measurements, general mechanism and time characteristics of various steps involved in the heterogeneous photocatalysis at TiO<sub>2</sub> have been suggested by Hoffmann [41]. Steps and their characteristic times are listed in Table (1.1).

**Table 1.1: A general mechanism of semiconductor photocatalysis at TiO<sub>2</sub> [41].**

Primary process	Characteristic times
Charge carrier generation	
$\text{TiO}_2 + h\nu \rightarrow h_{\text{vb}}^+ + e_{\text{cb}}^-$	Fast (fs)
Charge-carrier trapping	
$h_{\text{vb}}^+ + >\text{Ti}^{\text{IV}}\text{OH} \rightarrow \{>\text{Ti}^{\text{IV}}\text{OH}^\bullet\}^+$	Fast(10ns)
$e_{\text{cb}}^- + >\text{Ti}^{\text{IV}}\text{OH} \rightarrow \{>\text{Ti}^{\text{III}}\text{OH}\}$	Shallow trap(100ps) dynamic equilibrium
$e_{\text{cb}}^- + >\text{Ti}^{\text{IV}} \rightarrow >\text{Ti}^{\text{III}}$	Deep trap (10ns) irreversible
Charge-carrier recombination	
$e_{\text{cb}}^- + \{>\text{Ti}^{\text{IV}}\text{OH}^\bullet\}^+ \rightarrow >\text{Ti}^{\text{IV}}\text{OH}$	Slow (100ns)
$h_{\text{vb}}^+ + \{>\text{Ti}^{\text{III}}\text{OH}\} \rightarrow >\text{Ti}^{\text{IV}}\text{OH}$	Fast (10ns)
Interfacial charge transfer	
$\{>\text{Ti}^{\text{IV}}\text{OH}^\bullet\}^+ + \text{Red} \rightarrow >\text{Ti}^{\text{IV}}\text{OH} + \text{Red}^{\bullet+}$	Slow (100ns)
$\{>\text{Ti}^{\text{III}}\text{OH}\} + \text{Ox} \rightarrow >\text{Ti}^{\text{IV}}\text{OH} + \text{Ox}^{\bullet-}$	Very slow (ms)

*Note:*  $h_{\text{vb}}^+$ : photoholes,  $e_{\text{cb}}^-$ : photoelectrons,  $>\text{TiOH}$ : TiO<sub>2</sub> surface group, Red: Reductant, Ox: Oxidant.

According to this general mechanism, the overall photo-catalytic quantum efficiency is controlled by:

- 1) competition between the recombination of the charge carriers ( $e^-$ ,  $h^+$ ) and trapping of charge carriers
- 2) competition between recombination of trapped charge carriers and interfacial charge transfer (capture of charge carriers).

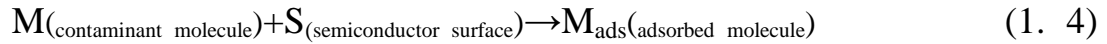
The suggested mechanisms for contaminant degradation by photo-excited semiconductors are divided into the following categories [42]:

A) Adsorption: for a catalytic reaction to occur, at least one and frequently all of the reactants must become attached to the surface (adsorption). Adsorption takes place by physical adsorption or chemisorption. Literature referred UV/TiO<sub>2</sub> photo-degradation process to Langmuir adsorption model, which postulated that:

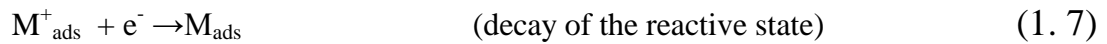
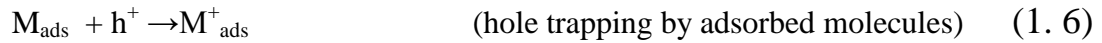
1. All catalyst surface sites are identical and have same adsorption activity.
2. There is no interaction between adsorbed molecules.
3. All same molecules adsorb by same mechanism, and adsorbed complexes have same structures.
4. The extent of adsorption is less than one complete monomolecular layer on the surface.

B) Direct Photo-Catalytic Pathway:

The mechanism of Langmuir-Hinshelwood photo-catalytic reaction, which occurs at a photo-chemically active surface after photo-excitation of the catalyst and producing electrons- holes is described as follows:



(adsorption/desorption Langmuir equilibrium)



The photo-excitation of the catalyst produces electrons and holes. The carrier (hole) may be trapped by the adsorbed molecule to form a reactive radical state, whose decay occurs through recombination with an electron. The chemical reaction yields the products and regenerates the original state of the catalyst surface(S).

### 1.3.2 ZnO photocatalytic reaction mechanism

UV or visible light is used to create electron hole pairs in the semiconductor, by exciting electrons from valence band to conduction band. The electrons then react with oxygen in the sample to form  $O_2^-$  whereas the holes react with surface hydroxyl groups to form OH $\cdot$  radicals. The radical species then react with organic molecule and oxidize them to mineral species such as  $CO_2$ ,  $H_2O$ , and possibly other compounds. These

processes are summarized in Figure (1.11) as shown below[43].

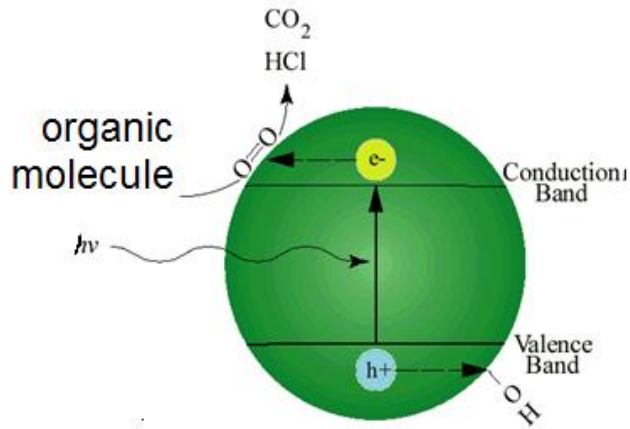
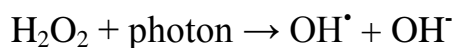
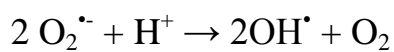
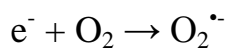
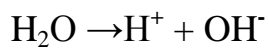


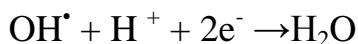
**Figure (1.11):** A schematic showing how ZnO semiconductor photocatalyst functions in degrading organic contaminants in water [43].

The basic reactions of the above-mentioned process are as follows [44]:





And the termination reactions are:



## 1.4 Reaction parameters studied

Several photo-catalytic chemical and physical parameters were studied such as: presence of oxygen, pH, initial contaminant concentration, catalyst amount, agitation rate, temperature, light wavelength and light intensity [45, 46]. Herrmann [47] summarized effects of these factors via plots of rates versus parameters involved.

## 1.5 Examples of contaminants studied

A number of chemical contaminants have been identified in water. These contaminants reach water supplies from various sources, including municipal and industrial discharges, urban and rural run-off, natural geological formations, drinking water distribution materials and the drinking water treatment process [48]. Hydroxyl and other oxygen-containing radicals are known to be present during the degradation of organic water pollutants in illuminated  $\text{TiO}_2$  photocatalyst slurries. It is proposed that the hydroxyl radical,  $\text{OH}^\bullet$ , is the primary oxidant in the photocatalytic system [49].

Photocatalytic decolorization of azo-dye orange II in water has been examined in an external UV light irradiation slurry photoreactor using zinc oxide (ZnO) as a semiconductor photocatalyst [50]. ZnO and activated carbon-supported ZnO were used in photo-degradation of methyl orange and phenazopyridine with direct solar light in aqueous solutions, both naked ZnO and AC/ZnO were highly efficient in mineralizing phenazopyridine, reaching complete removal in about 50 minutes, with AC/ZnO having the higher edge, the photo-degradation reaction was induced by the UV tail of the solar light [51, 52].

Also nano-ZnO has been applied in wastewater treatment by photocatalytic oxidation [53]. Furthermore, ZnO has been used to eliminate hazardous organic compounds, such as phenol, from wastewaters [54]. Silver modified titania photocatalyst [55, 56] and ZnO nanorods [57] were used in bacteria inactivation for drinking water disinfection. CdS sensitized ZnO was used in electrodes in photoelectrochemical Cells [58] and in photocatalytic degradation of organic contaminants [59]. Silver-loaded zinc oxide (Ag/ZnO) photocatalyst was fabricated by chemical deposition [60]. Enhancement of cyanide photocatalytic degradation was done using sol-gel ZnO sensitized with cobalt phthalocyanine [61].

Albagaia, a British environmental technology company, has developed and patented processes which utilize the photocatalysis with titanium dioxide in different states including slurries, but also in various immobilized forms applied as thin films. These technologies have been tested and proven

highly successful in destroying waste disposal products for the pharmaceutical industry and on highly toxic chemical agents. Further, Albagaia has shown the effectiveness of the technology in destroying  $\beta$ -estradiol in low concentrations in drinking water and is now working on the application of the technology to domestic water supplies of various kinds [62]. Benzoic acid, salicylic acid, phenol, 2-chlorophenol, 3-chlorophenol, 4-chlorophenol, nitrobenzene, methanol, ethanol, acetic acid and formic acid in aerated, aqueous suspensions of  $\text{TiO}_2$  were illuminated with near UV light [63].

### **1.6 Photodegradation of paracetamol**

Paracetamol has been in use as an analgesic for home medication for over 30 years and is accepted as a very effective treatment for the relief of pain and fever in adults and children. Paracetamol is also known as acetaminophen. Paracetamol is one of the most common drugs used in the world, and is manufactured in huge quantities. As shown in Figure (1.12) the starting material for the commercial manufacture of paracetamol is phenol, which is nitrated to give a mixture of the *ortho* and *para*-nitrophenol. The *o*-isomer is removed by steam distillation, and the *p*-nitro group reduced to a *p*-amino group. This is then acetylated to give paracetamol [64].

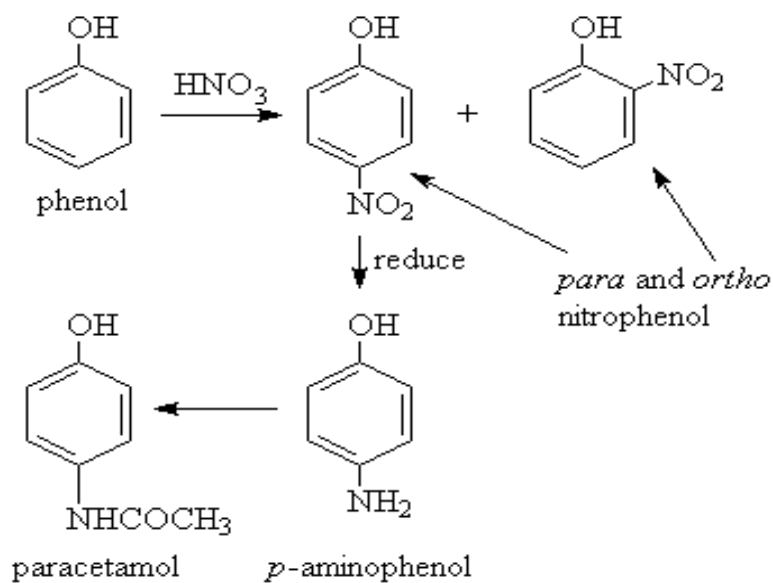


**Figure (1.12):** The commercial manufacture steps of paracetamol [64].

$\beta$ -cyclodextrin grafted titanium dioxide ( $\beta$ -CD/TiO<sub>2</sub>) was synthesized through photo- induced self assembly methods. After being modified by  $\beta$ -CD, the photocatalytic activities of TiO<sub>2</sub> samples increased by 2.3 times the degradation of paracetamol under visible light irradiation. The  $\beta$ -CD worked as sensitizer for TiO<sub>2</sub> in photodegradation of paracetamol [65]. Photocatalytic oxidation of paracetamol (acetaminophen) was investigated by Yang. UVC and UVA regions were used with and without TiO<sub>2</sub> catalyst. Up to 95% of paracetamol was degraded within 80 min using TiO<sub>2</sub>. In the absence of the catalyst, lower degradation rates were observed. Different reaction parameters were studied indicating future potential for TiO<sub>2</sub> catalyst in degrading paracetamol. Despite these advantages, the report did not study effect of direct solar light on paracetamol degradation. Moreover, the report limited its investigation to reaction rate, without

studying catalyst efficiency in terms of turn over number and quantum yield values [66].

## **1.7 General objective of this work**

### **Strategic objective:**

The strategic objective of this work is to find safe and economic processes to dispose pharmaceutical wastes. Paracetamol was chosen as a model pharmaceutical that is widely used. It is intended to purify water from pharmaceutical contaminant (paracetamol) by photodegradation using a safe and economic catalytic system, such as  $\text{TiO}_2$  or  $\text{ZnO}$  semiconducting materials in their powder/nanoparticle form. Using solar energy to completely mineralize the pharmaceutical waste in water is one target of this work.

### **Technical objectives:**

- 1- Preparing nano-sized powder of  $\text{TiO}_2$  and  $\text{ZnO}$  semiconductors. Which use UV light and solar light for paracetamol photodegradation and water purification.
- 2- Characterizing the prepared  $\text{TiO}_2$  and  $\text{ZnO}$  powders using XRD, SEM, UV/Visible spectra, and other techniques.

- 3- Studying effects of pH, contaminant concentration, catalyst concentration and temperature, on catalyst efficiency of these nano-powder materials in paracetamol degradation process.

## **1.8 Novelty of this work**

As discussed above, researchers studied photodegradation of pharmaceutical compounds in general, and paracetamol in particular. However, earlier studies used artificial UV or H<sub>2</sub>O<sub>2</sub> systems only. In this work, we intend to use direct solar light itself (including visible and UV portions). Moreover, we wish to study things that have not been studied before, such as catalyst efficiency. This will be studied by measuring values of turnover number and quantum yield. Factors that enhance efficiency will also be investigated for the first time.

## **1.9 Hypothesis**

It is assumed here that:

- a) Paracetamol is widely spread organic compound and needs to be completely removed from water by photocatalytic degradation.
- b) Using direct solar light in photodegradation studies would have application value for this study.

c)  $\text{TiO}_2$  is known to be not highly effective absorber for UV, whereas  $\text{ZnO}$  is known to absorb UV effectively. Therefore, we assume that  $\text{ZnO}$  will have higher efficiency than  $\text{TiO}_2$  in degrading paracetamol.

This work is intended to test these assumptions at lab scale level.

## Chapter 2

### Materials and Methods

#### 2.1 Materials

##### 2.1.1 Zinc oxide:

Commercial ZnO powder (Catalog no. 205532 with coagulate particle size of less than 5  $\mu\text{m}$ ) was purchased from Sigma Aldrich Co. and used as the photo-catalyst for water purification.  $\text{ZnCl}_2$  that was purchased from Sigma Co. and NaOH from Frutarom Co. were used for ZnO nanoparticle synthesis that was used as naked ZnO photocatalysts. ZnO with two different particles size ranges were used in the photodegradation experiments to study the effect of particle size on the photocatalytic activity in visible light, and were characterized by electronic absorption spectra, XRD and photoluminescence spectra as discussed below.

##### 2.1.2 Titanium dioxide:

$\text{TiO}_2$  powders (anatase and rutile) were purchased from A Johnson Matthey Company, and were characterized by electronic absorption spectra, XRD and photoluminescence spectra as discussed below.  $\text{TiCl}_3$  (12% in HCl solution) was purchased from Riedel-de Haen, as a 20% solution in HCl and NaOH was purchased from Sigma Aldrich Co. were used for  $\text{TiO}_2$  nanoparticle synthesis that was used in photocatalytic purification water.  $\text{TiO}_2$  with two different particle size ranges were used in the

photodegradation experiments to study the effect of particle size on the photocatalytic activity (in visible light).

### **2.1.3 Paracetamol:**

Was kindly donated by Pharmacare Co., Ramallah in pure form.

### **2.1.4 Other chemicals:**

Ethanol, HCl, and activated carbon (AC) was purchased from Aldrich Ltd, in pure form, with measured surface area  $850 \text{ m}^2/\text{g}$  [67].

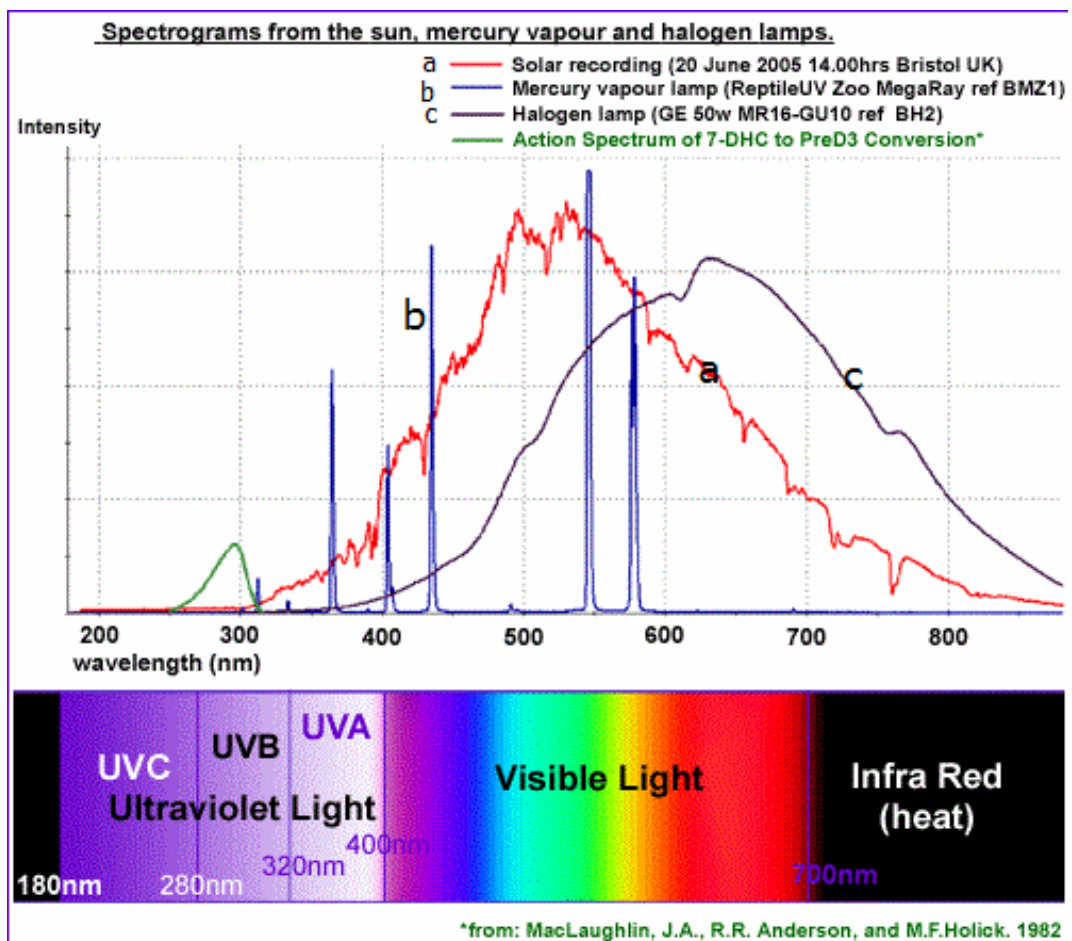
## **2.2 Instruments**

### **2.2.1 UV lamp**

Illumination in the UV range was carried out using an 300 W/230V mercury tungsten (Osram Ultra-Vitalux) lamp housed in a protection box with luminance (6000 lux,  $0.000878477 \text{ W}/\text{cm}^2$ ). Table (2.1) summarizes the features of the used UV lamp [68]. Its spectrum, is shown in Figure (2.1) in comparison with solar light and halogen spot lamp spectra [69]. It should be noted the mercury lamp has only one wavelength at 370 nm, that only exist in UV range, whereas solar light has a range 400- 300 nm in the UV range.

**Table (2.1): UV lamp specifications [68].**

<b>Model</b>	003313
<b>Lifespan (hours)</b>	1000
<b>Rated Wattage (W)</b>	300
<b>Lamp Voltage (V)</b>	230
<b>Light Technical Data</b>	UVA radiated power 315...400 nm, 13.6 W UVB radiated power 280...315 nm, 3.0 W

**Figure (2.1): Spectrograms for the a) sun, b) mercury vapor c) halogen lamps [69].**

### **2.2.2 UV-visible spectrophotometry**

UV/visible electronic absorption spectra were measured on a Shimadzu model TCC-260 spectrophotometer.

### **2.2.3 Lux meter**

A lux meter (Lx-102 light meter) was used to adjust light intensity that reaches the water sample in the photo-catalytic purification experiments.

### **2.2.4 pH meter**

A pH meter was used to adjust the reaction mixture pH as desired. Jenway 3510 pH.

### **2.2.5 Thermometer**

A mercury thermometer was used to measure temperature.

### **2.2.6 Centrifuge**

A Scientific Ltd model 1020 D.E. centrifuge was used for centrifugation purposes.

### **2.2.7 XRD**

Powder diffraction spectra were recorded, at room temperature, on a Bruker D-8 Advance diffractometer with graphite monochromatized Cu  $K_{\alpha}$  radiation ( $\lambda = 1.5406 \text{ \AA}$ ) in Laboratories of the Department of

Chemistry at King Saud University, Riyadh, Saudi Arabia. The data were recorded at  $2\theta$  steps of  $0.02^\circ$  with 1 s/step.

### **2.2.8 SEM**

A Field emission scanning electron microscopy was measured on a Jeol microscope, Model JSM-6700F, using the energy dispersive spectroscopic FE-SEM/EDS technique. SEM measurements were kindly made at ICMCB, University of Bordeaux, France.

## **2.3 Catalyst preparation**

### **2.3.1 Preparation of TiO<sub>2</sub> powder**

In a 250 mL conical flask a 200 mL distilled water and 4.00 g NaOH were placed. Then, TiCl<sub>3</sub> (12% in HCl solution) in a separatory funnel was added drop-wise with continuous stirring until the mixture became white in color. The resulting TiO<sub>2</sub> powder was decanted and washed with water 2- 3 times. We adjusted the pH in the range (3- 6). The powder was then separated from the mixture using a centrifuge (speed 5000 round per minute). The isolated powder was left to dry at room temperature [70].

### **2.3.2 Nanoparticle zinc oxide preparation**

ZnO nanoparticles were prepared by precipitation method. In a typical experiment, a 0.45 M aqueous solution of zinc chloride (ZnCl<sub>2</sub>) was prepared by dissolving 15.231 g in 200 mL distilled water, then the volume

was completed to 250 mL in a 250 mL volumetric flask, also 0.9 M aqueous solution of sodium hydroxide (NaOH) was prepared in distilled water with dissolving 9.000 g NaOH in 200 mL and completed to the volume in 250 mL volumetric flask. Then, NaOH solution was poured into a beaker and heated at about 55°C. The ZnCl<sub>2</sub> solution was added slowly dropwise (in about 40 minute) to the heated solution under high speed stirring (magnetically).

### **2.3.3 AC/catalyst (TiO<sub>2</sub>, ZnO) preparation**

The white catalyst (TiO<sub>2</sub>, ZnO) particle suspension (100 mL distilled water, containing about 32 g catalyst) was mixed with activated carbon (8 g) and stirred for one hour. The mixture was then heating with continuous stirring until the water vaporized. Then, the mixture dried in the oven at 120°C.

### **2.3.4 Stock solution preparation**

Three stock solutions were needed for photocatalytic experiment:

- Contaminant stock solution (1000 ppm) was prepared by dissolving paracetamol (0.10 g) in distilled water. The resulting solution was then diluted to 1.00 L with distilled water, and kept in the dark.
- Dilute solutions (0.05 M) of both HCl and NaOH were prepared for the purpose of controlling the pH in the catalytic reaction mixtures.

## 2.4 Calibration curve

Five known concentrations of paracetamol (0, 5, 10, 25, and 50 ppm) were prepared and measured by UV/visible spectrophotometer at  $\lambda_{\max}$  270 nm as shown in Figure (2.2). A calibration curve of absorbance vs. paracetamol concentration was then constructed, as shown in Figure (2.3).

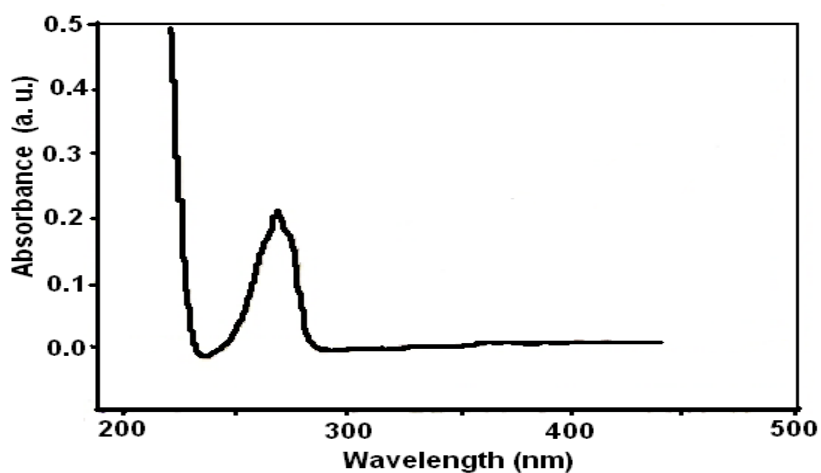


Figure (2.2): UV-visible spectrum of paracetamol.

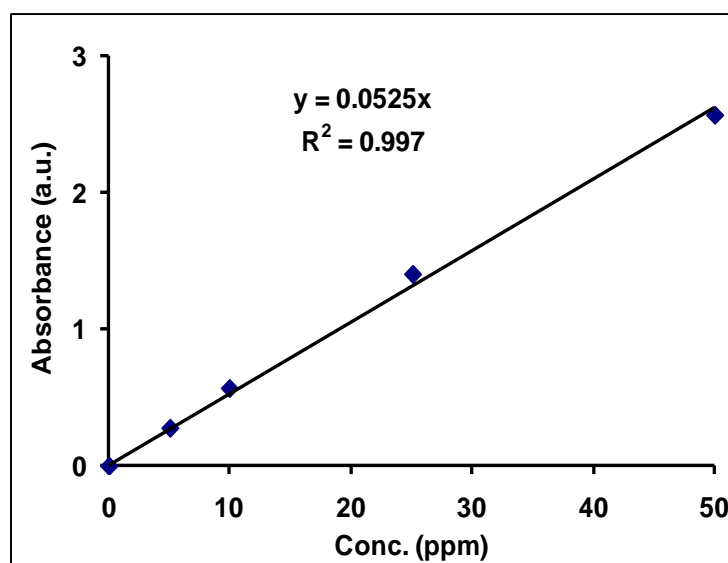


Figure (2.3): A calibration curve showing a plot of absorbance vs. paracetamol concentration (ppm). Measurements were conducted in aqueous media, at room temperature, the maximum wavelength was 270 nm.

## **2.5 Photo-catalytic experiments**

Catalytic experiments were conducted in a 100 mL magnetically stirred thermostated beaker. The out-side walls of the beaker was covered with aluminum foil to reflect back astray radiations. The glass beaker was dipped in controlled temperature water bath. Aqueous reaction mixtures (50 mL) of known concentrations of contaminant and catalyst were placed in the beaker. The pH was controlled as desired by adding drops of NaOH or HCl dilute solutions. The reaction mixture was then with stirring in the dark to allow adsorption of contaminant onto catalyst reach equilibrium. Part of the contaminant adsorbed onto the surface of the catalyst. Direct UV radiation using UV lamp was applied vertically to the photo-catalytic mixture surface. Reaction time was measured the moment irradiation was started. The change in contaminant concentration was measured with time. Small aliquots of solution were syringed out from reaction vessel at different reaction times then centrifuged (5000 round/minute for 5 minutes).Then, a clear solution taken and put in a quartz cell. The absorbance was measured for all solutions at different times using UV/visible spectrophotometry.

## **Chapter 3**

### **Results and Discussion**

#### **3.1 Introduction**

The main goal of this work was to assess the feasibility of using known types of semiconductors, such as  $\text{TiO}_2$  and  $\text{ZnO}$  in light driven photodegradation of organic contaminants. Paracetamol, which is a known medicinally active compound, was used here as a model for future safe degradation of pharmaceutical contaminants in water.  $\text{TiO}_2$  and  $\text{ZnO}$  were used as commercial and synthetic materials to photocatalyze degradation of paracetamol.  $\text{AC/TiO}_2$  and  $\text{AC/ZnO}$  were prepared as well. All these semiconductor materials were characterized and used to study the photodegradation of paracetamol using UV light for commercial (micro-sized) catalyst and direct sun light for synthetic (nano-sized) catalyst. The degradation reaction was conducted under different conditions. Effects of pH, catalyst amount and paracetamol concentration, on reaction rates were all studied.

#### **3.2 Photocatalyst characterization results**

##### **3.2.1 $\text{TiO}_2$ system**

##### **X-ray diffraction (XRD) of $\text{TiO}_2$ :**

XRD patterns were measured for commercial and prepared  $\text{TiO}_2$  powder as shown in Figures (3.1), (3.2) and (3.3).

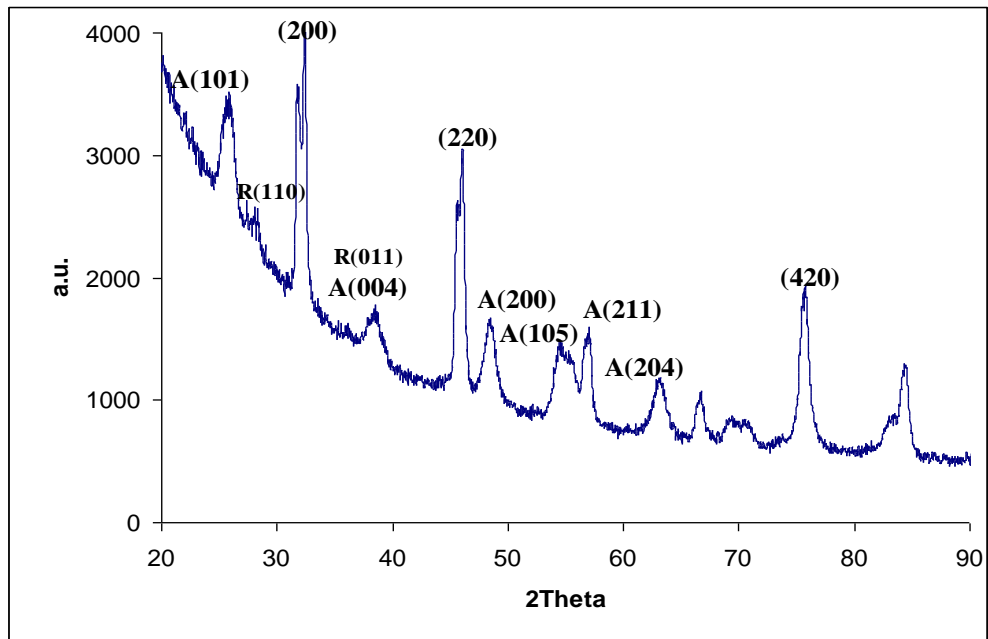


**Figure (3.1):** X-ray diffraction pattern for prepared TiO<sub>2</sub> nano-particles.

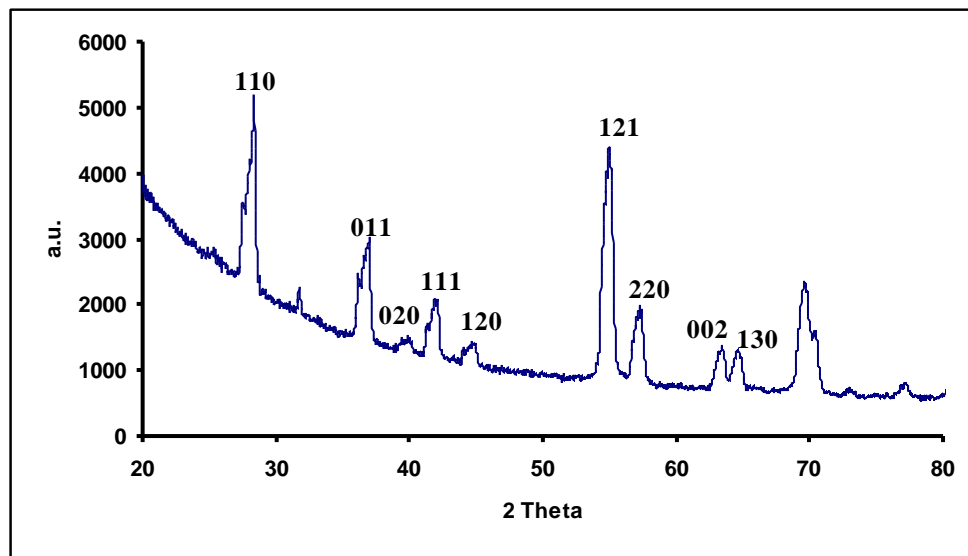


**Figure (3.2):** X-ray diffraction pattern for commercial TiO<sub>2</sub> rutile.

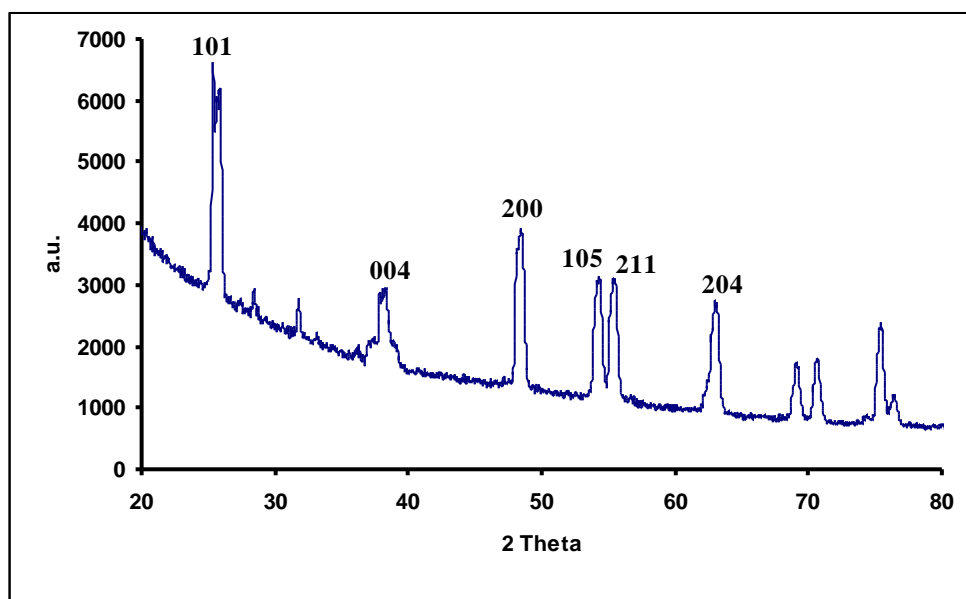


**Figure (3.3):** X-ray diffraction pattern for commercial TiO<sub>2</sub> anatase.

The XRD results were compared to earlier anatase and rutile literature [71, 72]. The XRD patterns showed that the prepared TiO<sub>2</sub> powder was a mixture of anatase and rutile forms. The anatase form was the major component, because the prepared TiO<sub>2</sub> powder was not annealed. Rutile is more stable than anatase, so rutile may be produced by annealing the anatase [12, 13]. However, as we demand the more active form, anatase, we did not wish to convert it to rutile. The three peaks at  $2\theta = 31, 45.5, 75$  belong to NaCl impurity, as evidenced from literature [73]. The impurity peaks appearing in the spectrum belong to resulting NaCl which results by reaction of HCl with TiCl<sub>3</sub> and NaOH. The Scherrer equation [74] was used to calculate the particle diameter,

$$d = K \lambda (\beta \cos\theta)$$

where  $K$  is the shape factor with a typical value of about 0.9,  $\lambda$  is the X-ray wavelength (0.15418 nm),  $\beta$  is the line broadening at half the maximum height (FWHM) in radians, and  $\theta$  is the Bragg angle,  $d$  is the mean size (averaged diameter of crystallites in nm) of the ordered (crystalline) domains [75], which may vary for different particles. Based on two different XRD peaks at (200) and (204) indices, The Scherrer equation shows that the average particle size for the prepared powder is 8.6 nm. The commercial powders showed 12.5 nm sizes for both anatase and rutile phases.

#### **Scanning electron microscopy (SEM) of TiO<sub>2</sub>:**

SEM images were used to investigate the surface morphology of the prepared TiO<sub>2</sub>, as shown in Figure (3.4). The Figure shows that the TiO<sub>2</sub> particle size was in the nano-scale, (~20- 25 nm). However, the SEM images did not show high resolution, which means that the particles are composed of smaller particles of ~8.6 nm in diameter, as found from XRD.

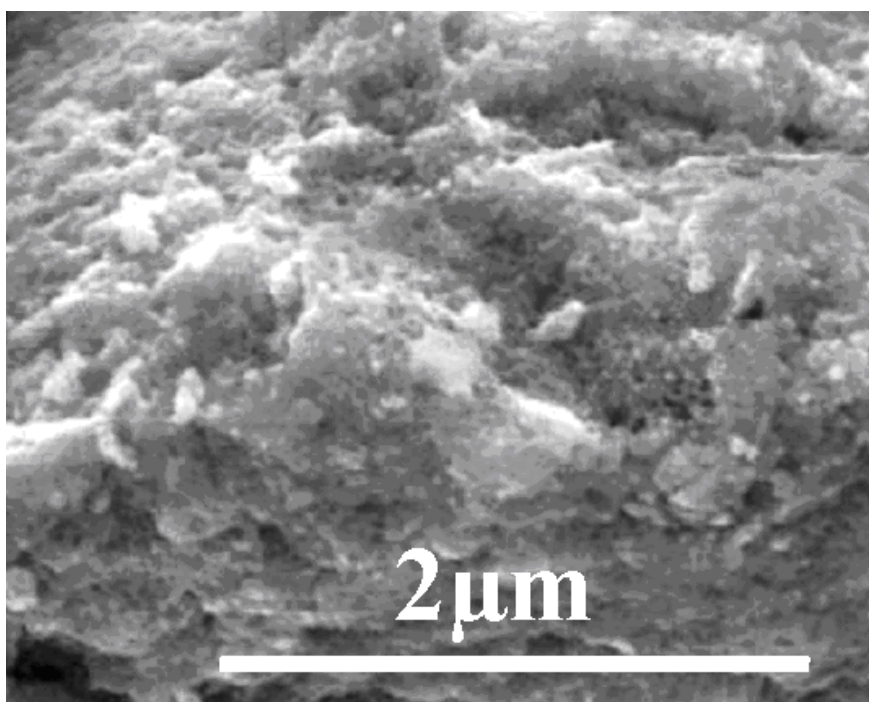


**Figure (3.4):** SEM images for prepared nano-particles of TiO<sub>2</sub>.

### **TiO<sub>2</sub> photoluminescence (PL) spectra:**

Photoluminescence emission spectra were studied for both commercial (rutile and anatase form) and prepared TiO<sub>2</sub> samples. Excitation was conducted using 226 nm wavelength. The observed emission peaks occurred at 366 nm for prepared TiO<sub>2</sub>, 385 nm for commercial anatase TiO<sub>2</sub>, and 378 nm for commercial rutile TiO<sub>2</sub> (Figure 3.5). The emission wavelengths show that the band gap was 3.20 eV. The spectra showed that the commercial powder has larger size than the prepared powder. With smaller particles, there are less atoms, and the band gap should be larger [15]. The emission peaks at 430 nm are due to presence of oxygen vacancies [76].

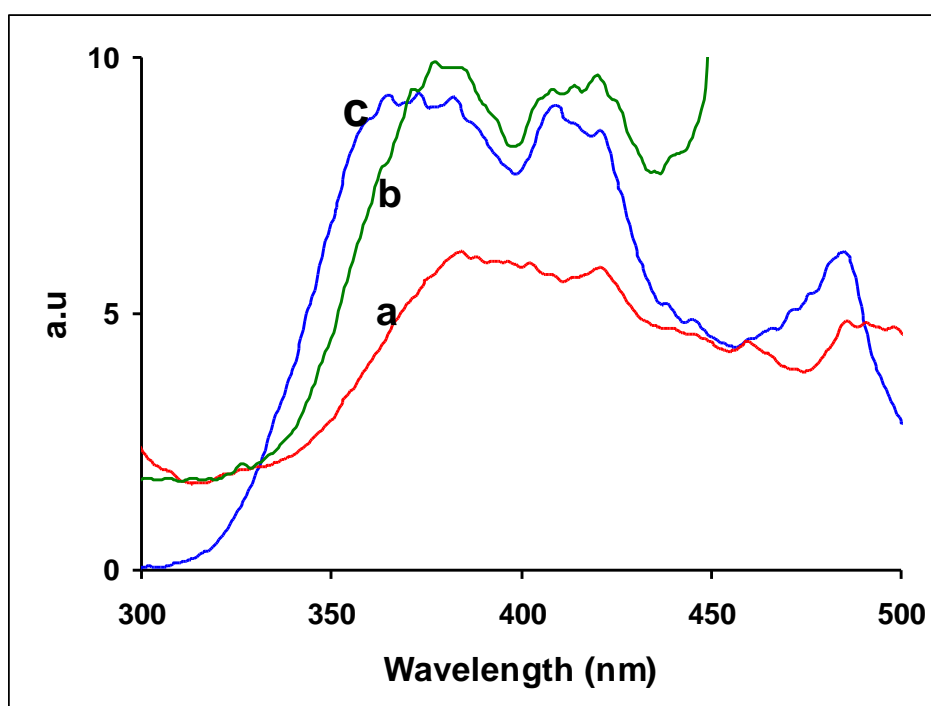


**Figure (3.5):** Photoluminescence spectra measured for TiO<sub>2</sub>: a) commercial anatase sample, b) commercial rutile sample, c) prepared nano-size, excitation wavelength was 226 nm.

### UV- visible spectral characterization of TiO<sub>2</sub>:

Electronic absorption spectra were measured for both commercial (anatase and rutile form) and for the prepared TiO<sub>2</sub> powders as shown in Figure (3.6). The TiO<sub>2</sub> spectrum showed maximum absorbance at 347 nm with a band gap ~3.0 eV for the prepared nano-sized particles of TiO<sub>2</sub>. Commercial TiO<sub>2</sub> powders showed absorption bands at 379 nm for anatase form, and 356 for rutile form. This is due to the commercial particles being larger in size than the prepared particles. It is known that larger particles have smaller band gap values [15].

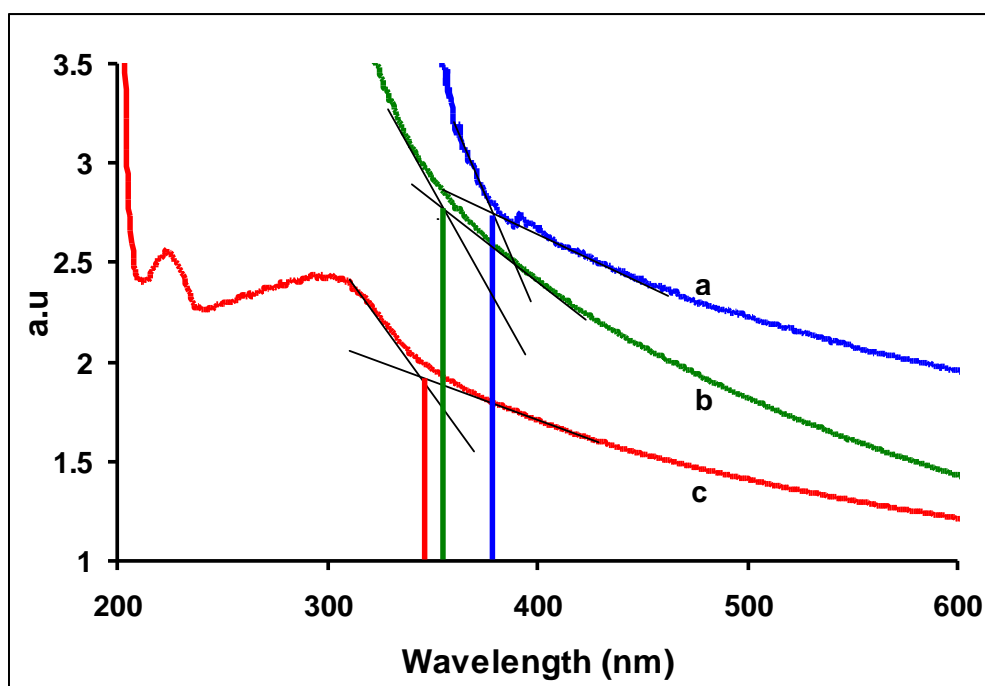


**Figure (3.6):** Solid state electronic absorption spectra measured for TiO<sub>2</sub> a) commercial anatase form, b) commercial rutile form, c) nano-particles powder.

### 3.2.2 ZnO system

Commercial ZnO powder and prepared nanoparticles were characterized using UV/Visible absorption spectrophotometry, photoluminescence spectrometry, XRD and SEM techniques.

#### UV-visible spectral characterization of ZnO:

The UV-Visible electronic absorption spectrum was measured for both commercial and prepared ZnO nanoparticles. Figure (3.7) shows the absorption band at  $\lambda_{\text{max}} = 379$  nm for commercial ZnO, and 371 nm for prepared ZnO. The Figure shows that the prepared powder has slightly shorter wavelength, due to wider band gap associated with smaller particles of the prepared powder. This is consistent with literature [32].

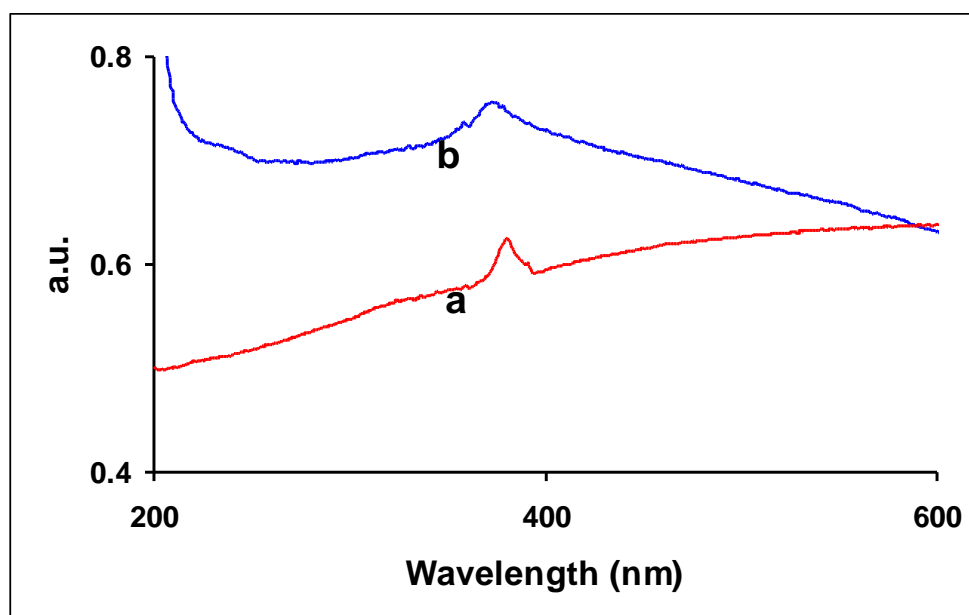


**Figure (3.7):** Electronic absorption spectra for a) commercial ZnO catalyst, b) ZnO nano-particles, suspension inside water.

### **Photoluminescence (PL) spectra of ZnO:**

Photoluminescence emission spectra were measured for both commercial and prepared ZnO nanoparticles, as shown in Figure (3.8). Emission peaks occurred at 388 nm for commercial ZnO, and 383 nm for prepared ZnO. The Figure shows that the commercial ZnO has longer emission wavelength due to its larger particle size. The PL spectral results are in parallel with the electronic absorption spectral results and with earlier literature [77, 78]. The band at  $\lambda = 440$  nm, is due to oxygen vacancies inside the particles, as discussed by literature [76].

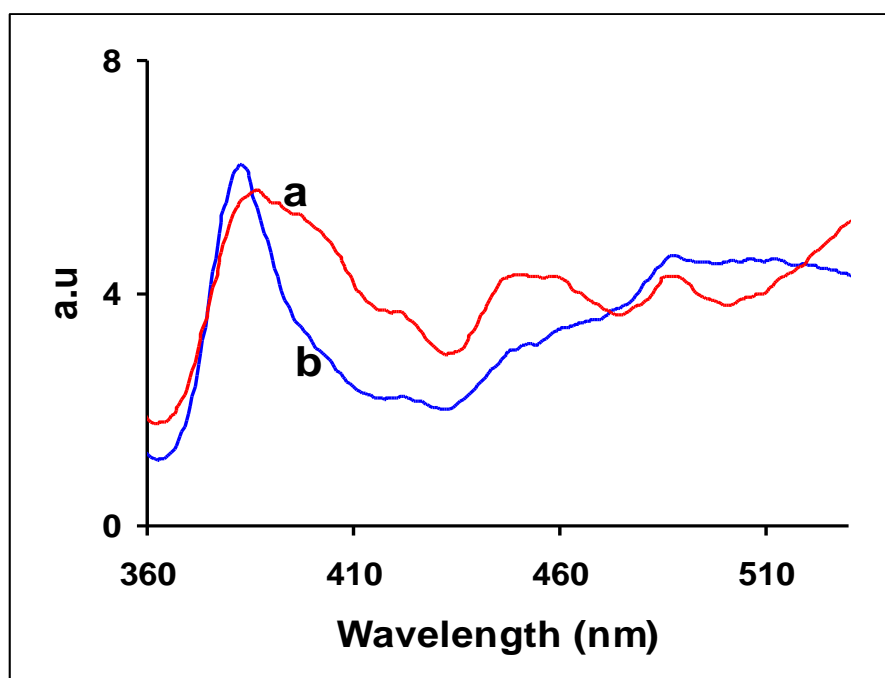


**Figure (3.8):** Photoluminescence spectra measured for a) ZnO commercial, b) ZnO nano-particles, excitation wavelength was 325 nm.

### **XRD study of ZnO:**

ZnO powders were characterized using XRD technique, as shown in Figures (3.9- 3.11). Particle size was calculated from XRD diffraction pattern of ZnO particles. The X-ray pattern showed a hexagonal wurtzite crystal type for ZnO particles, (Figure 3.9). This coincided with literature XRD pattern for wurtzite ZnO [79], Figure (3.10). Based on two different XRD peaks at (100) and (101) indices, the average ZnO particle diameter was 16 nm, as calculated by the Scherrer equation [74]. Commercial ZnO powder involved larger size (19.4 nm) as measured by XRD.

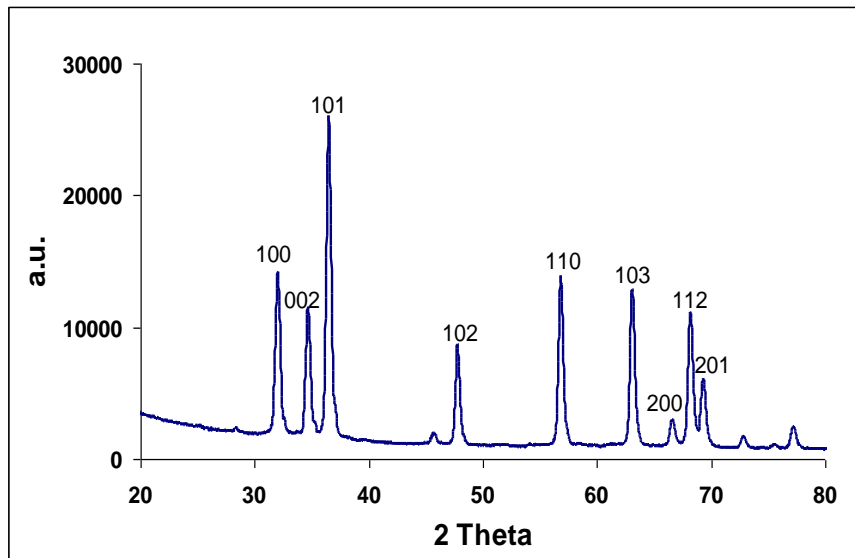


**Figure (3.9):** X-ray diffraction pattern for the prepared ZnO nano-particles.

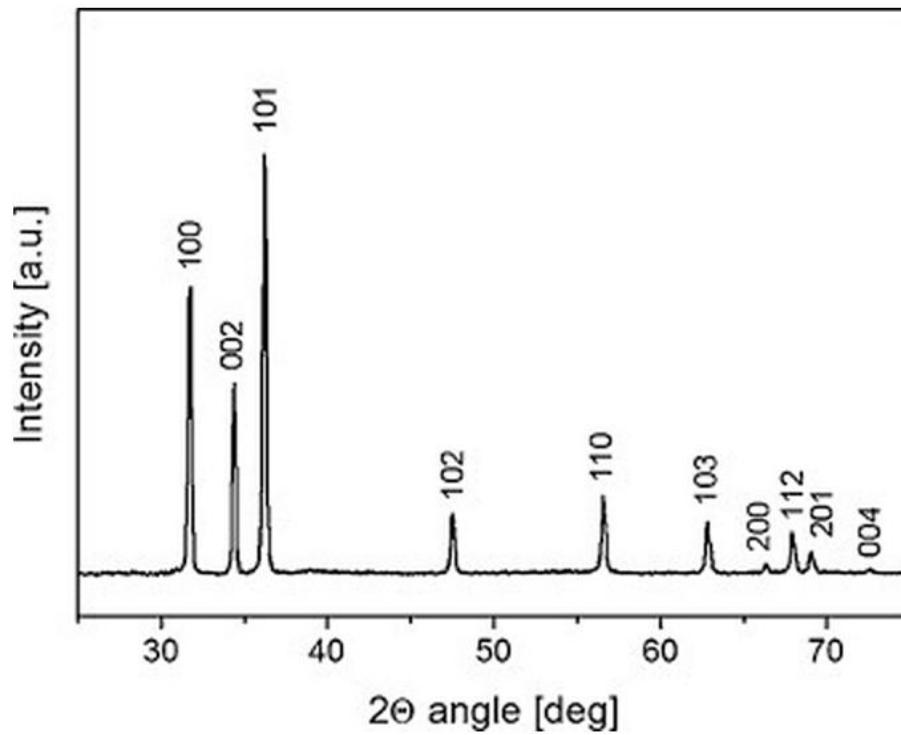


**Figure (3.10):** Literature X-ray diffraction pattern of nano zinc oxide (ZnO) particles [79].

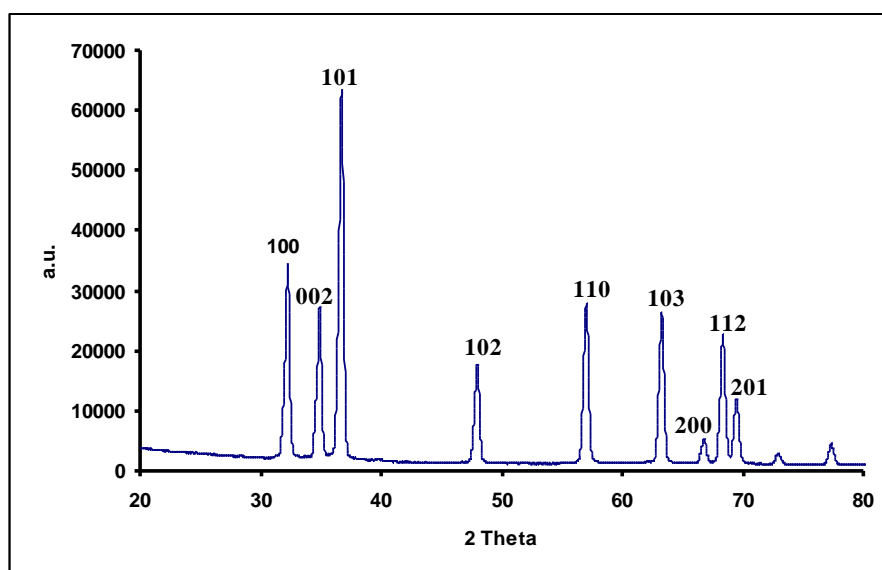


**Figure (3.11):** X-ray diffraction pattern for commercial ZnO.

### **SEM results of ZnO:**

SEM images were used to study the surface morphology and estimated size of prepared ZnO particles. SEM images showed elongated nanorods (rice-shaped) ZnO particles with about 10- 20 nm in width and nearly 100 nm in length. Surface morphology of the nanoparticles is shown in Figure (3.12). The crystallites observed by SEM involve coagulates of smaller particles, with ~16 nm in diameter, as calculated by XRD.

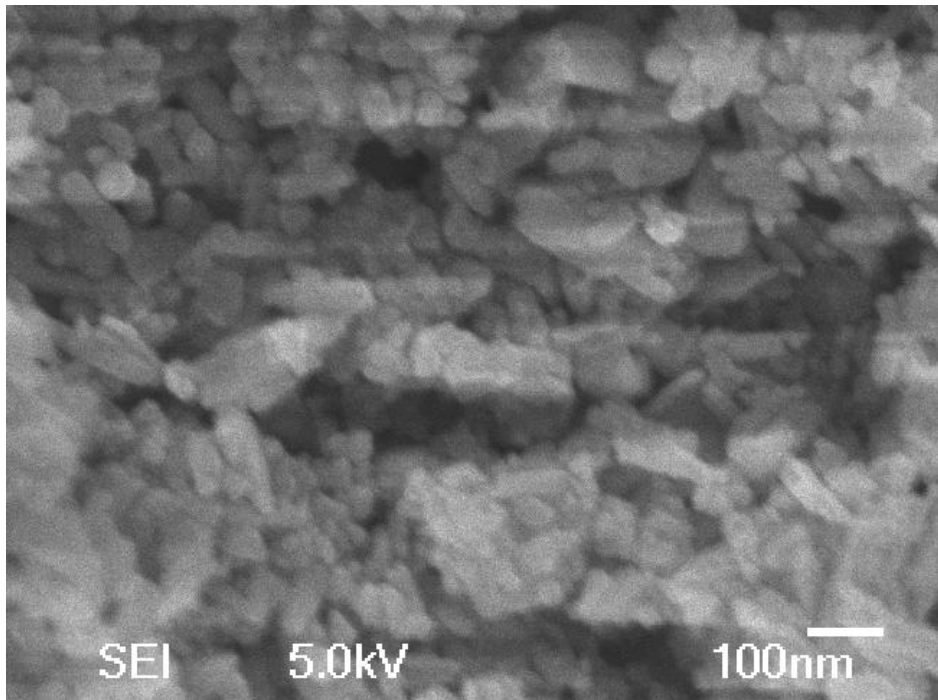


**Figure (3.12):** SEM images for the prepared ZnO nanoparticles.

### **3.3 Photocatalytic reaction results**

The photodegradation of paracetamol was studied under different conditions, and different catalyst systems.

#### **3.3.1 Commercial catalyst system**

Commercial  $\text{TiO}_2$  and ZnO systems were used to catalyze photodegradation of paracetamol contaminant in water using UV light.

##### **3.3.1.1 Commercial $\text{TiO}_2$ catalyst system**

###### ***Effect of contaminant concentration***

Under neutral conditions, the effect of contaminant concentration on degradation of paracetamol was studied using the  $\text{TiO}_2$  commercial system.

The paracetamol concentration was varied from 15 ppm to 45 ppm with constant catalyst ( $\text{TiO}_2$ ) loading 0.1 g/50mL. Figure (3.13) shows that the anatase form of  $\text{TiO}_2$  catalyzes the photodegradation process. The Figure shows that the overall reaction rate was not affected with increased contaminant concentration.

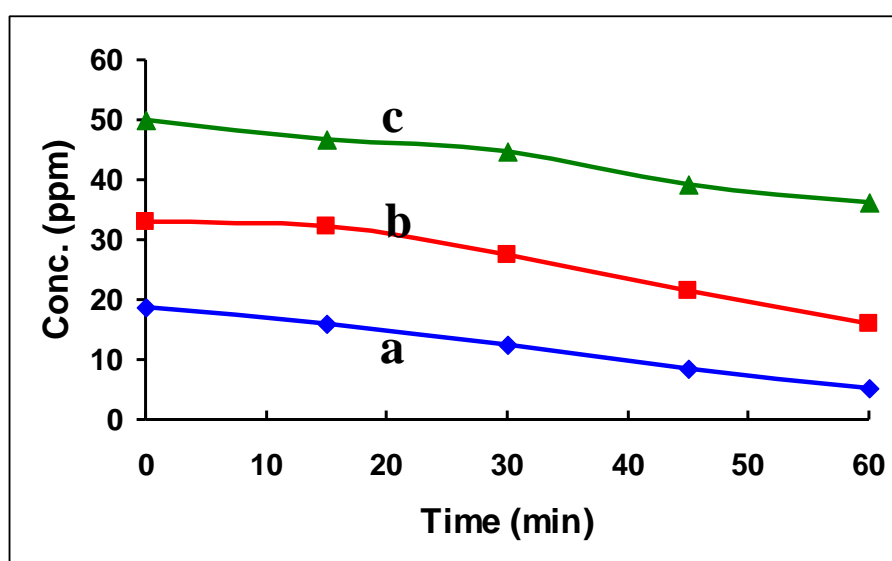


**Figure (3.13):** Effect of contaminant concentration on degradation of paracetamol using the  $\text{TiO}_2$  anatase system under UV light and neutral conditions: a) 15 ppm, b) 30 ppm, c) 45 ppm.

The turnover number, quantum yield, turnover frequency and overall rate values calculated after 60 minutes at different concentrations of paracetamol (15, 30 and 45 ppm) were not significantly affected as shown in Table (3.1).

**Table (3.1): Effect of contaminant concentration on values of turnover number (T.N.), turnover frequency (T.F.) ( $\text{min}^{-1}$ ), quantum yield (Q.Y.) and overall rate (ppm/min) for paracetamol degradation after 60 min, using the  $\text{TiO}_2$  anatase system under UV light.**

Nominal concentration (ppm)	Initial concentration (ppm)	Final concentration (ppm)	Turnover number	Turnover frequency ( $\text{min}^{-1}$ )	Quantum yield	Overall rate (ppm/min)
15	18.75	5.36	$3.54 \times 10^{-3}$	$0.06 \times 10^{-3}$	$10.08 \times 10^{-2}$	0.22
30	33.04	16.07	$4.50 \times 10^{-3}$	$0.08 \times 10^{-3}$	$12.78 \times 10^{-2}$	0.30
45	50.00	36.25	$3.64 \times 10^{-3}$	$0.06 \times 10^{-3}$	$10.35 \times 10^{-2}$	0.23

Where:

\*Turnover number (T.N.) = number of moles of reacted paracetamol / number of moles of  $\text{TiO}_2$  catalyst.

Number of contaminant moles reacted = (Initial concentration – Final concentration) in ppm  $\times (50 \times 10^{-6}) / \text{M.wt of paracetamol (151 g/mole)}$ .

Moles of catalyst ( $\text{TiO}_2$ ) =  $\text{Wt} / \text{MM} = 0.1 / 80 = 1.25 \times 10^{-3}$  mole

\*Turnover frequency (T.F.) = T.N. / time ( 60 minute )

\*Quantum yield (Q.Y.) = number of contaminant molecules reacted / total number of photons used.

$E \text{ (J)} = \text{Incident power per unit area} \times \text{Total area or incident power} \times \text{Exposure time in second}$

$$= [(0.000878477 \text{ W/cm}^2) \times 21.6 \text{ cm}^2] \times [60 \times 60 \text{ second}] = 68.31 \text{ J}$$

Assuming average wavelength of incident light is 385 nm for UV light and 555 nm for visible light (incident power per unit area =  $0.0146413 \text{ w/cm}^2$ ), then:

$$v = c/\lambda = 3 \times 10^8 \text{ ms}^{-1} / 385 \times 10^{-9} \text{ m} = 7.8 \times 10^{14} \text{ s}^{-1}$$

And from Planks equation,  $E \text{ (J)} = nh\nu$

$$n = J/h\nu = 68.31 / (7.8 \times 10^{14} \times 6.62 \times 10^{-34}) = 1.323 \times 10^{20} \text{ photons}$$

The rutile form of  $\text{TiO}_2$  failed to catalyze the photodegradation of paracetamol. This is shown in Figure (3.14) where no significant change in

paracetamol concentration was observed. Note that the measured contaminant concentration in each case is less than the originally used nominal concentration. The difference is due to adsorption onto catalyst surface.

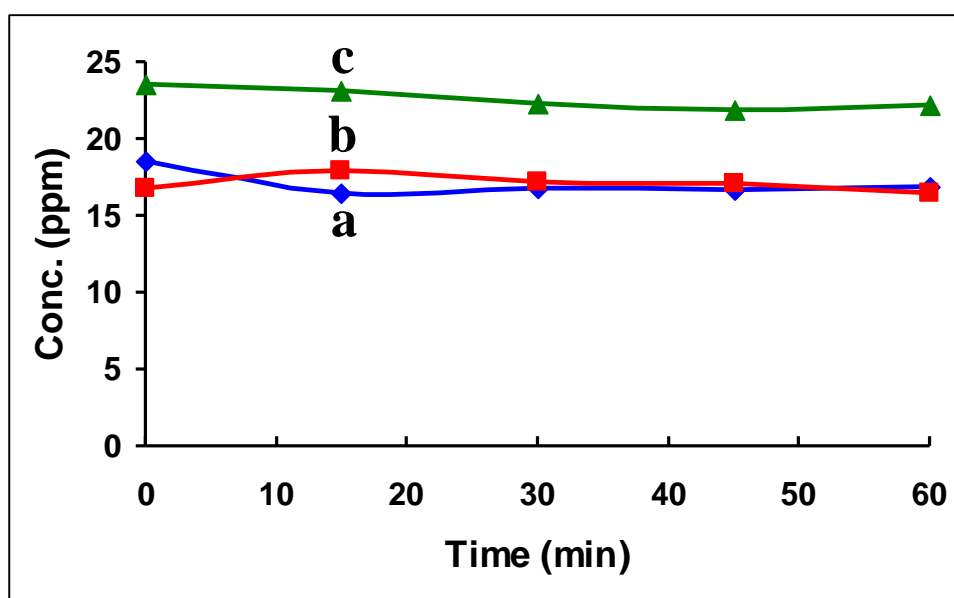


**Figure (3.14):** Effect of contaminant concentration on degradation of paracetamol using the TiO<sub>2</sub> rutile system under UV light and neutral conditions: a) 15 ppm, b) 30 ppm, c) 45 ppm.

### *Effect of catalyst concentration*

Under neutral conditions, the effect of concentration of TiO<sub>2</sub> in anatase form on photo-degradation of paracetamol by varying its amount, from 0.05 to 0.20 g/50mL solution, was investigated. (Figure 3.15) shows that TiO<sub>2</sub> anatase failed to catalyze the photodegradation of paracetamol by increasing the amount of TiO<sub>2</sub> anatase.

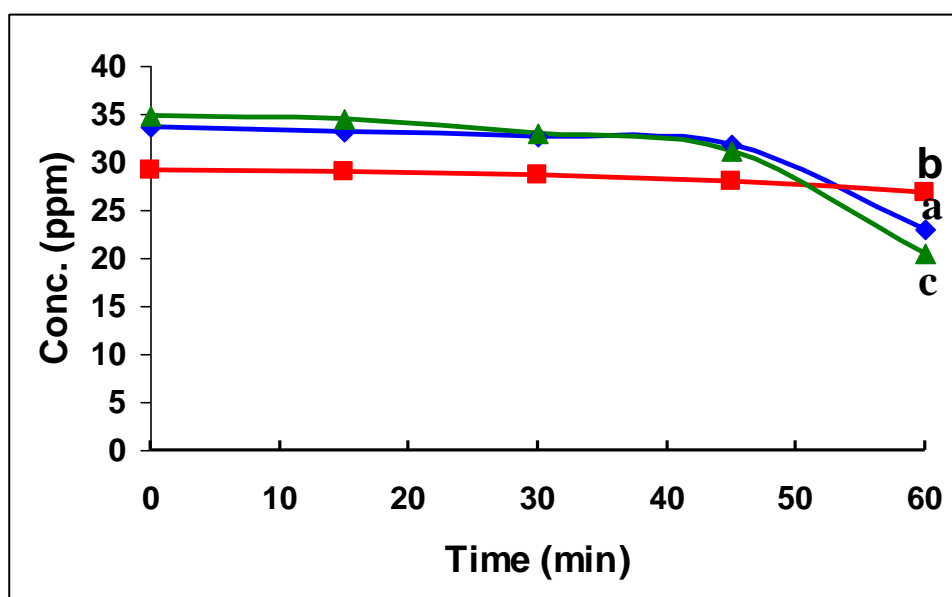


**Figure (3.15):** Effect of concentration of TiO<sub>2</sub> in anatase form on photo-degradation of paracetamol by varying its amount: a) 0.05 g, b) 0.1 g, c) 0.2 g under UV light and neutral conditions.

The results are summarized in Table (3.2). The Tables shows that the catalyst concentration did not have a tendency on values of turnover number, turnover frequency, quantum yield and overall rate.

**Table (3.2):** Effect of catalyst concentration on values of turnover number, turnover frequency ( $\text{min}^{-1}$ ), quantum yield and overall rate (ppm/min) for paracetamol degradation after 60 min, using TiO<sub>2</sub> in anatase form under UV light.

Catalyst wt (g)	Initial concentration (ppm)	Final concentration (ppm)	Turnover number	Turnover frequency ( $\text{min}^{-1}$ )	Quantum yield	Overall rate (ppm/min)
0.05	33.62	23.00	$5.60 \times 10^{-3}$	$0.93 \times 10^{-4}$	$8.00 \times 10^{-2}$	0.20
0.1	29.13	26.79	$0.62 \times 10^{-3}$	$0.10 \times 10^{-4}$	$1.78 \times 10^{-2}$	0.04
0.2	34.84	20.50	$1.90 \times 10^{-3}$	$0.32 \times 10^{-4}$	$10.75 \times 10^{-2}$	0.24

The rutile form of TiO<sub>2</sub> failed to catalyze the photodegradation of paracetamol. This is shown in Figure (3.16) where no significant change in paracetamol concentration was observed when using the rutile form as catalyst.

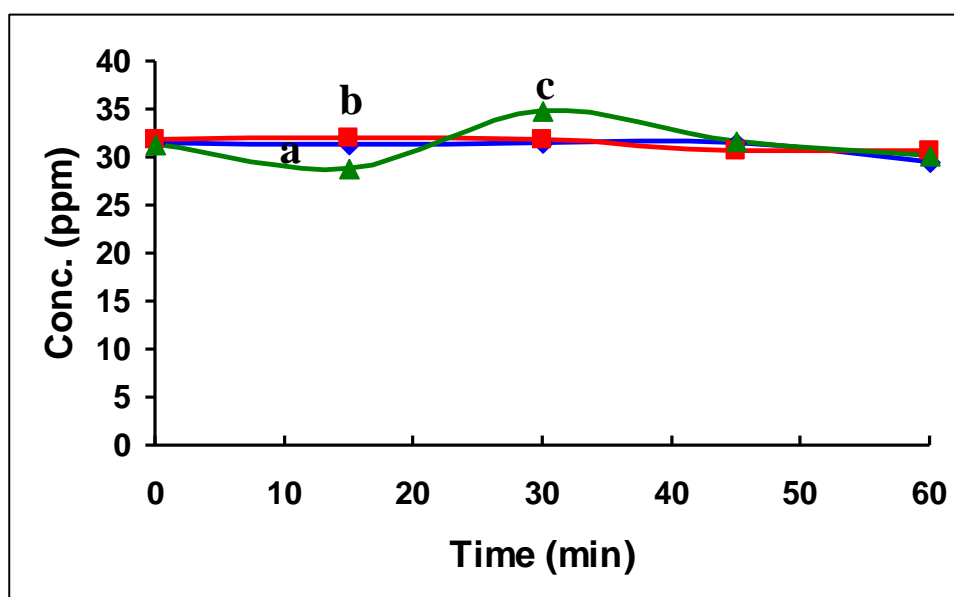


**Figure (3.16):** The photodegradation rate of paracetamol by varying the concentration of TiO<sub>2</sub> catalyst in the rutile form: a) 0.05 g, b) 0.1 g, c) 0.2 g under UV light and neutral conditions.

Values of turnover number, turnover frequency, quantum yield and overall rate for paracetamol degradation were calculated after 60 min. Table (3.3) shows the reaction rate was not affected by varying catalyst concentration.

**Table (3.3):** Effect of catalyst concentration on values of turnover number, turnover frequency ( $\text{min}^{-1}$ ), quantum yield and overall rate (ppm/min) for paracetamol degradation after 60 min, using TiO<sub>2</sub> catalyst in the rutile form under UV light.

Catalyst wt (g)	Initial concentration (ppm)	Final concentration (ppm)	Turnover number	Turnover frequency ( $\text{min}^{-1}$ )	Quantum yield	Overall rate (ppm/min)
0.05	31.48	29.47	$1.07 \times 10^{-3}$	$0.20 \times 10^{-4}$	$15.25 \times 10^{-3}$	0.024
0.1	31.79	30.62	$0.31 \times 10^{-3}$	$0.05 \times 10^{-4}$	$8.75 \times 10^{-3}$	0.020
0.2	31.35	30.23	$0.15 \times 10^{-3}$	$0.03 \times 10^{-4}$	$8.50 \times 10^{-3}$	0.020

### *Effect of pH*

Effect of pH on reaction rates of paracetamol degradation with UV-light lamp was investigated. The efficiency of TiO<sub>2</sub> in rutile form was more than anatase form in photo-degradation of paracetamol. Figures (3.17) and (3.18) were shown that. Photo-degradation of paracetamol was investigated under different pH values (Neutral pH=7, Acidic pH=3.5 and Basic pH=10) at constant catalyst (TiO<sub>2</sub>) loading 0.1 g/50mL. In Figure (3.17) the rutile TiO<sub>2</sub> showed higher reaction rate at basic medium.

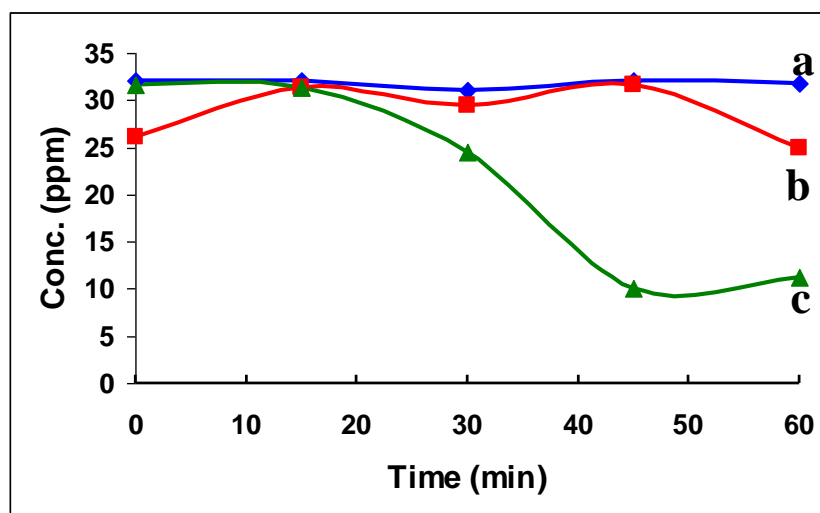


**Figure (3.17):** Effect of pH on reaction rates of paracetamol degradation with UV-light lamp using TiO<sub>2</sub> rutile: a) Neutral, b) Acidic, c) Basic.

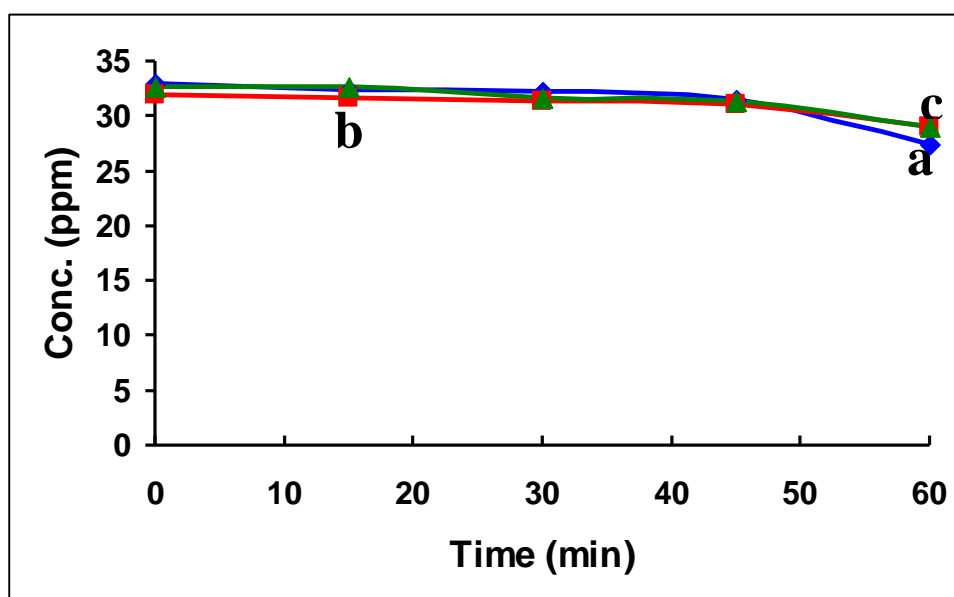


**Figure (3.18):** Effect of pH on reaction rates of paracetamol degradation with UV-light lamp using TiO<sub>2</sub> anatase: a) Neutral, b) Acidic, c) Basic.

The T.N., Q.Y., T.F. and overall rate values also showed higher values at pH = 10 (basic) as shown in Table (3.4) when using rutile form.

**Table (3.4):** Effect of pH on values of turnover number, turnover frequency (min<sup>-1</sup>), quantum yield and overall rate (ppm/min) for paracetamol degradation after 60 min, using rutile form of TiO<sub>2</sub> under UV light.

pH	Initial concentration (ppm)	Final concentration (ppm)	Turnover number	Turnover frequency (min <sup>-1</sup> )	Quantum yield	Overall rate (ppm/min)
Neutral	32.143	31.80	0.09X10 <sup>-3</sup>	0.002X10 <sup>-3</sup>	0.26X10 <sup>-2</sup>	0.01
Acidic	26.136	25.00	0.30X10 <sup>-3</sup>	0.005X10 <sup>-3</sup>	0.87X10 <sup>-2</sup>	0.02
Basic	31.660	11.20	5.42X10 <sup>-3</sup>	0.100X10 <sup>-3</sup>	15.50X10 <sup>-2</sup>	0.34

(Table 3.5) shows that the anatase catalyst did not have a tendency on values of turnover number, turnover frequency, quantum yield and overall rate.

**Table (3.5): Effect of pH on values of turnover number, turnover frequency ( $\text{min}^{-1}$ ), quantum yield and overall rate (ppm/min) for paracetamol degradation after 60 min, using anatase form of  $\text{TiO}_2$  under UV light.**

pH	Initial concentration (ppm)	Final concentration (ppm)	Turnover number	Turnover frequency ( $\text{min}^{-1}$ )	Quantum yield	Overall rate (ppm/min)
Neutral	33.0	27.47	$1.50 \times 10^{-3}$	$0.03 \times 10^{-3}$	$4.25 \times 10^{-2}$	0.100
Acidic	32.0	29.03	$0.79 \times 10^{-3}$	$0.01 \times 10^{-3}$	$2.24 \times 10^{-2}$	0.050
Basic	32.7	29.00	$1.00 \times 10^{-3}$	$0.02 \times 10^{-3}$	$2.80 \times 10^{-2}$	0.062

### 3.3.1.2 Commercial ZnO catalyst system

#### *Effect of contaminant concentration*

Under neutral conditions, effect of initial paracetamol concentration on overall rate of degradation was studied under UV light. The degradation rate was higher with higher contaminant concentration as shown in Figure (3.19).

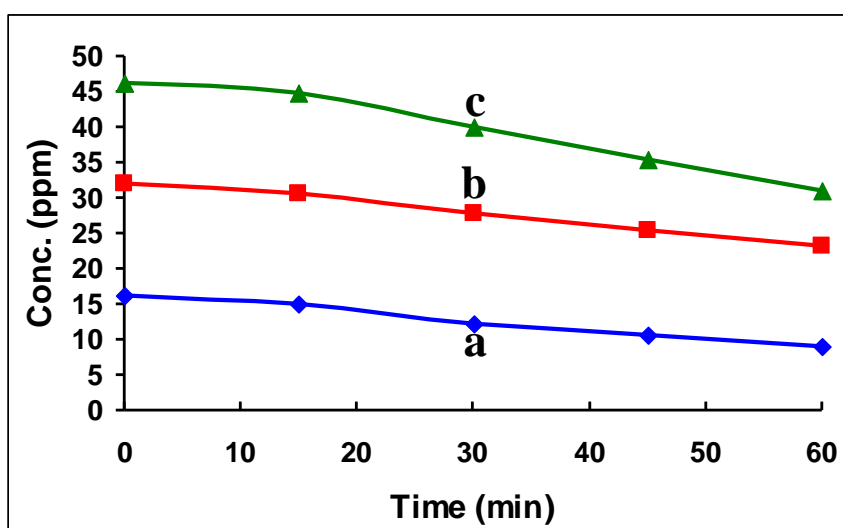


**Figure (3.19):** Effect of initial paracetamol concentration on overall rate of degradation under UV light and neutral conditions, using ZnO commercial: a) 15 ppm, b) 30 ppm, c) 45 ppm.

Turnover number, turnover frequency, quantum yield and overall rate values were calculated after 60 minutes using different concentrations of paracetamol (15, 30 and 45 ppm) at constant ZnO 0.1 g/50mL. The values increased by increasing paracetamol concentration, as shown in Table (3.6).

**Table (3.6): Effect of initial paracetamol concentration on values of turnover number, turnover frequency ( $\text{min}^{-1}$ ), quantum yield and overall rate (ppm/min) for paracetamol degradation after 60 min, using ZnO commercial under UV light.**

Nominal concentration (ppm)	Initial concentration (ppm)	Final concentration (ppm)	Turnover number	Turnover frequency ( $\text{min}^{-1}$ )	Quantum yield	overall rate (ppm/min)
15	16.22	8.96	$2.0 \times 10^{-3}$	$0.03 \times 10^{-3}$	$5.50 \times 10^{-2}$	0.121
30	32.09	23.23	$2.4 \times 10^{-3}$	$0.04 \times 10^{-3}$	$6.75 \times 10^{-2}$	0.150
45	46.30	31.02	$4.1 \times 10^{-3}$	$0.07 \times 10^{-3}$	$11.50 \times 10^{-2}$	0.255

### *Effect of catalyst concentration*

The effect of ZnO catalyst concentration on degradation of paracetamol (30 ppm) was investigated under neutral conditions. The overall rate of reaction increased with increasing catalyst amount as shown in Figure (3.20).

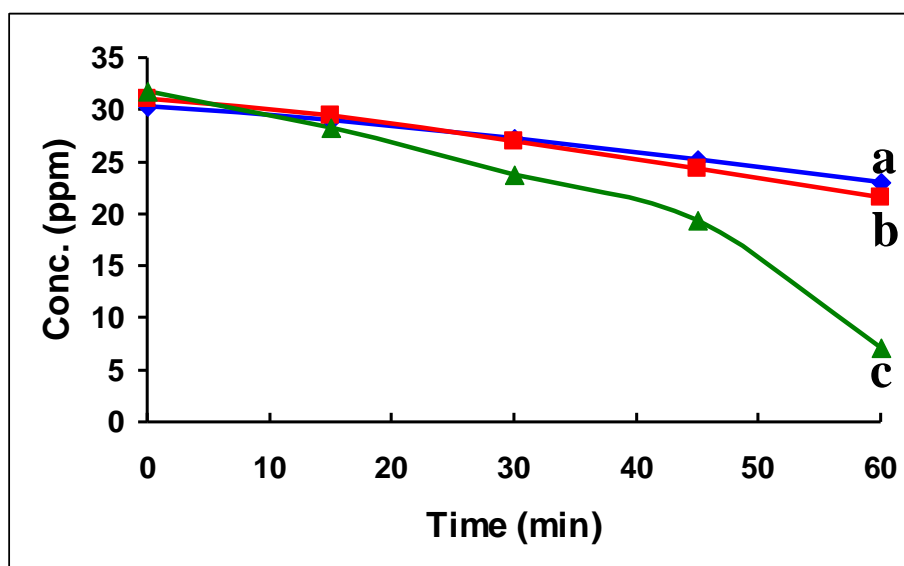


**Figure (3.20):** Effect of ZnO catalyst concentration on degradation of paracetamol under UV light and neutral conditions: a) 0.05 g, b) 0.1 g, c) 0.2 g.

T.N., T.F., Q.Y. and overall rate reaction were calculated after 60 minutes using different catalyst amounts (0.05, 0.1 and 0.2 g). The overall rate reaction and Q.Y. values increased by increasing catalyst amount, while the T.N. and T.F. values decreased to a certain value then increased, as shown in Table (3.7).

**Table (3.7):** Effect of ZnO catalyst concentration on values of turnover number, turnover frequency ( $\text{min}^{-1}$ ), quantum yield and overall rate (ppm/min) for paracetamol degradation after 60 min, using ZnO commercial under UV light.

Catalyst wt (g)	Initial concentration (ppm)	Final concentration (ppm)	Turnover number	Turnover frequency ( $\text{min}^{-1}$ )	Quantum yield	overall rate (ppm/min)
0.05	30.34	23.020	$4.0 \times 10^{-3}$	$0.67 \times 10^{-4}$	$5.5 \times 10^{-2}$	0.122
0.1	31.00	21.600	$2.5 \times 10^{-3}$	$0.42 \times 10^{-4}$	$7.0 \times 10^{-2}$	0.160
0.2	31.82	7.154	$3.3 \times 10^{-3}$	$0.60 \times 10^{-4}$	$18.6 \times 10^{-2}$	0.410

### 3.3.2 Nano-catalyst systems

Nanoparticle  $\text{TiO}_2$  and  $\text{ZnO}$  systems were prepared and used to photocatalyze paracetamol contaminant using direct solar light.

#### 3.3.2.1 $\text{TiO}_2$ system

0.2 g  $\text{TiO}_2$  nano-particles, commercial  $\text{TiO}_2$  rutile and  $\text{TiO}_2$  anatase were used for photodegradation of neutral 30 ppm paracetamol solution under direct solar light. Figure (3.21) shows values of remaining contaminant paracetamol concentration measured with time. As the Figure shows, the commercial  $\text{TiO}_2$  in anatase form catalyzed the photodegradation process faster than the nano-particles  $\text{TiO}_2$  did.

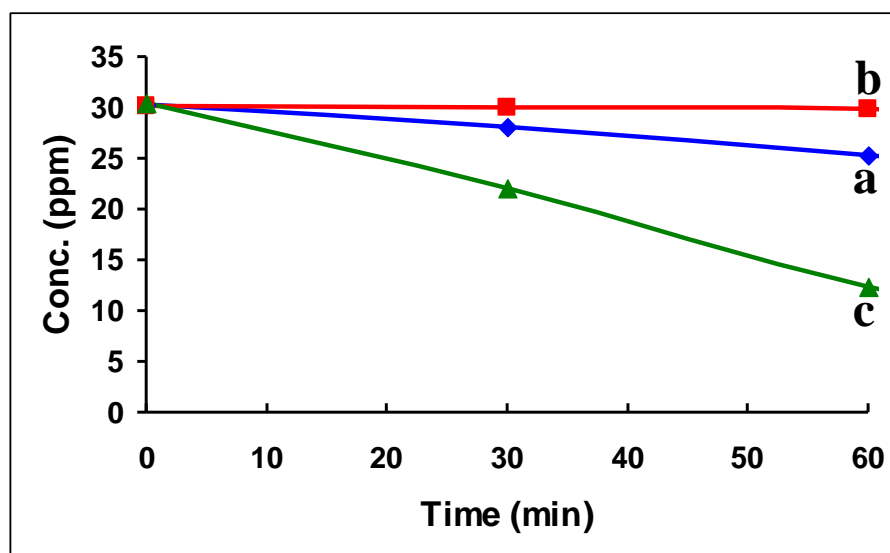


**Figure (3.21):** Photodegradation of neutral 30 ppm paracetamol solution under direct solar light and neutral conditions, using  $\text{TiO}_2$  nano-particles and  $\text{TiO}_2$  commercial: a)  $\text{TiO}_2$  nano-particle, b)  $\text{TiO}_2$  R, c)  $\text{TiO}_2$  A.

T.N., T.F., Q.Y. and overall rate reaction were calculated after 60 minutes using different TiO<sub>2</sub> systems. Table (3.8) shows that values were higher for TiO<sub>2</sub> anatase, nano-particles TiO<sub>2</sub> and TiO<sub>2</sub> rutile, respectively.

**Table (3.8): Effect of TiO<sub>2</sub> systems on values of turnover number, turnover frequency (min<sup>-1</sup>), quantum yield and overall rate (ppm/min) for paracetamol degradation after 60 min, using TiO<sub>2</sub> nano-particles and TiO<sub>2</sub> commercial under direct sun light.**

Catalyst	Initial concentration (ppm)	Final concentration (ppm)	Turnover number	Turnover frequency (min <sup>-1</sup> )	Quantum yield	overall rate (ppm/min)
TiO <sub>2</sub> nano.	30.24	25.35	0.65X10 <sup>-3</sup>	0.01X10 <sup>-3</sup>	7.50X10 <sup>-3</sup>	0.1
TiO <sub>2</sub> R	30.10	29.90	0.03X10 <sup>-3</sup>	0.00X10 <sup>-3</sup>	0.31X10 <sup>-3</sup>	0.0
TiO <sub>2</sub> A	30.43	12.42	2.40X10 <sup>-3</sup>	0.04X10 <sup>-3</sup>	28.75X10 <sup>-3</sup>	0.3

### 3.3.2.2 ZnO system

0.2 g ZnO nano-particles and commercial were used for photodegradation of neutral paracetamol solution (30 ppm) under direct sun light. Figure (3.22) shows that commercial ZnO catalyst system was more effective in paracetamol photodegradation.

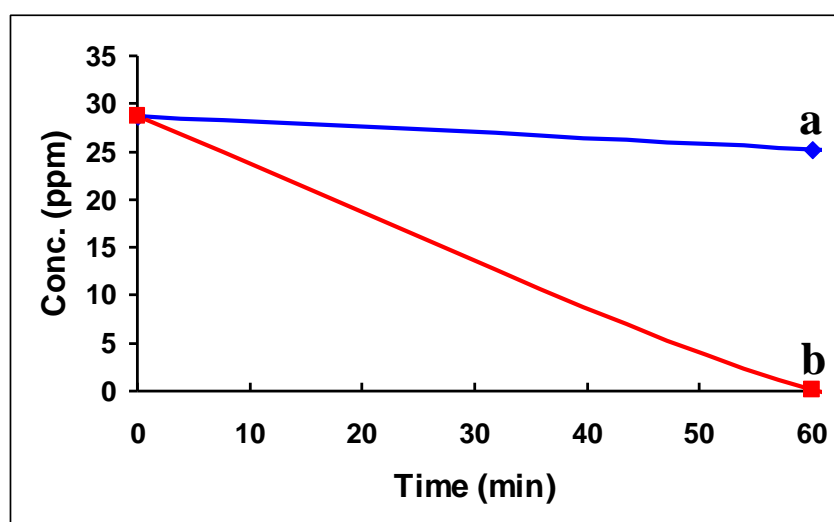


**Figure (3.22):** ZnO nano-particles and commercial in photodegradation of neutral paracetamol solution (30 ppm) under direct sun light and neutral conditions: a) ZnO nano-particle, b) ZnO commercial.

The values of T.N., Q.Y., T.F., and overall rate reaction for commercial ZnO catalyst system were higher than those for the nano-particles counterpart, as shown in Table (3.9).

**Table (3.9): Effect of ZnO nano-particles and commercial on values of turnover number, turnover frequency ( $\text{min}^{-1}$ ), quantum yield and overall rate (ppm/min) for paracetamol degradation after 60 min under direct sun light.**

Catalyst	Initial concentration (ppm)	Final concentration (ppm)	Turnover number	Turnover frequency ( $\text{min}^{-1}$ )	Quantum yield	overall rate (ppm/min)
ZnO nano.	28.75	25.20	$0.96 \times 10^{-3}$	$0.01 \times 10^{-3}$	$1.13 \times 10^{-2}$	0.06
ZnO comm.	28.7	0.08	$7.70 \times 10^{-3}$	$0.13 \times 10^{-3}$	$9.00 \times 10^{-2}$	0.48

### 3.3.2.3 $\text{TiO}_2$ and ZnO nano-systems

0.2 g nano-catalysts were used for photodegradation of neutral 30 ppm paracetamol solution (100 mL). Figure (3.23) shows that ZnO nano-catalyst was more overall reaction rate than  $\text{TiO}_2$  nano-catalyst under direct sun light. Then the values of T.N., T.F., Q.Y. and overall rate for ZnO nano-catalyst was more as shown in Table (3.10).

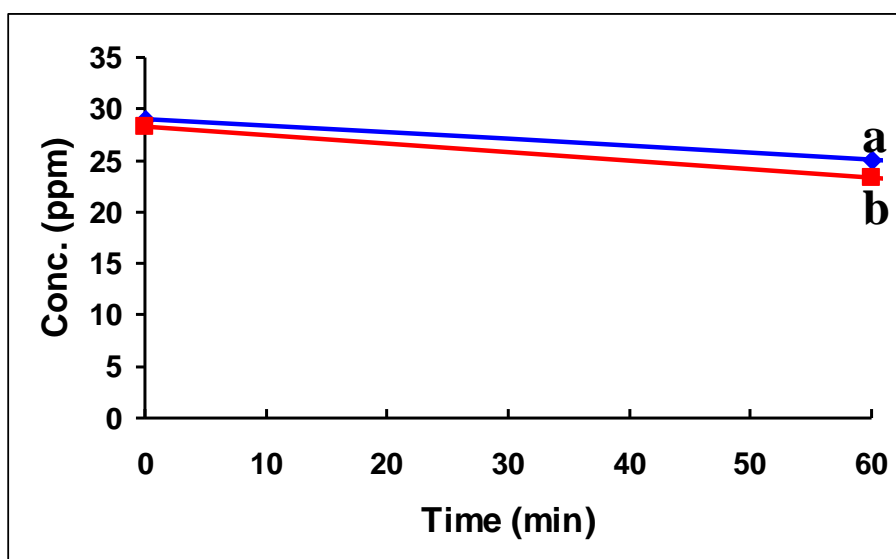


**Figure (3.23):** TiO<sub>2</sub> and ZnO nano-catalysts in photodegradation of neutral 30 ppm paracetamol solution: a) TiO<sub>2</sub> nano-particle, b) ZnO nano-particle.

**Table (3.10):** Effect of TiO<sub>2</sub> and ZnO nano-catalyst on values of turnover number, turnover frequency (min<sup>-1</sup>), quantum yield and overall rate (ppm/min) for paracetamol degradation after 60 min under direct sun light.

Catalyst	Initial concentration (ppm)	Final concentration (ppm)	Turnover number	Turnover frequency (min <sup>-1</sup> )	Quantum yield	overall rate (ppm/min)
TiO <sub>2</sub> nano.	29.02	25.13	1.04X10 <sup>-3</sup>	1.7X10 <sup>-5</sup>	12.50X10 <sup>-3</sup>	0.065
ZnO nano.	28.33	23.28	1.34X10 <sup>-3</sup>	2.2X10 <sup>-5</sup>	15.63X10 <sup>-3</sup>	0.080

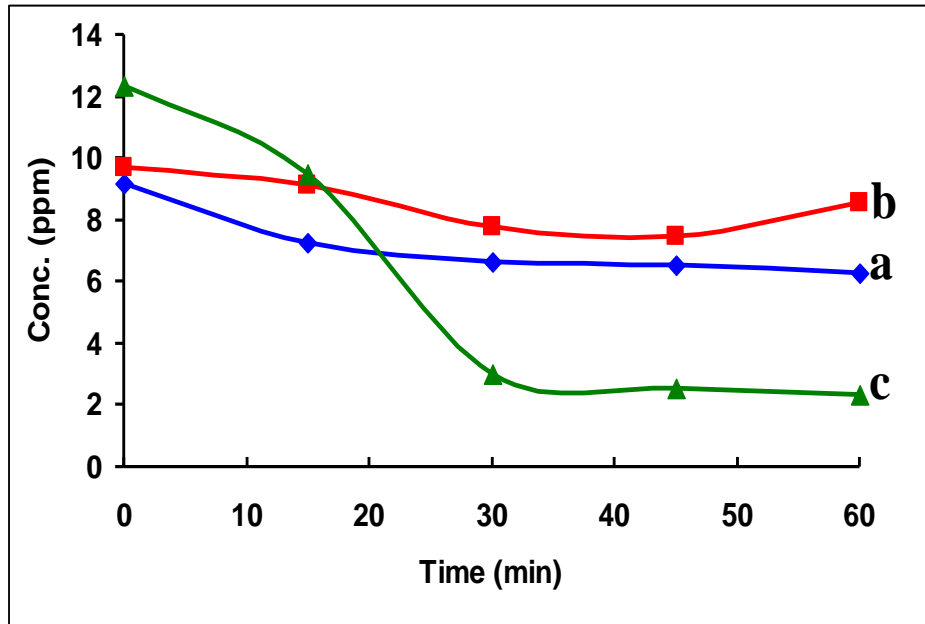
### 3.3.3 AC-Supported catalyst systems

AC/Catalyst (commercial TiO<sub>2</sub> rutile, commercial TiO<sub>2</sub> anatase and nano-particles) and (ZnO commercial and nano-particles) were used for photodegradation of paracetamol. UV light was used in case of supported commercial TiO<sub>2</sub> and ZnO, whereas direct sun light was used for supported

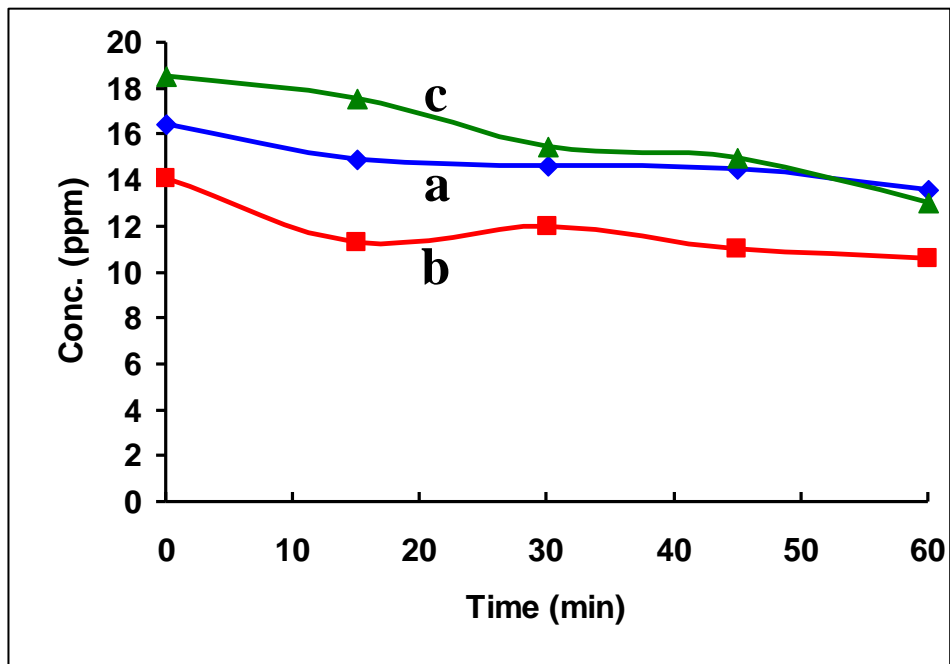
nano-sized  $\text{TiO}_2$  and  $\text{ZnO}$ . AC/Anatase > active than AC/Rutile under different pH values.

### ***Effect of contaminant concentration***

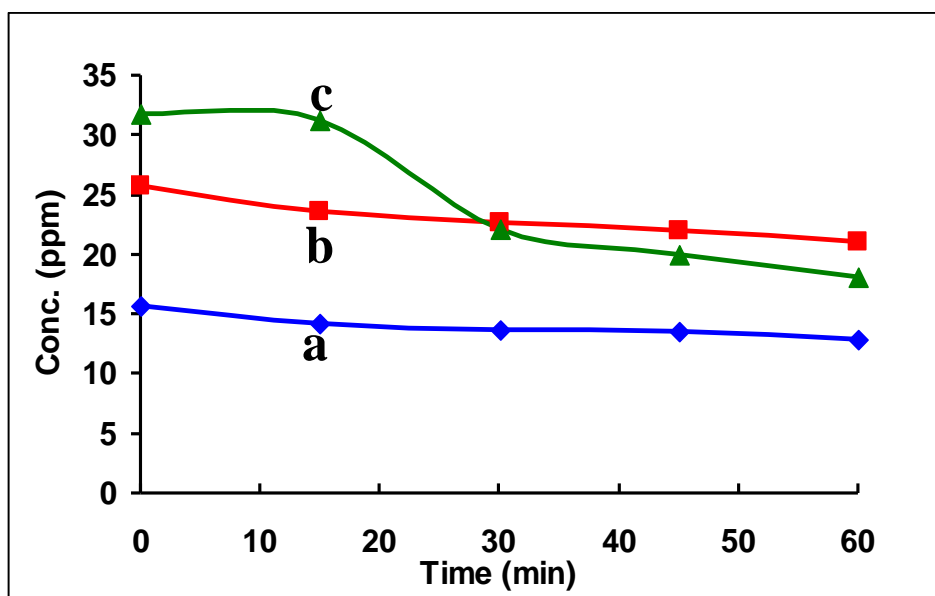
Under neutral conditions, effect of initial paracetamol concentration on overall rate of degradation under UV light was studied. The initial paracetamol concentration was varied from 60 ppm to 100 ppm, with constant AC/catalyst (commercial) amount 0.12 g/50mL. Figures (3.24 i, ii, iii, iv) show the effect of contaminant concentration on overall rate values, for different catalyst systems. The results are summarized in Table (3.12). In each paracetamol concentration, the overall photodegradation catalyst efficiency varied as: AC/ZnO > AC/ $\text{TiO}_2$  (A) > AC/ $\text{TiO}_2$  (R), respectively. On the other hand, different paracetamol concentration affected overall rate of photodegradation of paracetamol. In case of AC/ZnO catalyst system, the contaminant concentration showed no systematic effect on rate of photodegradation reaction. But when using AC/ $\text{TiO}_2$  (A), the photodegradation reaction rate increased to a certain value then decreased when increasing paracetamol concentration. There was no significant effect on overall reaction rate when using AC/ $\text{TiO}_2$  (R), as it was ineffective, as shown in Table (3.11).



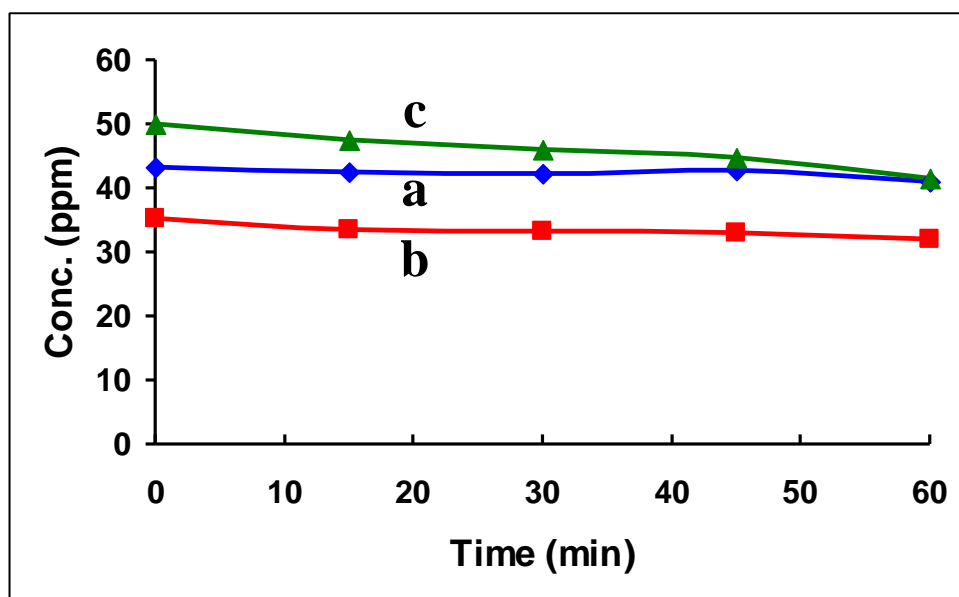
i)



ii)



iii)



iv)

**Figure (3.24):** Effect of initial paracetamol concentration on overall reaction rate of degradation for different catalyst systems (a: AC/TiO<sub>2</sub> R, b: AC/TiO<sub>2</sub> A, c: AC/ZnO) under UV light and neutral conditions: i) 60 ppm, ii) 70 ppm, iii) 85 ppm, iv) 100 ppm.

**Table(3.11): Effect of paracetamol concentration on values of turnover number, turnover frequency ( $\text{min}^{-1}$ ), quantum yield and overall rate (ppm/min) for paracetamol degradation after 60 min, using different commercial catalyst systems under UV light.**

Contaminant concentration (ppm)	Catalyst	Turnover number	Turnover frequency ( $\text{min}^{-1}$ )	Quantum yield	overall rate (ppm/min)
60	AC/TiO <sub>2</sub> R	$0.63 \times 10^{-3}$	$0.11 \times 10^{-4}$	$2.16 \times 10^{-2}$	0.05
	AC/TiO <sub>2</sub> A	$0.25 \times 10^{-3}$	$0.04 \times 10^{-4}$	$0.88 \times 10^{-2}$	0.02
	AC/ZnO	$2.20 \times 10^{-3}$	$0.40 \times 10^{-4}$	$7.51 \times 10^{-2}$	0.20
70	AC/TiO <sub>2</sub> R	$0.63 \times 10^{-3}$	$0.11 \times 10^{-4}$	$2.16 \times 10^{-2}$	0.05
	AC/TiO <sub>2</sub> A	$0.76 \times 10^{-3}$	$0.13 \times 10^{-4}$	$2.60 \times 10^{-2}$	0.06
	AC/ZnO	$1.20 \times 10^{-3}$	$0.20 \times 10^{-4}$	$4.10 \times 10^{-2}$	0.10
85	AC/TiO <sub>2</sub> R	$0.61 \times 10^{-3}$	$0.10 \times 10^{-4}$	$2.08 \times 10^{-2}$	0.05
	AC/TiO <sub>2</sub> A	$1.10 \times 10^{-3}$	$0.20 \times 10^{-4}$	$3.65 \times 10^{-2}$	0.08
	AC/ZnO	$3.03 \times 10^{-3}$	$0.51 \times 10^{-4}$	$10.33 \times 10^{-2}$	0.23
100	AC/TiO <sub>2</sub> R	$0.47 \times 10^{-3}$	$0.10 \times 10^{-4}$	$1.63 \times 10^{-2}$	0.04
	AC/TiO <sub>2</sub> A	$0.73 \times 10^{-3}$	$0.10 \times 10^{-4}$	$2.50 \times 10^{-2}$	0.06
	AC/ZnO	$3.90 \times 10^{-3}$	$0.65 \times 10^{-4}$	$13.25 \times 10^{-2}$	0.14

### ***Effect of pH***

Effect of pH on reaction rates of paracetamol degradation with UV light were investigated using constant amount of AC/catalyst (0.12 g) and 70 ppm paracetamol solution (50 mL).

#### **\*AC/TiO<sub>2</sub> rutile**

Paracetamol degradation reaction using AC/TiO<sub>2</sub> rutile system was investigated in using different pH values in the range (3.5- 10) under UV light. The catalytic efficiency was higher at higher pH value (basic pH = 10) as shown in Figure (3.25).

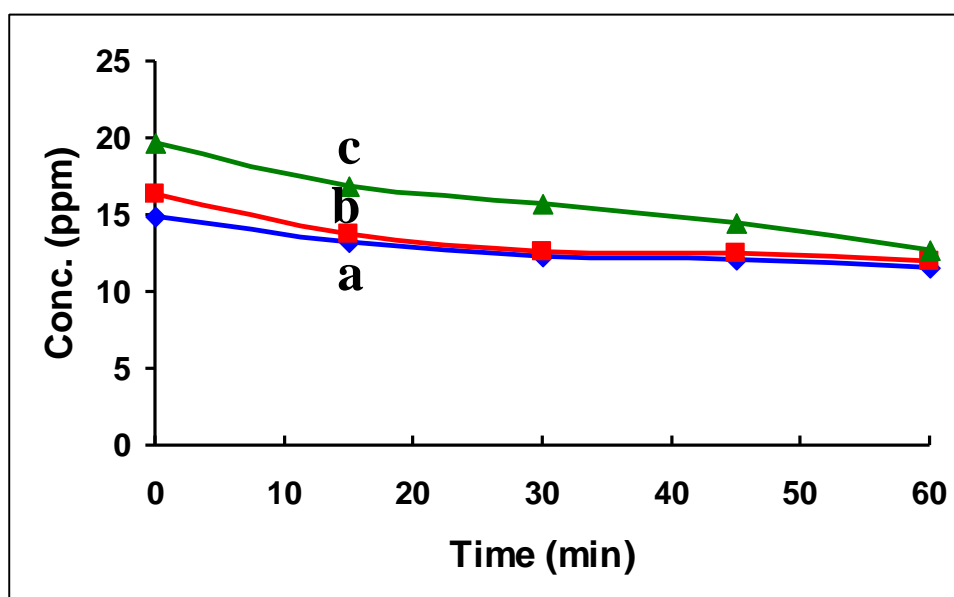


**Figure (3.25):** Paracetamol degradation reaction using AC/TiO<sub>2</sub> rutile system at different pH values in the range (3.5- 10) under UV light: a) Neutral, b) Acidic, c) Basic.

The values of T.N., Q.Y., T.F. and overall rate were calculated after 60 minutes at different pH values. Table (3.12) shows that the values increase by increasing the basicity of the paracetamol solution.

**Table (3.12):** Effect of pH on values of turnover number, turnover frequency (min<sup>-1</sup>), quantum yield and overall rate (ppm/min) for paracetamol degradation after 60 min, using AC/TiO<sub>2</sub> rutile system with UV light.

pH	Initial concentration (ppm)	Final concentration (ppm)	Turnover number	Turnover frequency (min <sup>-1</sup> )	Quantum yield	Overall rate (ppm/min)
Neutral	14.86	11.53	0.73X10 <sup>-3</sup>	0.01X10 <sup>-3</sup>	2.50X10 <sup>-2</sup>	0.060
Acidic	16.37	12.00	1.00X10 <sup>-3</sup>	0.02X10 <sup>-3</sup>	3.30X10 <sup>-2</sup>	0.073
Basic	19.73	12.69	1.50X10 <sup>-3</sup>	0.03X10 <sup>-3</sup>	5.25X10 <sup>-2</sup>	0.120

**\*AC/TiO<sub>2</sub> anatase**

Paracetamol degradation reaction using AC/TiO<sub>2</sub> anatase system was investigated in solution using different pH values under UV light.

The catalytic efficiency did not vary with value of pH in the range (3.5-10). At higher pH value the overall reaction rate was higher, as shown in Figure (3.26).

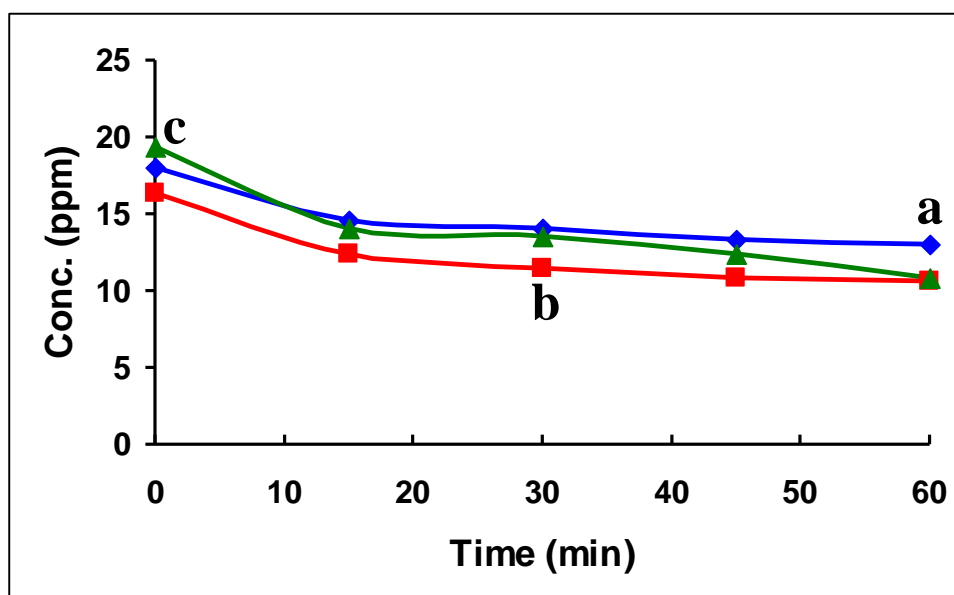


**Figure (3.26):** Paracetamol degradation reaction using AC/TiO<sub>2</sub> anatase system using different pH values under UV light: a) Neutral, b) Acidic, c) Basic.

The values of T.N., Q.Y. and T.F. were calculated, as shown in Table (3.13). All these values were slightly increased by increasing the basicity of paracetamol solution.

**Table (3.13):** Effect of pH on values of turnover number, turnover frequency (min<sup>-1</sup>), quantum yield and overall rate (ppm/min) for paracetamol degradation after 60 min, using AC/TiO<sub>2</sub> anatase system with UV light.

pH	Initial concentration (ppm)	Final concentration (ppm)	Turnover number	Turnover frequency (min <sup>-1</sup> )	Quantum yield	overall rate (ppm/min)
Neutral	18.06	13.00	1.13X10 <sup>-3</sup>	0.02X10 <sup>-3</sup>	3.88X10 <sup>-2</sup>	0.08
Acidic	16.33	10.6	1.30X10 <sup>-3</sup>	0.02X10 <sup>-3</sup>	4.33X10 <sup>-2</sup>	0.10
Basic	19.39	10.82	1.90X10 <sup>-3</sup>	0.03X10 <sup>-3</sup>	6.50X10 <sup>-2</sup>	0.14

**\* AC/ZnO commercial**

Effect of pH on overall reaction rate of paracetamol degradation with UV light lamp was investigated. The efficiency of AC/ZnO system in photo-degradation of paracetamol, (Figure 3.27), was investigated at different pH values. The overall reaction rate decreased by increasing the acidity of paracetamol solution. The Figure shows that under neutral or basic conditions, the reaction reached equilibrium in short time (60 min). whereas under acidic conditions it continued its progress for prolonged time.

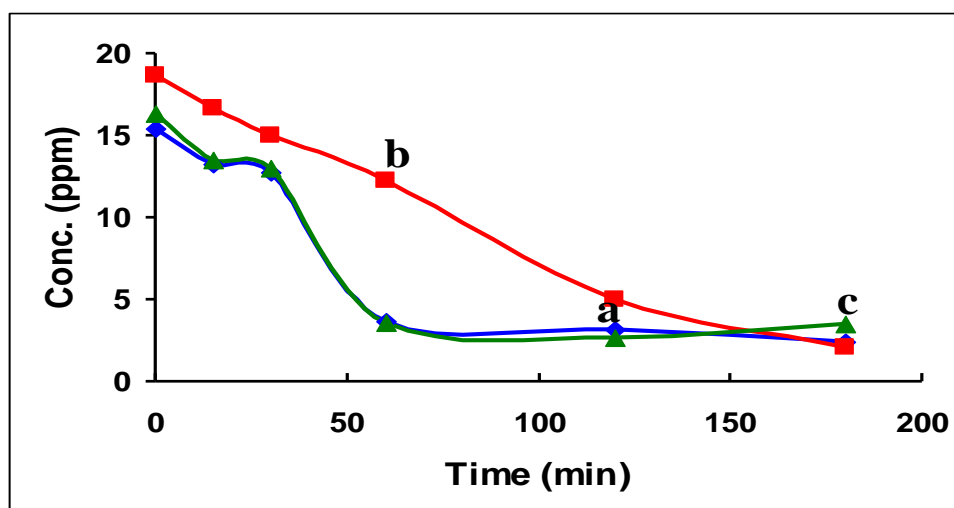


**Figure (3.27):** Effect of pH on reaction rate of paracetamol degradation with UV light lamp using AC/ZnO (commercial) catalyst: a) Neutral, b) Acidic, c) Basic.

Values of T.N., T.F., Q.Y. and overall reaction rate are summarized in Table (3.14). The Table shows that the values increased by increasing the pH value 3.5, 7, 10 respectively.

**Table (3.14): Effect of pH on values of turnover number, turnover frequency ( $\text{min}^{-1}$ ), quantum yield and overall rate (ppm/min) for paracetamol degradation after 60 min using AC/ZnO (commercial) catalyst with UV light.**

pH	Initial concentration (ppm)	Final concentration (ppm)	Turnover number	Turnover frequency ( $\text{min}^{-1}$ )	Quantum yield	Overall rate (ppm/min)
Neutral	15.44	3.65	$2.70 \times 10^{-3}$	$0.045 \times 10^{-3}$	$9.0 \times 10^{-2}$	0.20
Acidic	18.68	12.22	$1.43 \times 10^{-3}$	$0.024 \times 10^{-3}$	$4.9 \times 10^{-2}$	0.11
Basic	16.31	3.60	$2.81 \times 10^{-3}$	$0.050 \times 10^{-3}$	$9.6 \times 10^{-2}$	0.21

**\* AC/TiO<sub>2</sub> nano-particles and AC/ZnO nano-particles**

0.24 g AC/TiO<sub>2</sub> and AC/ZnO nano-particles were used for photodegradation of neutral 60 ppm paracetamol solution (100 mL) under direct sun light. Figure (3.28) shows the overall photo-degradation reaction rate using the two supported catalyst types. The synthetic AC/ZnO reaction rate was higher than overall reaction rate for synthetic AC/TiO<sub>2</sub>.

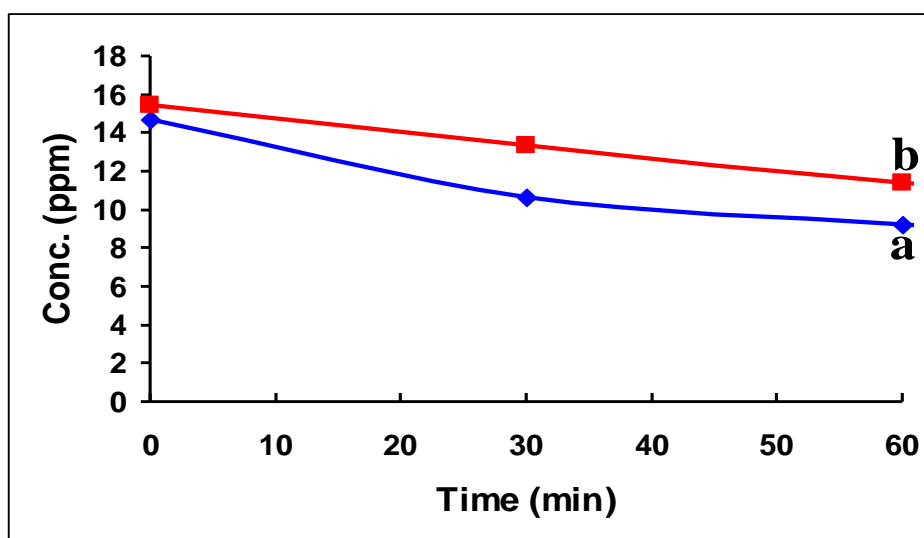


**Figure (3.28):** AC/TiO<sub>2</sub> and AC/ZnO nano-particles for photodegradation of neutral 60 ppm paracetamol solution (100 mL) under direct sun light: a) AC/ZnO nano-particle, b) AC/TiO<sub>2</sub> nano-particle.

Turnover number, quantum yield and turnover frequency calculated after 60 minutes for each catalyst system were shown in Table (3.15). All values for AC/ZnO nano. were higher than values for AC/TiO<sub>2</sub> nano.

**Table (3.15): Effect of catalyst on values of turnover number, turnover frequency (min<sup>-1</sup>), quantum yield and overall rate (ppm/min) for paracetamol degradation after 60 min, using AC/Catalyst nano. under direct sun light.**

Catalyst	Initial concentration (ppm)	Final concentration (ppm)	Turnover number	Turnover frequency (min <sup>-1</sup> )	Quantum yield	Overall rate (ppm/min)
AC/ZnO nano.	14.71	9.21	1.2X10 <sup>-3</sup>	0.020X10 <sup>-3</sup>	17.5X10 <sup>-3</sup>	0.10
AC/TiO <sub>2</sub> nano.	15.42	11.43	0.87X10 <sup>-3</sup>	0.015X10 <sup>-3</sup>	12.5X10 <sup>-3</sup>	0.07

**\* AC/TiO<sub>2</sub> anatase and AC/TiO<sub>2</sub> rutile**

Samples (0.12 g) of AC/TiO<sub>2</sub> anatase and AC/TiO<sub>2</sub> rutile were used for photodegradation of acidic (pH= 3.5) paracetamol (70 ppm) for three hours under UV light. As shown in Figure (3.29), AC/TiO<sub>2</sub> anatase catalyzed the photodegradation process faster than AC/TiO<sub>2</sub> rutile did.

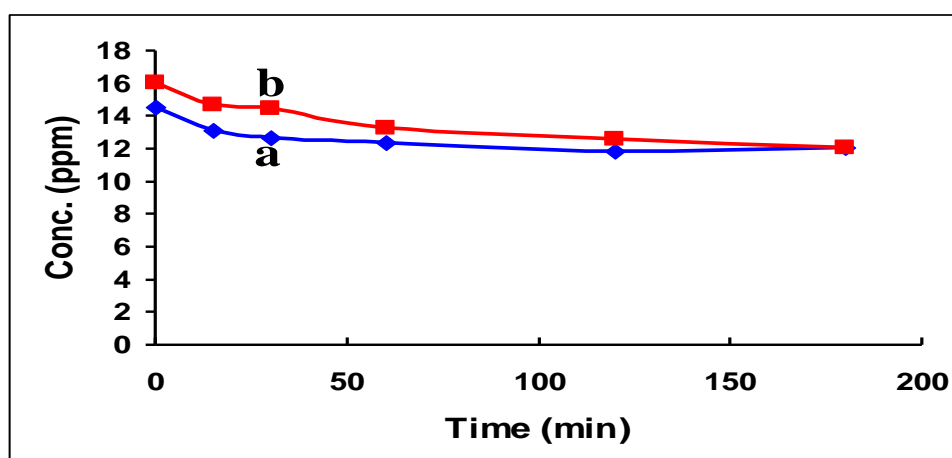


**Figure (3.29):** AC/TiO<sub>2</sub> forms (anatase and rutile) for photodegradation of acidic 70 ppm paracetamol solution (100 mL) under UV light: a) AC/TiO<sub>2</sub> rutile, b) AC/TiO<sub>2</sub> anatase.

Turnover number, quantum yield, turnover frequency and overall rate calculated after 60 minutes for each catalyst system were shown in Table (3.16). All values for AC/TiO<sub>2</sub> anatase were higher than values for AC/TiO<sub>2</sub> rutile.

**Table (3.16): Effect of AC/TiO<sub>2</sub> commercial catalysts (anatase and rutile) on values of turnover number, turnover frequency (min<sup>-1</sup>), quantum yield and overall rate (ppm/min) for paracetamol degradation after 60 min under UV light.**

Catalyst	Initial concentration (ppm)	Final concentration (ppm)	Turnover number	Turnover frequency (min <sup>-1</sup> )	Quantum yield	overall rate (ppm/min)
AC/TiO <sub>2</sub> R	14.53	12.35	4.80X10 <sup>-4</sup>	0.08X10 <sup>-4</sup>	16.5X10 <sup>-3</sup>	0.04
AC/TiO <sub>2</sub> A	16.04	13.27	6.13X10 <sup>-4</sup>	0.10X10 <sup>-4</sup>	21.0X10 <sup>-3</sup>	0.05

### 3.4 General discussion

In this work two types of metal oxides  $\text{TiO}_2$  and  $\text{ZnO}$  semiconducting materials have been used as photocatalysts for paracetamol degradation with UV or direct solar light.  $\text{TiO}_2$  was used either as commercial powder (in the micro-scale size) or as synthetic powder (in the nano-scale size).  $\text{ZnO}$  powder was also used as commercial (micro-sized) or synthetic (nano-sized).

The commercial micro-scale catalyst systems were first used to degrade paracetamol in the UV region. This was to reassess earlier literature reports [66] where UV light was used to degrade paracetamol in water. However, as UV light is costly, it is advisable to use solar light which is non-costly. As solar light that reaches earth involves about 5% UV only, it is thus necessary to investigate efficiency of all catalyst systems described above under solar light. Our main object is thus focused on using direct solar light in degrading paracetamol using the  $\text{TiO}_2$  and  $\text{ZnO}$  catalyst systems. This shows novelty of this work. All catalytic reaction results described earlier in this section will be discussed now.

Based on Figure (2.1), it should be noted that the mercury lamp used here did not yield radiation with enough UV waves, whereas solar radiation contained a tail in the UV range. These facts explain why solar radiation was more efficient in some cases than the used mercury lamp.

### **3.4.1 Catalytic reaction results**

#### **3.4.1.1 Commercial catalyst systems**

##### **3.4.1.1.1 Commercial TiO<sub>2</sub> systems**

Commercial TiO<sub>2</sub> particles showed little efficiency in catalyzing the photodegradation of paracetamol under the used UV light, while the anatase form was effective under direct sun light. This is consistent with earlier literature where anatase form is more efficient than rutile phase of TiO<sub>2</sub> [80]. Different kinetic parameters were investigated for photodegradation of paracetamol using TiO<sub>2</sub> commercial (anatase and rutile) under UV light, in order to enhance catalyst activity.

##### ***Effect of contaminant concentration***

Under neutral conditions, at lower contaminant concentrations, both anatase and rutile forms failed to catalyze the photodegradation of paracetamol. Increasing contaminant concentration, using either anatase or rutile forms, did not enhance degradation reaction rate under UV. This result is consistent with literature [66], where increasing contaminant concentration did not enhance reaction rate.

##### ***Effect of catalyst concentration***

Effect of increasing catalyst (both rutile and anatase) concentration was studied under UV radiation. In both systems, increasing catalyst

concentration did not affect the rate. Literature studies show different behaviors regarding effect of catalyst concentration on photodegradation rate [81]. Increasing catalysts concentration should increase rate. This because increasing catalyst dosage, total active surface area increases, hence availability of more active sites on catalyst surface [82]. In some reports, increasing catalyst loading increased reaction rate up to a limit [66]. This is because when more catalyst is used, the catalyst particles screen the radiation and prevent it from reaching catalyst sites inside the reaction mixture. This may lower the reaction rate.

### *Effect of pH*

At lower pH values, both anatase and rutile failed to catalyze the photodegradation of paracetamol in neutral and acidic media, under UV. At higher pH values (basic media), the rutile phase showed higher reaction rate, whereas the anatase could not function. This is consistent with earlier literature [81]. This may be attributed to the electrostatic interactions between the H atom at the OH groups on surface of TiO<sub>2</sub> catalyst and paracetamol anions (resulting at higher pH). Such interactions lead to more adsorption of the latter on the metal oxide support [66, 83]. Moreover, the effect of pH can be attributed to enhanced formation of OH<sup>•</sup> radicals, because at higher pH more hydroxide ions are available on TiO<sub>2</sub> surface and can be easily oxidized to form the radical OH<sup>•</sup> [84, 85]. This consequently increases the efficiency of paracetamol degradation at higher pH.

Effect of pH on TiO<sub>2</sub> catalytic efficiency can also be understood in terms of zero point charge concept. For TiO<sub>2</sub>, the zero point charge is around pH 6.4 [86]. This means that at higher pH values (more basic) the TiO<sub>2</sub> surface becomes more negative with surface OH groups, as H<sup>+</sup> are removed from surface OH groups. Therefore at higher pH the TiO<sub>2</sub> surface attracts more paracetamol molecules by interaction of the O<sup>-</sup> with H atoms of the paracetamol. This explains what at least rutile TiO<sub>2</sub> activity has been increased with higher pH.

#### **3.4.1.1.2 Commercial ZnO system**

Commercial ZnO was used in photodegradation of paracetamol under UV light and direct solar light. In both cases, the commercial ZnO catalyzed the photodegradation of paracetamol. Under UV light different kinetic parameters were investigated for photodegradation of paracetamol using ZnO commercial. Effect of pH was not studied in case of commercial ZnO catalyst [87].

#### ***Effect of contaminant concentration***

Photodegradation reaction rate increased by increasing paracetamol concentration, under UV. Values of T.N., T.F. and Q.Y. were also increased by increasing paracetamol concentration. This shows the importance of this work, where the process can function under different contaminant concentrations. This behavior is consistent with earlier literature describing other different photocatalytic reactions [51, 52].

### *Effect of catalyst concentration*

Overall rate reaction and quantum yield were increased with increasing catalyst amount, under UV. The values of T.N. and T.F. did not significantly change with increasing catalyst concentration. This is consistent with earlier literature where increasing catalyst concentration may increase rate to a certain limit [51, 81]. Other reports showed that increasing catalyst amount lowered reaction rate [88, 89]. The catalyst amount should increase rate by providing more active sites [81]. However, the screening effect may also lower the rate when catalyst amount is increased [89]. Therefore, the two factors may should be considered while explaining kinetics of photo-catalyzed degradation reactions. In this work, the first fact was the dominant factor. Increasing catalyst concentration increased rate and Q.Y. . The constant values of T.N. and T.F. values also indicate that efficiency of catalyst per molecule remained constant even with increasing catalyst concentration.

#### **3.4.1.2 Activated carbon-supported commercial catalysts (AC/catalysts)**

The commercial catalyst systems were supported onto activated carbon for two reasons: Firstly, to increase the rate of degradation; and, Secondly, to make catalyst separation from reaction mixture easier. Both TiO<sub>2</sub> and ZnO catalyst systems were therefore supported onto AC surfaces. General comparison for AC-supported vs. no supported was made. Effects of

different kinetic parameters on photodegradation of paracetamol were also studied under UV [52].

#### **3.4.1.2.1 AC/TiO<sub>2</sub> System**

Supporting commercial TiO<sub>2</sub> onto activated carbon surfaces enhanced its catalytic activity under UV. Both supported anatase and rutile TiO<sub>2</sub> phases showed higher efficiency values than their unsupported counterparts. The reason is due to ability of AC surface to adsorb contaminant molecules and bring them closer to catalyst sites. The hydrophilic nature of AC further helps such adsorption of contaminant molecules [90]. Moreover, supporting the catalyst particles onto AC surface made them easier to isolate from reaction mixture.

#### **3.4.1.2.2 AC/ZnO system**

The AC/ZnO is hydrophilic in nature as it readily mixes with water. The system is physically easy to isolate from water by simple filtration. Supporting commercial ZnO onto activated carbon increased its efficiency under UV radiation. The results are consistent with earlier literature [52]. This is because the AC brings the contaminant molecules closer to the catalyst sites by effective adsorption. Moreover, the AC keeps the ZnO particles uniformly distributed as individual particles, which helps expose them more to radiation.

### *Effect of contaminant concentration*

Under constant paracetamol concentration, the overall photodegradation reaction rate varied with type of supported catalyst as: AC/ZnO > AC/TiO<sub>2</sub> (A) > AC/TiO<sub>2</sub> (R). On other hand, paracetamol concentration affected the rate of reaction as described in Table (3.11). By increasing paracetamol concentration, the AC/ZnO efficiency showed no systematic effect on rate of photodegradation reaction. Rate may decrease by increasing contaminant concentration. However, as paracetamol absorbs light at  $\lambda = 385$  nm (near UV light), therefore increasing its concentration may block UV light from the catalyst surface. This may lower rate of reaction [51]. This is consistent with earlier results on different catalyst systems. The AC/TiO<sub>2</sub> anatase efficiency increased with increasing paracetamol concentration up to a certain value, as shown in Table 3.11.

Different explanations for contaminant concentration effect on reaction rate are proposed, all of which rely on the adsorption of contaminant molecules on the solid surface in a Langmuire Hinshelwood model [91]. As contaminant initial concentration increases above certain limits, more contaminant molecules are adsorbed onto the surface of AC/ZnO. This prohibits adsorption of other species such as O<sub>2</sub>, which is necessary for the reaction to occur. Moreover, with higher contaminant concentrations more light screening is expected to occur.

### *Effect of pH*

In case of AC/ZnO catalyst, the overall reaction decreased by increasing the acidity (lower pH) of paracetamol contaminant solution. Lowering the rate in acidic media is attributed to the amphoteric behavior of ZnO. As shown earlier in equations 1.2 and 1.3, in Chapter 1 earlier, ZnO is unstable at low and high pH values [92]. The values of overall rate, T.N., T.F. and Q.Y. increased with increasing the pH value. This is consistent with earlier literature [51]. Literature showed that ZnO may have highest efficiency under neutral conditions [51]. In this work, reaction was slower in acidic media due to two reasons: firstly, due to conversion of ZnO into other species, and secondly, due to paracetamol to easily carry positive charge at the N atom and to become as ammonium salt. The ammonium salt may not easily adsorb onto the ZnO surface, which then carries OH groups. Under neutral conditions, the paracetamol has Lewis basic center which may easily attach the ZnO surface OH groups, and the rate becomes faster.

The effect of pH on AC/ZnO efficiency is also attributed to its zero point charge value being 9.3 [93]. Therefore, at higher pH the ZnO surface is expected to involve negative charges. Such negative charges may attract H atoms on paracetamol molecules, and may enhance their adsorption onto the catalyst sites.

The AC/TiO<sub>2</sub> anatase catalyst system activity was higher in basic media. This resembles earlier reports about TiO<sub>2</sub> catalysts systems supported onto silica [94]. TiO<sub>2</sub> is more stable than ZnO under different pH values. The increased efficiency in catalyst at higher pH value could thus be explained based on ability of the paracetamol to adsorb onto TiO<sub>2</sub> surface more than at lower pH values. The efficiency of AC/TiO<sub>2</sub> rutile also increased under basic conditions. This can be explained in similar manner like the anatase system. Effect of pH on TiO<sub>2</sub> activity has already been discussed in section 3.4.1.1.1.

### **3.4.1.3 Nano-particle catalyst systems**

Synthetic TiO<sub>2</sub> and ZnO particles were prepared and used in paracetamol photodegradation reaction. The particles were in the nano-size scale, TiO<sub>2</sub> nano-particles (8.6 nm) and ZnO nano-particles (16 nm) were used in photodegradation of paracetamol under direct sun light. Each of them was compared with its commercial counterpart. Details of results are discussed below.

#### **3.4.1.3.1 Nano TiO<sub>2</sub> system**

Prepared nano TiO<sub>2</sub> particles (8.6 nm) were used in photodegradation of paracetamol under direct solar light in neutral solutions. The results show that the nano-particles were less efficient than the commercial anatase but more efficient than the commercial rutile form. With smaller TiO<sub>2</sub> particle size, value of band gap increases. Therefore, the nano-particles need UV

rather than visible light. However, as particle size is smaller, the relative surface area increases, which makes the catalyst more active. Despite its larger particle size, and lower relative surface area, the anatase catalyst was more active than the nano-scale catalyst, due to lower band gap of the former [15]. The rutile system showed very low efficiency, as discussed earlier in this work and in earlier literature [80]. The ability of commercial anatase and nano-TiO<sub>2</sub> particles to catalyze the reaction under solar light is due to availability of UV tail in the solar light [15].

#### **3.4.1.3.2 Nano ZnO system**

The overall rate reaction for commercial ZnO (5 µm) catalyst system was higher than for synthetic ZnO (16 nm) under direct sun light. The effect of size on the photodegradation efficiency can be ascribed to the following reasons: when the size of ZnO crystals decreases, the relative number of particles dispersed in the solution will increase, resulting in enhancement of the photon absorbance. With smaller particles the relative surface area of ZnO photocatalyst should also increase, which should promote adsorption of more paracetamol molecules on the surface and increase efficiency [92]. The results showed that the commercial ZnO was more active than the nano ZnO particles. The reason is thus due to value of  $E_{bg}$ . As the commercial powder has larger size, it has smaller  $E_{bg}$ , as discussed above. Therefore, the commercial powder will have more chance to absorb in the wavelength range closer to visible light (longer wavelength).

Comparison between nano ZnO with nano-TiO<sub>2</sub> catalyst systems, showed that the former is more active. This is due to higher absorptivity values for the ZnO system than the TiO<sub>2</sub>, as described in literature [83].

#### **3.4.1.4 AC/catalyst nano-particle systems**

AC/TiO<sub>2</sub> and AC/ZnO nano-particles were used in photodegradation reaction of paracetamol under direct sun light. The synthetic AC/TiO<sub>2</sub> showed nearly similar efficiency to naked synthetic TiO<sub>2</sub>. Presence of activated carbon, with high surface area, should as an effective absorbent to concentrate paracetamol molecules around the loaded TiO<sub>2</sub> and then bring them closer to catalyst active sites. The absorbed paracetamol could also be supplied to the loaded TiO<sub>2</sub> mostly by surface diffusion. Activated carbon may also prevent recombination of electron-hole pairs as reported earlier [95]. AC may also increase catalyst efficiency by keeping TiO<sub>2</sub> particles away from each other and increasing their exposure to light. In this work, the AC did not show significant effect on catalyst efficiency. This is because the features shown above possibly counteract each other. Ability of AC to absorb contaminant molecules is offset by other factors such as light screening.

The synthetic AC/ZnO was more efficient than naked synthetic ZnO. The AC can increase adsorption of contaminant molecules and bring them closer to ZnO catalyst sites, and can keep ZnO particles away from each other.

The overall reaction of AC/ZnO nano-particles was higher than AC/TiO<sub>2</sub> nano-particles. This is due to efficiency of synthetic ZnO being higher than that for synthetic TiO<sub>2</sub>, discussed above. The high absorptivity of ZnO to UV radiation [81] makes it an efficient degradation catalyst under direct solar light. ZnO catalyzes degradation reactions with UV tail that approaches our earth, which accounts for 5– 8% of solar radiation on earth surface. ZnO particles have been used to degrade different organic contaminants in water [47, 51, 81, 83, 89, 92, 94, 96- 104]. The results show that the catalyst with highest activity was the AC/ZnO (nano-particle) system. In addition to increasing ZnO catalyst efficiency, the AC made its recovery also easier [90, 105, 106]. Therefore, we recommend to focus future research on AC supported ZnO systems.

**Conclusions:**

- 1) Both ZnO and TiO<sub>2</sub> powders have been investigated as photocatalysts for photodegradation of paracetamol as a model pharmaceutical contaminant in water under different conditions. Both commercial and prepared powders were investigated.
- 2) ZnO catalyst was more efficient than TiO<sub>2</sub> catalyst in photodegradation of paracetamol under both UV and direct sun light.
- 3) Commercial anatase showed higher efficiency than synthetic TiO<sub>2</sub> under direct sun light.
- 4) Commercial TiO<sub>2</sub> rutile was effective only in UV at higher pH values.
- 5) Commercial ZnO showed higher efficiency than synthetic ZnO.
- 6) Supporting catalysts onto activated carbon surfaces enhanced their activity under both UV and direct sun light.
- 7) Supported commercial ZnO was more efficient than supported anatase TiO<sub>2</sub> under UV.
- 8) When paracetamol concentration and pH were varied, the AC/TiO<sub>2A</sub> and AC/ZnO<sub>comm.</sub> catalyst systems showed different behaviors.
- 9) AC/ZnO<sub>nano.</sub> was more efficient than AC/TiO<sub>2nano.</sub> under direct sun light.

**Suggestions for further work:**

- 1) Using ZnO and TiO<sub>2</sub> as photoatalytic substances to degrade paracetamol and other pharmaceutical wastes at pilot plant scale.
- 2) Using other semiconductor catalysts in photodegradation of paracetamol.
- 3) Applying the ZnO, TiO<sub>2</sub>, AC/ZnO and AC/TiO<sub>2</sub> catalysts in different chemical pollutants, such as fertilizers, pesticides, drugs and other water pollutants.
- 4) Using other methods for ZnO and TiO<sub>2</sub> nano-particles preparation to achieve smaller particle size with higher efficiency.
- 5) Supporting the catalysts on other supports, such as sand and clay.
- 6) Using other types of mercury lamps which emit radiations with more UV fractions for basic study purposes.
- 7) Study reactions for longer exposure times.
- 8) Study effect of oxygen flow rate.
- 9) Study influence of other aqueous ions (interference) on reaction rate.

## References

- [1] <http://www.hull.ac.uk/coastalobs/general/environment/pollution.html>  
(Accessed Nov. 25, 2012).
- [2] [http://www.bcb.uwc.ac.za/sci\\_ed/grade10/ecology/conservation/poll.htm](http://www.bcb.uwc.ac.za/sci_ed/grade10/ecology/conservation/poll.htm)  
(Accessed Nov. 25, 2012).
- [3] [en.wikipedia.org/wiki/Purified\\_water](http://en.wikipedia.org/wiki/Purified_water) (Accessed Nov. 25, 2012).
- [4] A. Zyoud. **Nanoparticle CdS-sensitized TiO<sub>2</sub> catalyst for photo-degradation of water organic contaminants: Feasibility assessment and natural-dye alternatives**, Ph.D.Thesis, An-Najah National University, Palestine, (2009), p.1.
- [5] <http://en.wikipedia.org/wiki/Ultraviolet> (Accessed Jan. 3, 2013)
- [6] B. G. Yacobi, **Semiconductor Materials: An Introduction to Basic Principles**, Springer, (2003), pp. 1- 3.
- [7] M. Anpo, **Utilization of TiO<sub>2</sub> photocatalysts in green chemistry**, *Pure Appl. Chem.*, **72**, (2000), pp. 1265– 1270.
- [8] R. Benedix, F. Dehn, J. Quaas, M. Orgass, **Application of titanium dioxide photocatalysis to create self-cleaning building materials**, *LACER*, No. 5, (2000), pp. 157- 168.

[9] A. Mills, R. H. Davies and D. Worsley, **Water purification by semiconductor photocatalysis**, *Chem. Soc. Rev.*, **22**, (1993), pp. 417- 425.

[10] [http://en.wikipedia.org/wiki/Titanium\\_dioxide](http://en.wikipedia.org/wiki/Titanium_dioxide) (Accessed Jan. 3, 2013)

[11] G. El, M. Chen, L. Dubrovinsky, P. Gillet, G. Graup, **An ultradense polymorph of rutile with seven-coordinated titanium from the Ries crater**, *Science*, **293** (5534), (2001), pp. 1467– 70.

[12] J. Jamieson, B. Olinger, **Pressure temperature studies of anatase, brookite, rutile and TiO<sub>2</sub> II: A discussion**, *Mineral. Notes*, **54**, (1969), p. 1477.

[13] N. N. Greenwood, A. Earnshaw, **Chemistry of the Elements**, Oxford: Pergamon, (1984), pp. 1117– 19.

[14] A. Fujishima, K. Honda, **Electrochemical photolysis of water at a semiconductor electrode**, *Nature*, **238** (5358), (1972), pp. 37– 8.

[15] O. Carp, C.L. Huisman, A. Reller, **Photoinduced reactivity of titanium dioxide**, *Progr. Solid State Chem.*, **32**, (2004), pp. 33– 177

[16] T. Ohno, K. Sarukawa, M. Matsumura, **Photocatalytic activity of pure rutile particles isolated from TiO<sub>2</sub> powder by dissolving the anatase component in HF solution**, *Phys. Chem. B*, **105**, (2001), pp. 2417- 2420.

[17] A. Fujishima, K. Hashimoto, T. Watanabe, **TiO<sub>2</sub> photocatalysis fundamentals and application**, BKC Inc. Tokyo, Japan (1999), p. 125.

[18] D. Devilliers, Süd-Chemie, Inc. **Semiconductor photocatalysis: Still an active research area despite barriers to commercialization**, *Energie*, **17**, (2006), pp. 1- 6

[19] TIME's Best Inventions of 2008, (Accessed Jan. 3, 2013).

[20] I. K. Konstantinou, T. A. Albanis, **TiO<sub>2</sub>-assisted photocatalytic degradation of azo dyes in aqueous solution: Kinetic and mechanistic investigations**, *App. Cat. B: Env.*, **49**, (2004), p. 1. ([http://en.wikipedia.org/wiki/Titanium\\_dioxide](http://en.wikipedia.org/wiki/Titanium_dioxide))

[21] J. Winkler, *Titanium Dioxide*. Hannover: Vincentz Network, (2003), pp. 115- 116. ISBN 3-87870-148-9.

[22] H. Chen, Z. Xie, X. Jin, C. Luo, C. You, Y. Tang, D. Chen, Z. Li, and X. Fan, **TiO<sub>2</sub> and N-doped TiO<sub>2</sub> induced photocatalytic inactivation of staphylococcus aureus under 405 nm LED blue light irradiation**, *Int. J. Photoenergy*, (2012), pp. 1- 5.

[23] J. Dharma, A. Pital, Perkin Elmer, Inc. **Simple method of measuring the band gap energy value of TiO<sub>2</sub> in the powder form using a UV/Vis/NIR Spectrometer**.

([http://www.perkinelmer.com/Content/applicationnotes/app\\_uvvisnirmeasurebandgapenergyvalue.pdf](http://www.perkinelmer.com/Content/applicationnotes/app_uvvisnirmeasurebandgapenergyvalue.pdf))

[24] A. Hernandezbattez, R. Gonzalez, J. Viesca, J. Fernandez, J. Diazfernandez, A. MacHado, R. Chou, J. Riba, **CuO, ZrO<sub>2</sub> and ZnO nanoparticles as antiwear additive in oil lubricants**, *Wear*, **265**, (2008), p. 422.

[25] M. De Liedekerke, 2.3. **Zinc Oxide (Zinc White): Pigments, Inorganic, 1**, *Ullmann's Encyclopedia of Industrial Chemistry*, Wiley on-line Library, 2006.

[26] N. N. Greenwood, A. Earnshaw, **Chemistry of the Elements** (2nd ed.), (Chapter 29) Butterworth–Heinemann, Oxford, U.K., (1997), pp. 1201- 1224, ISBN 0080379419.

[27] E. Wiberg, A. F. Holleman, *Inorganic Chemistry*. Elsevier, (2001), p.1291- 1300 (chapter XXIII), ISBN 0-12-352651-5.

[28] U. Özgür, Y. I. Alivov, C. Liu, A. Teke, M. A. Reshchikov, S. Doğan, V. Avrutin, S. J. Cho, **A comprehensive review of ZnO materials and devices**, *J. Appl. Phys.*, **98**, (2005), p. 041301.

[29] S. Talam, S. R. Karumuri, N. Gunnam, **Synthesis, characterization and spectroscopic properties of ZnO nanoparticles**, *international scholarly research network, ISRN Nanotechnology*, (2012), p.1- 6.

[30] J. Zhou, F. Zhao, Y. Wang, Y. Zhang, and L. Yang, **Size controlled synthesis of ZnO nanoparticles and their photoluminescence properties**, *J. Luminesc.*, **122- 123**, (2007), pp. 195– 197.

[31] N.Tamaekong, C. Liewhiran, A. Wisitsoraat, S. Phanichphant, **Flame-spray-made undoped zinc oxide films for gas sensing applications**, *Sensors (Basel)*, **10**, 2010, pp. 7863- 7873.

[32] Q. Peng, Qin, **ZnO nanowires and their application for solar cells**, **School of Environmental & Chemical EngineeringNanchang Hangkong UniversityNanchang**, 330063, China

[33] Y. D. Jin, J. P. Yang, P. L. Heremans, **Single-layer organic light-emitting diode with 2.0% external quantum efficiency prepared by spin-coating**, *Chem. Phys. Lett.*, **320**, (2000), pp. 387– 392.

[34] X. Wang, Y. Ding, C. J. Summers, Z. L. Wang, **Large-scale synthesis of six-nanometer-wide ZnO nanobelts**, *J. Phys. Chem. B*, **108**, (2004), pp. 8773– 8777.

[35] N. Chestnoy, T. D. Harris, R. Hull, L. E. Brus, **Luminescence and photophysics of CdS semiconductor clusters: the nature of the emitting electronic state**, *J. Phys. Chem.* **90**, (1986), pp. 3393– 3399.

[36] J. R. Heath, J. J. Shiang, **Covalency in semiconductor quantum dots**, *Chem. Soc. Rev.*, **27**, (1998), pp. 65– 71.

[37] M. H. Huang, Y.Wu, H. Feick, N. Tran, E.Weber, P. Yang, **Catalytic growth of zinc oxide nanowires by vapor transport**, *Adv. Mater.*, **13**, (2001), pp. 113– 116.

[38] G. Williams, P. V. Kamat, **Graphene-semiconductor nanocomposites: excited-state interactions between ZnO nanoparticles and graphene oxide**, *Langmuir*, **25**, (2009), pp. 13869– 13873.

[39] B. S. Rao, B. R. Kumar, V. R. Reddy, T. S. Rao, **Preparation and characterization of CdS nanoparticles by chemical co-precipitation technique**, *Chalcogen. Lett.*, **8**, (2011), pp. 177– 185.

[40] <http://www.csemuae.com/pdfs/Wastewater%20Treatment%20using%20Solar%20UV%20radiation.pdf> (Accessed Jan. 3, 2013).

[41] M. R. Hoffmann, S. T. Martin, W. Y. Choi, D. W. Bahnemann, **Environmental applications of semiconductor photo-catalysis**, *Chem. Rev.*, **9**, (1995), pp. 69- 96.

[42] Reference 4, p. 16.

[43] C. J. Philippopoulos, M. D Nikolaki, **Photocatalytic processes on the oxidation of organic compounds in water**, *New Trends Technol.*, **9**, (2010), p. 89.

[44] A. G. Rinc, C. Pulgarin, N. Adler, P. Peringer, **Interaction between E. coli inactivation and DBP-precursors dihydroxybenzene isomers in the photocatalytic process of drinking-water disinfection with TiO<sub>2</sub>**, *Photochem. Photobiol A.*, **139**, (2001), pp. 233– 241.

[45] D. Chen, A. K. Ray, **Photocatalytic kinetics of phenol and its derivatives over UV irradiated TiO<sub>2</sub>**, *Appl. Catal. B: Environ.*, **23**, (1999), pp. 143- 157.

[46] V. Augugliaro, V. Loddo, L. Palmisano, M. Schiavello, **Performance of heterogeneous photocatalytic systems: Influence of operational variables on photoactivity of aqueous suspension of TiO<sub>2</sub>**, *Catalysis*, **153**, (1995), pp. 32- 40.

[47] J. M. Herrmann, Heterogeneous photocatalysis: **Fundamentals and applications to the removal of various types of aqueous pollutants**, *Catal. Today*, **53**, (1999), pp. 115- 129.

[48] R. L. Calderon, **The epidemiology of chemical contaminants of drinking water**, *Food Chem. Toxicol.*, **38**, (2000), p. S13– S20.

<http://www.sciencedirect.com/science/article/pii/S0278691599001337>

[49] C. S. Turchi, D. F. Ollis, **Photocatalytic degradation of organic water contaminants: Mechanisms involving hydroxyl radical attack**, *J. Catal.*, **122**, (1990), pp. 178- 192

<http://www.sciencedirect.com/science/article/pii/002195179090269P>

[50] J. Nishio, M. Tokumura , H.T. Znad, Y. Kawase , **Photocatalytic decolorization of azo-dye with zinc oxide powder in an external UV**

**light irradiation slurry photoreactor**, *J. Hazard. Mater.*, **138**, (2006), pp. 106-115.

[51] H. S. Hilal, G. Y. M. Al-Nour , A. Zyoud, M. H. Helal and I. Saadeddin, **Pristine and supported ZnO catalysts for phenazopyridine degradation with direct solar light**, *Solid State Sci.*, **12**, (2010), pp. 578–586.

[52] H. S. Hilal, G. Y. M. Nour, A. Zyoud , **Photo-degradation of methyl orange with direct solar light using ZnO and activated carbon supported ZnO**, Chapter 6 in **Water Purification**, Eds. Nikolaj Gertsen and Linus Sonderby, Novascience Publ., NY, (2009), pp. 227- 246, ISBN: 978-1-60741-599-2.

[53] M. Zhao, Z. Juan, **Wastewater treatment by photocatalytic oxidation of Nano-ZnO**, *Global Environ. Policy Japan*, **12**, (2008), pp. 1-9.

[54] A. Fortuny, C. Bengoa, J. Font, A. Fabregat, **Bimetallic catalysts for continuous catalytic wet air oxidation of phenol**, *J. Hazard. Mater. B.*, **64**, (1999), pp. 181– 193.

[55] A. Sobczyński, A. Dobosz, **Water purification by photocatalysis on semiconductors**, *Polish J. Environ. Studies*, **10**, (2001), pp. 195- 205.

[56] X. Pan, I. Medina-Ramirez, R. Mernaugh, J. Liu, **Nanocharacterization and bactericidal performance of silver modified titania photocatalyst**, *Coll. Surf. B*, **77**, (2010), pp. 82– 89.

[57] A. Sapkota, S. Baruah, O. Shipin, J. Dutta, **Photocatalytic inactivation of bacteria with ZnO nanorods, the 3rd Thailand nanotechnology conference**, 2009 Dec 21- 22, Asian Institute of Technology, Klong Luang.

[58] T. C. Dang, D. L. Pham, H. L. Nguyen, V. H. Pham., **CdS sensitized ZnO electrodes in photoelectrochemical cells**, *Adv. Nat. Sci.: Nanosci. Nanotechnol.*, **1**, (2010), pp.1- 6.

[59] G. Al-Nour, **Photocatalytic degradation of organic contaminants in the presence of graphite supported and unsupported ZnO modified with CdS particles**, M.Sc. Thesis, An-Najah National University, Palestine, 2009.

[60] S. Seki, T. Sekizawa, K. Haga, T. Sato, M. Takeda, Y. Seki, Y. Sawada, K. Yubuta, T. Shishido, **Effects of silver deposition on 405 nm light-driven zinc oxide photocatalyst**, *J. Vac. Sci. Technol*, **28**, (2010), pp.1- 6.

[61] R. R. Salinas-Guzman, J. L. Guzman-Mar, L. Hinojosa-Reyes, J. M. Peralta-Hernandez, A. Hernandez-Ramirez, **Enhancement of cyanide**

**photocatalytic degradation using sol–gel ZnO sensitized with cobalt phthalocyanine**, *J. Sol-Gel Sci. Technol.*, **54**, (2010), p.1- 7.

[62] M. Hitchman, G. Tyrie, S. Barfield, M. Park, **Photocatalysis in industrial water treatment –An operational technology**, Albagaia Ltd, Edinburgh, United Kingdom.

<http://albagaia.com/images/AlbagaiaPhotocatalyticWaterTreatment.pdf>

[63] R. W. Matthews, Purification of water with near—U.V. **illuminated suspensions of titanium dioxide**, *Water Res.*, **24**, (1990), pp. 539- 673.

[64][http://www.ch.ic.ac.uk/rzepa/mim/drugs/html/paracet\\_text.htm](http://www.ch.ic.ac.uk/rzepa/mim/drugs/html/paracet_text.htm)  
(Accessed Jan. 5, 2013).

[65] X. Zhang, F. Wu, N. Deng, **Degradation of paracetamol in self-assembly  $\beta$ -cyclodextrin/TiO<sub>2</sub> suspension under visible irradiation**, *Catal. Commun.*, **11**, (2010), pp. 311- 502.

[66] L. Yang , L. E. Yu, M. B. Ray, **Degradation of paracetamol in aqueous solutions by TiO<sub>2</sub> photocatalysis**, *Water Res.*, **42**, (2008), pp. 3480 – 3488.

[67] H.S. Hilal, L.Z. Majjad, N. Zaatar, A. El-Hamouz, **Dye-effect in TiO<sub>2</sub> catalyzed contaminant photo-degradation: Sensitization vs. charge-transfer formalism**, *Solid State Sci.*, **9**, (2007), pp. 9- 15.

[68] <http://www.svetila.com/en/ultra-vitalux-300w-1170.html> (Accessed Jan. 5, 2013).

[69] J. A. MacLaughlin, R. R. Anderson, M. F. Holick, **Spectral character of sunlight modulates photosynthesis of previtamin D3 and its photoisomers in human skin**, *Science*, **216**, (1982), pp. 1001- 1003.

[70] Y. Bessekhoud, D. Robert, J. V. Weber, **Preparation of TiO<sub>2</sub> nanoparticles by Sol-Gel route**, *Int. J. Photoenergy*, **5**, (2003), p. 153.

[71] M. Pfanzelt, P. Kubiak, M. Fleischhammer, **M. Wohlfahrt-Mehrens, TiO<sub>2</sub> rutile—An alternative anode material for safe lithium-ion batteries**, *J. Power Sources*, **196**, (2011), pp. 6815– 6821.

[72] C. H. Sun, X. H. Yang, J. S. Chen , Z. Li , X. W. Lou , C. Li , S. C. Smith , G. Q. (Max) Lu, H. G. Yang, **Higher charge/discharge rates of lithium-ions across engineered TiO<sub>2</sub> surfaces leads to enhanced battery performance**, *Chem. Commun.*, **46**, (2010), pp. 6129- 6131

[73] M. Kondo, S. Adachi, **Optical Properties of NaCl: Sn<sup>+2</sup> Phosphor Synthesized from Aqueous NaCl/SnCl<sub>2</sub> /HCl Solution**, *ECS J. Solid State Sci. Technol.*, **2**, (2013), pp. R9- R15.

[74] Shape factor (X-ray diffraction), U.S. Department of Energy, Office of Scientific and Technical Information, available on: [http://www.osti.gov/engage/rrpedia/Shape\\_factor\\_%28Xray\\_diffraction%29](http://www.osti.gov/engage/rrpedia/Shape_factor_%28Xray_diffraction%29)

action%29#cite\_note-0 (Accessed Jan. 5, 2013).

[75] [http://depts.washington.edu/chemcrs/bulkdisk/chem364A\\_spr05/notes\\_Lecture-Note-11.pdf](http://depts.washington.edu/chemcrs/bulkdisk/chem364A_spr05/notes_Lecture-Note-11.pdf) (Accessed Jan. 5, 2013).

[76] S. Lopez-Romero, **Growth and characterization of ZnO cross-like structures by hydrothermal method**, *Revista Matéria*, **14** (2009) 716-724.

[77] C. Y. Lee, T. Y. Tseng, S. Y. Li, P. Lin, **Growth of zinc oxide nanowires on silicon (100)**, *TKJSE.*, **6**, (2003), pp. 127- 132.

[78] D. Sridevi, K. V. Rajendran, **Synthesis and optical characteristics of ZnO nanocrystals**, *Bull. Mater. Sci.*, **32**, (2009), pp. 165– 168.

[79] D. Calestani, M. Zha, R. Mosca, A. Zappettini, M.C. Carotta, V. Di Natale, L. Zanotti, **Growth of ZnO tetrapods for nanostructure-based gas sensors**, *Sens. Actuators, B*, **144**, (2010), pp.472– 478.

[80] C. G. Silva, J. L. Faria, **Anatase vs. rutile efficiency on the photocatalytic degradation of clofibrac acid under near UV to visible irradiation**, *Photochem. Photobiol. Sci.*, **8**, (2009), pp. 705- 711.

[81] S.K. Kansal, M. Singh, D.Sud, **Studies on photodegradation of two commercial dyes in aqueous phase using different photocatalysts**, *J. Hazard. Mater.*, **141**, (2007), pp. 581– 590.

[82] M.S.T. Gonclaves, A.M.F. Oliveira-Campose, E.M.M.S. Pinto, P.M.S. Plasencia, M.J.R.P. Queiroz, **Photochemical treatment of solutions of azo dyes containing TiO<sub>2</sub>**, *Chemosphere*, **39**, (1999), p. 781.

[83] S. Sakthivel, B. Neppolian, B.V. Shankar, B. Arabindoo, M. Palanichamy, V. Murugesan, **Solar photocatalytic degradation of azo dye: comparison of photocatalytic efficiency of ZnO and TiO<sub>2</sub>**, *Sol. Ener. Mater. Sol. Cells*, **77**, (2003), pp. 68.

[84] Zheng et al. , 1997 (Zheng, S.R., Huang, Q.G., Zhou, J., Wang, B.K., **A study on dye photoremoval on TiO<sub>2</sub> suspension solution**, *J. Photochem. Photobiol. A Chem.*, **108** (2– 3), (1997), pp. 235– 238).

[85] Galindo et al., 2000 (Galindo, C., Jacques, P., Kalt, A., **Photodegradation of the aminoazobenzene acid orange 52 by three advanced oxidation processes: UV/H<sub>2</sub>O<sub>2</sub>, UV/TiO<sub>2</sub> and VIS/TiO<sub>2</sub>: Comparative mechanistic and kinetic investigations**, *J. Photochem. Photobiol. A*, **130**, (2000), pp. 35– 47).

[86] J.- C. Chou, L. P. Liao, **Study on pH at the point of zero charge of TiO<sub>2</sub> pH ion-sensitive field effect transistor made by the sputtering method**, *Thin Solid Films*, **476**, (2005), pp. 157– 161.

[87] S. B. Park, H. C. Shin, W. Lee, W. I. Cho, H. Jang, **Improvement of capacity fading resistance of LiMn<sub>2</sub>O<sub>4</sub> by amphoteric oxides**, *J. Power Sources*, **180**, (2008), pp. 597– 601.

- [88] A. Akyol, H.C. Yatmaz, M. Bayramoglu, **Photocatalytic decolorization of Remazol Red RR in aqueous ZnO suspensions**, *Appl. Catal. B: Environ.*, **19**, (2004), p. 54.
- [89] N. Daneshvar, D. Salari, A.R. Khataee, **Photocatalytic degradation of azo dye acid red 14 in water on ZnO as an alternative catalyst to TiO<sub>2</sub>**, *J. Photochem. Photobiol. A: Chem.*, **157**, (2003), pp. 111- 116.
- [90] G. Li Puma, A. Bono, D. Krishnaiah, J. G. Collin, **Preparation of titanium dioxide photocatalyst loaded onto activated carbon support using chemical vapor deposition: A review paper**, *J. Hazard. Mater.*, **157**, (2008), pp. 209– 219.
- [91] D.S. Tsoukleris, A.I. Kontos, P. Aloupogiannis, P. Falaras, **Photocatalytic properties of screen-printed titania**, *Catal. Today*, **124**, (2007), p. 110
- [92] N. Daneshvar, S. Aber, M.S. Seyed Dorraji, A.R. Khataee, M.H. Rasoulifard, **Preparation and investigation of photo-catalytic properties of ZnO nanocrystals: effect of operational parameters and kinetic study**, *Int. J. Chem. Biomol. Eng.*, **1**, (2008), pp. 1307– 7449.
- [93] D. W. Bahnemann, C. Kormann, M. R. Hoffmann, **Preparation and characterization of quantum size zinc oxide: A detailed spectroscopic study**, *J. Phys. Chem.*, **91**, (1987), pp. 3789- 3798.

[94] A. H. Zyoud, H. S. Hilal, **Silica-supported CdS-sensitized TiO<sub>2</sub> particles in photo-driven water purification: Assessment of efficiency, stability and recovery future perspectives, Chapter 5 in Water Purification, Eds. Nikolaj Gertsen and Linus Sønderby, Novascience Publ., NY, (2009), pp. 203- 226. ISBN: 978-1-60741-599-2.**

[95] Y. Li, X. Li, J. Li, J. Yin, **Photocatalytic degradation of methyl orange by TiO<sub>2</sub>-coated activated carbon and kinetic study, *Water Research*, **40**, (2006), pp. 1119 – 1126.**

[96] J.M. Herrmann, C. Duchamp, M. Karkmaz, B.T. Hoai, H. Lachheb, E. Puzenat, C. Guillard, **Environmental green chemistry as defined by photocatalysis, *J. Hazard. Mater.*, **145**, (2007), pp. 624– 629.**

[97] K. Byrappa, A.K. Subramani, S. Anadada, K.M. Lokanatha Rai, R. Dinesh, M. Yoshimura, **Photo-catalytic degradation of rhodamine B dye using hydrothermally synthesized ZnO, *Bull. Mater. Sci.*, **29**, (2006), pp. 433– 438.**

[98] R. Ali, O.B. Siew, **Photo-degradation of new methylene blue N in aqueous solution using zinc oxide and titanium dioxide as catalyst, *J. Teknol.*, **45**, (2006), pp. 31– 42.**

[99] N. Daneshvar, D. Salari, A.R. Khataee, **Photo-catalytic degradation of azo dye acid red 14 in water as an alternative catalyst to TiO<sub>2</sub>, *J. Photochem. Photobiol. A: Chem.*, **162**, (2004), pp. 317– 322.**

[100] K. Mohamed, K. Nada, **pH effect on the photo-catalytic degradation of the chlorpyrifus from insecticide morisbana by ZnO in aquoues medium**, *Bull. Environ. Res.*, **9**, (2006), pp. 23– 31.

[101] A.J. Abbas, K.H. Salih, H.H. Falah, **Photo-catalytic degradation of textile dyeing waste water using titanium dioxide and zinc oxide**, *E-J. Chem.*, **5**, (2008), pp. 219– 223.

[102] H. Wang, C. Xie, W. Zhang, S. Cai, Z. Yang, Y. Gui, **Comparison of dye degradation efficiency using ZnO power with various size scales**, *J. Hazard. Mater.*, **141**, (2007), pp. 645– 652.

[103] C. Lizama, J. Freer, J. Baeza, H.D. Mansilla, **Optimized photo-degradation of Reactive blue 19 on TiO<sub>2</sub> and ZnO suspensions**, *Catal. Today*, **76**, (2002), pp. 235– 246.

[104] B. Rohe, W.S. Veeman, M. Tausch, **Synthesis and photo-catalytic activity of silane-coated and UV-modified nano scale zinc oxide**, *Nano Technol.*, **17**, (2006), pp. 277– 282.

[105] K. Byrappa, A.K. Subramani, S. Ananda, K.M. L Rai, M.H. Sunitha, B. Basavalingu, K. Soga, **Impregnation of ZnO onto activated carbon under hydrothermal conditions and its photocatalytic properties**, *J. Mater. Sci.*, **41**, (2006), pp. 1355– 1362.

[106] N. Sobana, M. Swaminathan, **Combination effect of ZnO and activated carbon for solar assisted photocatalytic degradation of Direct Blue 53**, *Sol. Energy Mater. Sol. Cells*, **91**, (2007), pp. 727– 734.

جامعة النجاح الوطنية

كلية الدراسات العليا

استخدام  $ZnO$  و  $TiO_2$  كحفازات ضوئية في تحطيم المخلفات الصيدلانية المنتشرة:

تأثير حجم حبيبة الحفاز وتثبيتته على السطوح

إعداد

شادية أحمد حسني حجاوي

إشراف

أ.د حكمت هلال

د. عاهد الزيود

قدمت هذه الرسالة استكمالاً لمتطلبات الحصول على درجة الماجستير في الكيمياء بكلية الدراسات العليا في جامعة النجاح الوطنية في نابلس فلسطين.

2013

ب

استخدام  $ZnO$  و  $TiO_2$  كحفازات ضوئية في تحطيم المخلفات الصيدلانية المنتشرة:

تأثير حجم حبيبة الحفاز وتثبيته على السطوح

إعداد

شادية أحمد حسني حجاوي

إشراف

أ.د. حكمت هلال

د. عاهد الزيود

الملخص

هناك الكثير من الطرق المستخدمة في تحطيم المخلفات الصيدلانية المنتشرة والملوثة للماء. ومن الطرق التي تعد من أفضل الوسائل لتتقية الماء بدون آثار جانبية هو استخدام الحفازات الضوئية مثل أكسيد التيتانيا و أكسيد الزنك. يعتبر هذان الحفازان من أشباه الموصلات التي تمتلك فجوة طاقة واسعة، لذلك فإن عملية تهيج الإلكترونات تتطلب وجود الأشعة فوق البنفسجية.

تم في هذه الدراسة استخدام أكسيد التيتانيا وأكسيد الزنك التجارية والمصنعة في المختبر، والتي تم تشخيصها بواسطة أشعة X والمجهر الماسح والوميض الضوئي والإمتصاص الضوئي، في تتقية الماء من المخلفات الصيدلانية مثل البراسيتامول عن طريق التحطيم الضوئي. حيث استخدم كلا الحفازين بأحجام مختلفة في تحطيم البراسيتامول. استخدم الحفاز التجاري تحت لمبة الأشعة فوق البنفسجية بينما الحفاز المصنع في المختبر تحت أشعة الشمس المباشرة. كما تم في هذه الدراسة تثبيت الحفاز على سطح الكربون المنشط. أجريت عملية التحطيم الضوئي للبراسيتامول تحت تأثير عدة عوامل مثل تركيز الملوث وتركيز الحفاز ودرجة الحموضة.

أظهرت النتائج في هذه الدراسة أن أكسيد التيتانيا التجاري بنوعيه (أنتيز و روتيل) ليس له فاعلية عالية في تحطيم البراسيتامول تحت الأشعة فوق البنفسجية. أما تحت أشعة الشمس المباشرة فتظهر فاعلية أكسيد التيتانيا التجاري (أنتيز) اكبر من النانو في عملية التحطيم. كما بينت نتائج هذه الدراسة أن أكسيد التيتانيا التجاري (روتيل) يعمل تحت الأشعة فوق البنفسجية على درجة حموضة عالية للوسط المائي الملوث بالبراسيتامول. أما أكسيد الزنك التجاري فله

فاعلية كبيرة نسبيا في التحطيم تحت كل من الأشعة فوق البنفسجية و أشعة الشمس المباشرة. وجد تحت تأثير الأشعة فوق البنفسجية أن فاعلية أكسيد التيتانيا (أنتيز) أكبر بقليل من أكسيد الزنك التجاري. بينما تحت أشعة الشمس المباشرة فإن أكسيد الزنك التجاري أكثر فاعلية في التحطيم من أكسيد التيتانيا (أنتيز). كذلك أكسيد الزنك النانو أكثر فاعلية من أكسيد التيتانيا النانو تحت أشعة الشمس المباشرة.

أما بالنسبة للحفازين المثبتين على سطح الكربون المنشط فإن الكربون زاد من تحفيز سطح الحفاز المستخدم في التحطيم الضوئي. فقد زاد الكربون المنشط من فاعلية أكسيد التيتانيا وأكسيد الزنك التجاريين تحت الأشعة فوق البنفسجية والنانو تحت أشعة الشمس المباشرة. حيث أظهرت الدراسة أن أكسيد التيتانيا النانو والمثبت له فاعلية في التحطيم أكبر من أكسيد التيتانيا التجاري والمثبت تحت أشعة الشمس المباشرة. أما أكسيد الزنك التجاري والمثبت، فله فاعلية أكبر من أكسيد التيتانيا (أنتيز) والمثبت، تحت الأشعة فوق البنفسجية. كما أن فاعلية أكسيد الزنك النانو والمثبت أكبر من أكسيد التيتانيا النانو والمثبت تحت أشعة الشمس المباشرة.

وباختصار تبين هذه الدراسة أن أكسيد التيتانيا وأكسيد الزنك المثبتين على سطح الكربون المنشط لهما حسنات في زيادة فاعليتهما في التحطيم كذلك في سهولة فصلهما من الوسط المائي بعد انتهاء عملية تحطيم الملوث.

